Comparison of Geothermal Structures at Tauhara Geothermal Field, New Zealand and Muara Laboh, Indonesia

A thesis submitted in partial fulfilment of the requirements for the degree of

Master of Science in Geology

at the

University of Canterbury

by

Joe Struthers

2019

Abstract

Understanding the relationships between geological features and hydrothermal fluid pathways is critical for effective geothermal site investigation, exploration and production. Feed zones found within wells indicate fluid conduits. This work demonstrates the development of a workflow using Leapfrog Geothermal modelling software to test which parameters of a given geothermal field influence where these feed zones occur. Two sites were chosen to develop the process: Tauhara, New Zealand, and Muara Laboh, Indonesia. These sites are both situated in extensional environments but have different lithologies, structures and, based on previous studies, are hypothesized to have different geothermal system controls.

This research focused on constructing lithology, structure, temperature, and feed zone models to investigate the attributes conventionally understood to influence permeability. The relationships between these were examined using offset distance and combined modelling. Experimentation through iterative reworking was used to improve the efficiency of the workflow. Comparisons were made between the two sites to test the versatility of the interpretive process, and to develop some initial interpretations of the factors controlling feed zones at both sites.

The study found that the two sites shared similar structural attributes, both sites are in a transtensional basin, a result of strike-slip and normal faulting processes. Tauhara has permeable lithologies which are subject to caldera collapse structures, particularly at the caldera margins. There is also evidence to show that interaction between the Taupo Volcanic Zone (TVZ) and North Island Shear Belt (NISB) provide key pathways for the circulation of hydrothermal fluids. Muara Laboh has some permeable strata but circulation is more reliant on fracturing proximate to the faulting within the pull-apart basin, with limited areas of hydrothermal circulation. There is still an opportunity to build on this framework, by improving the technical accuracy of the models (for example if more wells are drilled at the sites) and developing additional components in the combined models (for example pressure and alteration).

Table of Contents

Table of Figures

Acknowledgements

A huge thank you to my supervisors, Marlene and Jim for their help throughout, not only the MSc, but the PMEG too. Marlene, thanks for keeping Jim and I under control, making sure that whatever we were plotting was realistic, and for always managing to give great feedback, no matter where you were in the world. Your passion for teaching and education is obvious in your work, it was no surprise when you won the UC Science Teaching Award earlier this year. Jim, your wisdom, encouragement, and unrelenting support throughout the project has been vital. Your encyclopedic knowledge of the TVZ and all things volcanic has been invaluable. I'd say it's about time we catch up for a beer at the staff club.

Jeremy O'Brien, Brennan Williams and the Seequent team: thanks, for your endorsement for the Callaghan Fellowship, for helping me get set up with the software and your patience teaching me how to use it.

Thank you to Fabian Sepúlveda and Contact Energy, Novi Ganefianto, Marino Baroek and Supreme Energy, for your valuable data, support and advice over the last 12 months.

Thank you to Callaghan Innovation and MBIE for your funding throughout the year.

Thank you to the friends I've made during my adventure through student life. To my mates in room 466, I'm sure now that I'm gone, you'll be able to actually get some work done. Becca and Geena, thanks for all the rides to and from uni. You're the best, did I ever tell you that? It's been real.

Lastly, thanks fam: Mum, Dad, Mitch, and the animals. Mum and Dad for the Sunday Skype sessions to catch up on our respectively unexciting lives, making sure that I'm going alright, the supply packages, and the visits. Thanks, mum, for somehow managing to find, and send me, every new news article about advances in the geothermal industry. Mitch, I'm looking forward to the day when you can't give me grief about being the only one with a full-time job. See you soon.

1 Introduction

There is evidence for both spatially heterogeneous and dynamically evolving permeability in high temperature geothermal systems (Siratovich et al., 2016). This is exhibited at the surface by alteration and surface manifestations which are the surface expression of the high temperature reservoir below (e.g. Lagat, 2007). The nature of the alteration and the chemistry of the springs give indications of the potential temperature of the deeper resource and fluid composition. The spatial distribution of thermal features can give insight into the nature of permeability below the ground (e.g. faults, permeability caps, etc.) (Majorowicz, & Embry, 1998; Mayer et al., 2016). Exposed extinct systems, likewise, give insight into permeability evolution through time and alteration stages which may have been present when the geothermal system was active (Mordensky et al., In Press).

This study will characterise the relationship between fluid flow and hydrothermal alteration in two different geologic settings; one in a caldera rift basin in the Taupo Volcanic Zone (TVZ), the other in volcanic highland straddling the Sumatra Fault Zone in Indonesia, using current literature with subsurface geological data and fracture analysis. This study will shed light on the discrete nature of fluid flow in geothermal systems near large structures, and the more homogenous but unevenly distributed nature of permeability in a caldera-rift type environment (Spinks et al., 2005; Hurwitz et al., 2007).

3D modelling will help to understand the shape and nature of the different hydrothermal alteration zones, give context to the equilibrium state of the systems and indicate the typical shapes of permeable high temperature zones associated with high temperature geothermal systems in the different geologic settings.

1.1 Geothermal Systems

A geothermal system is characterized by its heat source, the composition of the circulating hydrothermal fluids, and the geology that the system is active within (Boden, 2016; Rosenberg, 2017). These systems are a result of 10 to 100 ka of evolution and will likely have experienced many different geological phases or processes - most of which can be traced/interpreted (Oze et al., 2017). The term geothermal field is used to describe the anthropogenic features/structures built round/within the system.

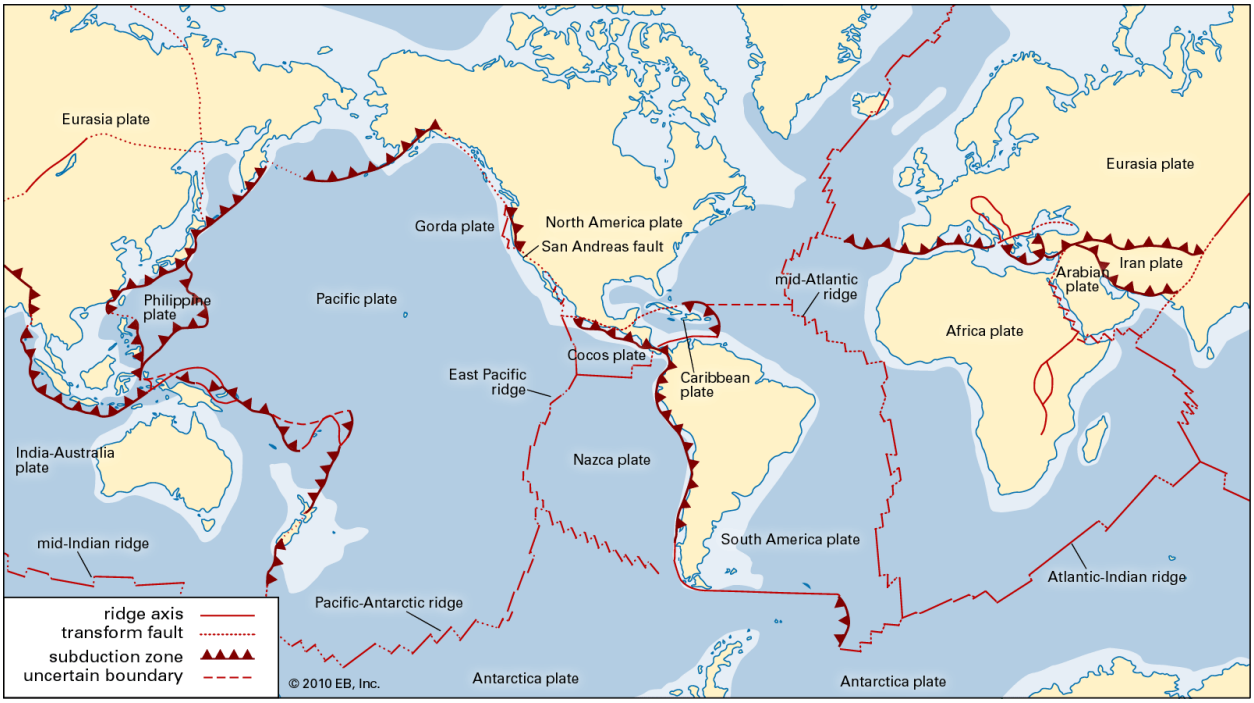

Figure 1.1: Global plate boundaries. Retrieved from https://www.britannica.com/science/world-map

Geothermal reservoirs are more frequent at plate boundaries (See Fig 1.1); areas where magma is shallow, or the crust is more permeable, and display higher temperature gradients (McClintock et al., 2016; Stelling et al., 2016) (Fig. 1.2). Geothermal systems contain fluids that circulate through permeable strata & faults and will typically have an insulating rock to entrap heat. A heat source, recharge fluids, permeable rock, and enough time for heat transfer over a large enough area, are the prerequisites for a geothermal system. Most geothermal systems therefore relate to late stage magma intrusion into the upper crust, and many are related to resurgence (Kennedy et al., 2018). However, where there is a high rate of extension, as in the TVZ, resurgence may not occur. Geothermal systems are not located in the most recent areas of volcanism, instead they seem to be much more controlled by macrostructures (Wilson & Rowland, 2015).

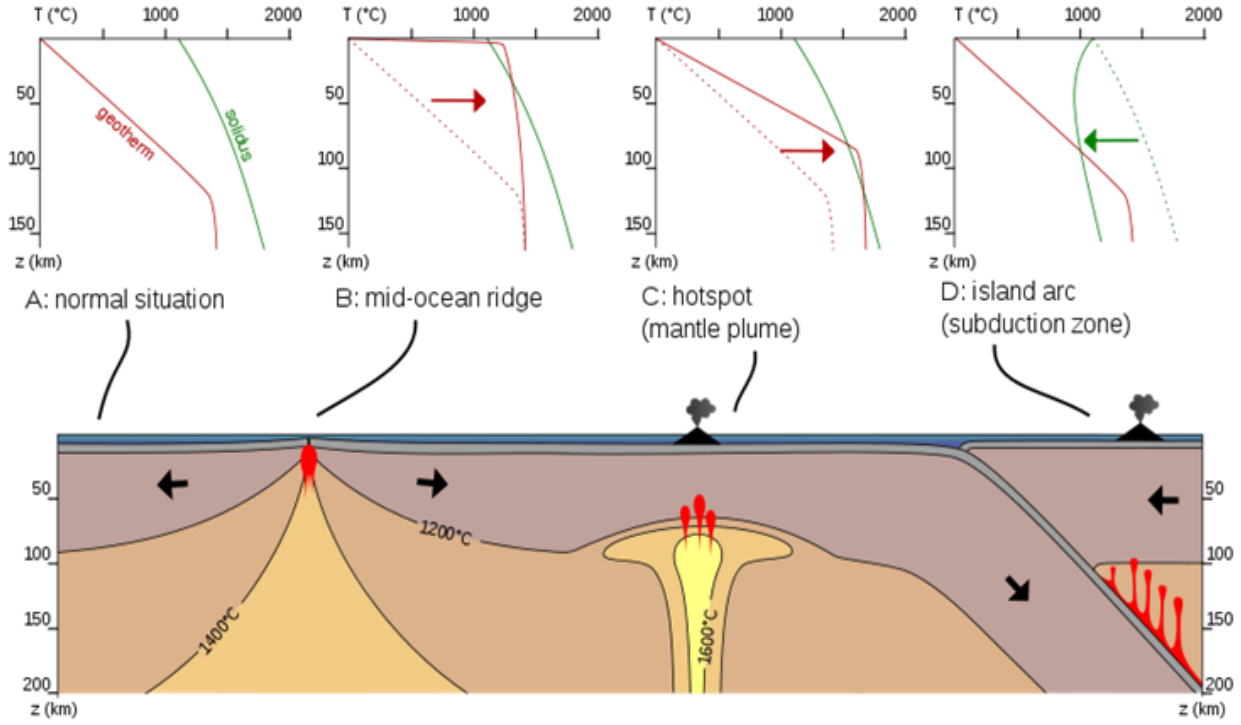

Figure 1.2: A geothermal system requires high temperatures exceptionally close to the surface. This shows how different setting effect geothermal gradients. The geotherm represents the natural rate of change in temperature. The solidus represents the temperatures where a rock will begin to partially melt. Sourced from https://commons.wikimedia.org/wiki/File:Partial_melting_asthenosphere_EN.svg

1.2 Components of a Geothermal Reservoir

1.2.1 Geology

Intrusive events are understood to be a result of buoyancy disequilibria (Wyering, 2015). Local stress patterns dictate the intrusions position within the strata as well as the geometry. The resulting bodies are typically either planar or amorphous. The introduction of hydrothermal fluid and alteration is commonly associated with intrusions/intrusive events and are the source of heat in a convective geothermal system (Stimac et al., 2019) (Fig 1.3).

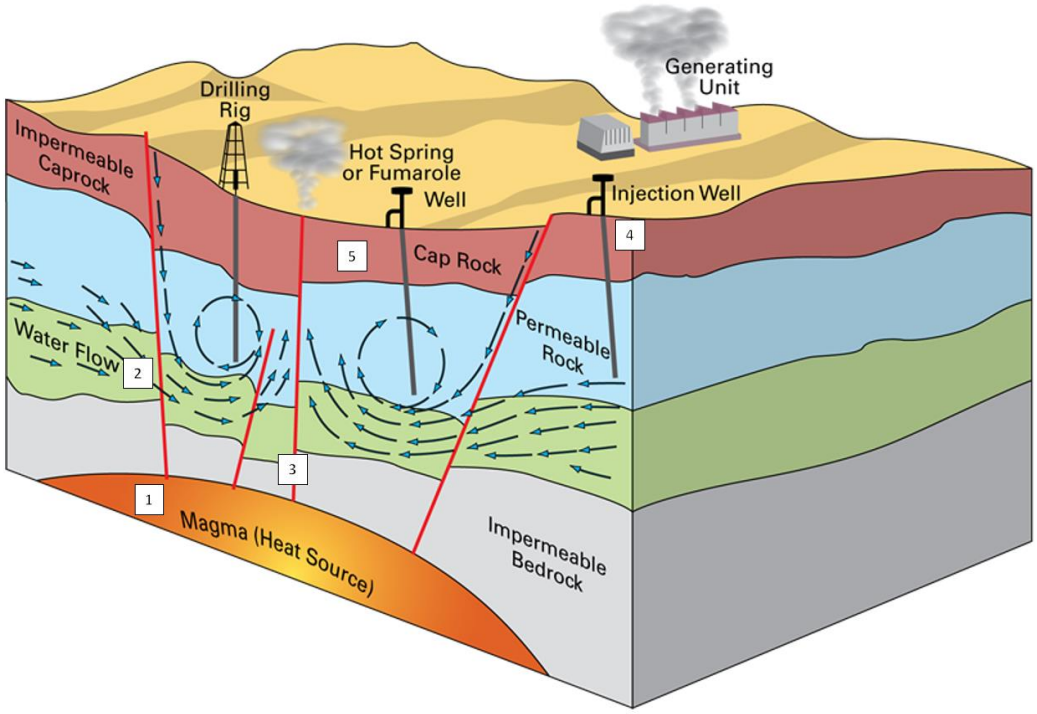

Figure 1.3: A typical convective geothermal system. Numbers refer to parts of the system discussed in the text Retrieved from: https://www.bgs.ac.uk/research/energy/geothermal/home.html

Both Tauhara and Muara Laboh are established hosts of convective geothermal systems (Fig. 1.3), fulfilling several geological features required for this type of system (Grant & Bixley, 2011; Truesdell et al., 1995): 1. Hot magmas transfer heat through geology to heat up circulating water. The magmas undergo circulation as well, maintaining high temperatures throughout the life of the reservoir; this is necessary as the temperature of a non-circulating magma (e.g. an intrusion) will eventually reach equilibrium with the local geothermal gradient. 2. Cold water infiltration (usually meteoric) permeate down through areas of high permeability e.g. 3. faults, fractures or permeable rock (Ármannsson, 2013) ,, this process is called reservoir replenishment and can carried out anthropogenically using injection wells 4. in cases of reservoir exploitation (e.g. hydrothermal power generation). The cold water is heated and chemically interacts with magma, becoming a hydrothermal fluid (Browne, 1978, Browne). Hotter, they are more buoyant and rise to the top of the reservoir, also using permeability features as flow pathways. In most cases the hottest temperatures are at the center of the reservoir, as the outer margins are cooled by the replenishing waters. 5. Cap rocks are another feature of most, but not all, geothermal systems (Grant & Bixley, 2011) and have been measured at both Tauhara and Muara Laboh (Rosenberg, 2017). These zones of impermeable rock

such as clays that form the constraints of the reservoir. Clays have high surface to area ratios; this gives them higher electrical resistivity (measured as Ohm-metres or Ω·m) than most other types of rock. As clays are highly impermeable, resistivity surveys can be used to deduce areas of low permeability in a reservoir and can be used to identify lateral and vertical reservoir extents using electrical conductivity (resistivity) surveys (Bibby et al., 2009.).

1.2.2 Permeability

Microstructures refer to the small-scale structures of a rock mass that allow fluid to pass through. This is typically expressed as effective porosity or matrix permeability. Microstructures also include geometry and rock texture, which is especially relevant for geothermal veining. These features are useful for making inferences about a range of system characteristics, including paleo flow, metamorphism and mineralization. Oliver & Bons (2001) provide a classification system which can be used to describe the relationships between observations, and the suggested orogenic environment. Recent studies by Siratovich et al. (2016) and Cant et al. (2018) have demonstrated the relationship between fracture and pore-based permeability at Rotokawa geothermal field.

Response of permeability to confining pressure is partially due to the internal rock textures, which cause variability in pore architecture. Cant et al. (2018) suggest that there are distinct relationships between permeability and confining pressure which are a function of the pore shapes and textures within the rock.

Convective flow in a geothermal system radiates away and upwards from the intrusive heat source (Fig. 1.3). This occurs more effectively in a host rock with higher permeability, typically in coarser grained materials, but can become reduced by fine grained material, like silt or mudstones. Flow can, however, still occur in materials comprised of lots of thin layers (Lagat, 2007) with open bedding planes.

Faulting is largely related to the tectonic structure and history of the area. Most geothermal areas, including the two study areas, are related to extension, and many are in rifted arcs, such as the two areas of study.

- *Temperature* - This has the largest influence on alteration. Mineral-forming or altering reactions occur at specific temperatures. Minerals are most stable at their formation temperature.
- *Fluid composition* - Elements and minerals available in the fluids and its pH control alteration rate and type.

- *Pressure* - Geothermal fields are typically low-pressure environments. This limits any metamorphic style alteration. The main influence of this is to maintain high-temperature groundwater and hydrothermal fluids in liquid form.
- *Porosity/Permeability* - This controls the area of the rock that can interact with the fluid, and provides space required for mineral precipitation/deposition.
- *Duration* - There should always be a start and end of a geothermal system. Extinct geothermal systems occur where there is no new introduction of heat. Active systems at active plate boundaries may have regular heat addition.

1.3 Aims and Objectives

The techniques described in this section seek to answer the outlined objectives - considering the limitations of the project. The objectives are:

- Review available literature and collect data
- Use Leapfrog Geothermal software, provided by Seequent, for model input and assessment
- Use Data, provided by Contact Energy and Supreme Energy, to develop auxiliary models. These will be used to assess the geothermal properties of each reservoir.
- Establish relationship between geology, temperature and feed zones
- Compare the two sites to better understand controls on geothermal systems.

1.4 Scientific Merit

Global warming and the goal established by many governments worldwide to reduce carbon emissions provides incentives for the development of renewable energy projects.

Geothermal power generation has disadvantages but can be highly effective in the correct context (Hammons, 2004, White & Chambefort, 2016). Limitations include the requirement for a geothermal reservoir as well as the initial setup costs. Reservoirs are typically only located at tectonic plate boundaries, or in areas where the Earth's outer crust is thin. An advantage is their ability to produce base power regardless of weather conditions (Ellabban et al., 2014).

The overarching aim of this project is to develop methodologies that can be applied to better constrain areas which exhibit geothermal potential. Results will include identifying temperature gradients, permeability, flow rates, structural geological features, and fluid pathways. Understanding these features

and their relationships to one another will be applied to the 3D models created. These models will help improve the operation of the existing field at Tauhara, help plan developments at Muara Laboh, and be useful elsewhere for a better understanding of geothermal systems.

McClintock et al. (2016) estimates an additional 3600 MW of available power within the TVZ, but currently only 854 MW is utilised for power generation. The locations of geothermal reservoirs within the TVZ make generation and distribution more practical than the current transport from hydro power systems in the South Island. The geothermal fields are also used as a direct heat source in small quantities in the central North Island timber and tourism industries and provide a minor contribution to domestic heating (Ministry of Business, Innovation & Employment, 2016).

Indonesia is estimated to have the largest geothermal potential in the world Balat et al., 2009; Pambudi, 2018)). Approximately 1.1 - 1.3 GW of a 28.5 GW potential geothermal resource is currently used for power generation and there are government plans to increase the resource utilization to 12.3 GW by 2025 (Ellebban et al., 2014; Beereport et al., 2011).

2 Study areas

2.1 Tauhara

2.1.1 Regional setting

The Tauhara geothermal field is located within the Taupo Volcanic Zone (TVZ) (Fig. 2.1). The TVZ is a back-arc basin, formed due to subduction of the Pacific plate below the Australian plate (Fig. 2.2). Extension in the TVZ ranges from ~7mm/year (in the south) to ~15mm/year (in the north) (O'Brien, 2010, Wilson et al., 1995).

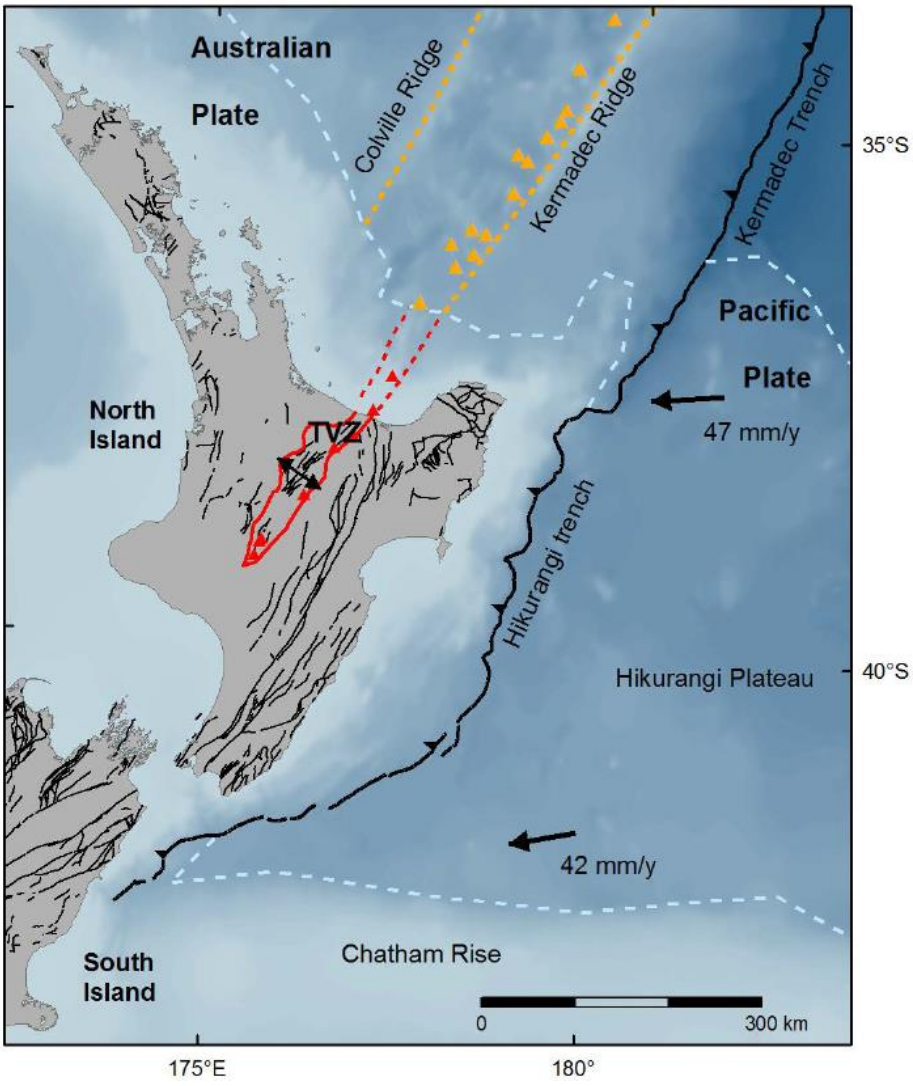

Figure 2.1: Tectonic features of the North Island, New Zealand (Rosenberg, 2017). The black lines within the Taupo Volcanic Zone (TVZ) margins represent the TVZ extensional faulting system, the North Island Shear Belt (NISB) strike-slip faulting is not included.

The central part of the zone is dominated by eight predominantly silicic calderas (Cole & Spinks, 2009; Wilson et al., 1995; Wyering, 2015), and most of the geothermal areas are related to these (Fig. 2.3, 2.4). Davidson (2014) notes that the highest flow rates are observed close to caldera margins. In the TVZ the main graben faults are NNE-trending, a result of the extensional. There is evidence of cross fracturing due to the North Island Shear Belt (NISB) which may also have an influence on permeability (Cole, 1990; Jasim et al., 2015; Seebeck et al., 2014; Spinks et al., 2005; Sepúlveda et al., 2012).

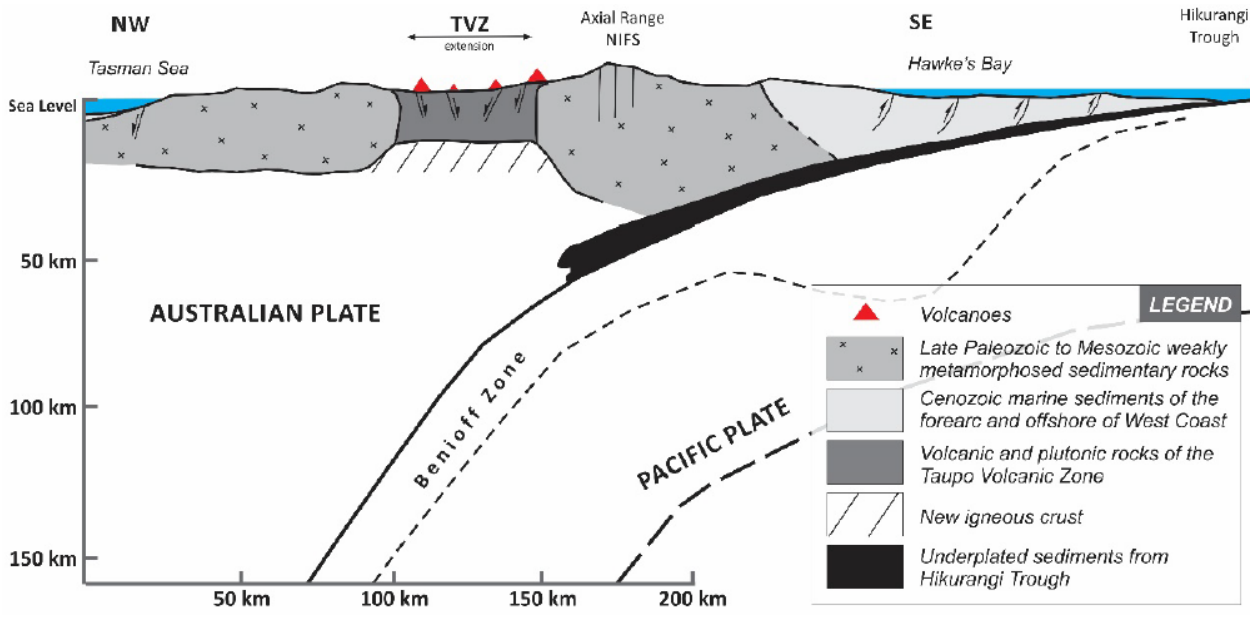

Figure 2.2: Tectonics of the North Island/TVZ (Nemeth & Kosik, 2019)

The TVZ is host to at least 20 geothermal fields, with the central part of TVZ containing a much greater proportion of higher temperature geothermal systems (Fig. 2.3) associated with the rhyolitic volcanism (Davidson 2014, Milicich, Bardsley et al. 2014). Wairakei-Tauhara is one of these systems, with Tauhara being the eastern/south-eastern section of the field (Fig. 2.4).

The central section of TVZ is dominated by rhyolite volcanoes, although there are some small andesitic volcanoes along the eastern side of central TVZ, while the northern end of TVZ is again dominated by andesitic and dacite volcanoes (Cole, 1978; Wilson et al., 1995; Wilson & Rowland, 2015; Ashwell et al., 2013; Davidson, 2014, Milicich et al., 2014). TVZ is currently the most active and productive area of rhyolitic volcanism on Earth, with over 25 caldera forming eruptions in the last 1.6 Ma (Wilson et al., 2009).

The Tauhara geothermal system, which is part of the combined Wairakei-Tauhara geothermal complex, is thought to be >60ka (Rosenberg, 2017). The geothermal system is fed from magmatic and meteoric water and steam. Hydrothermal fluids of greater than 300°C circulate and follow pathways from 3-1 km deep through faulted basement rock, lava bodies and pyroclastics (Rosenberg, 2017). General characteristics of the TVZ include a highly fractured and permeable subsurface, capping structures, proximate to lakes or rivers, and low topographic terrain (Browne, 1984). Of these characteristics, studies carried out by Ratouis & Zarrock (2016) indicate that capping lithologies provide the largest control reservoir development and dictate the geothermal pathways. As well as this, groundwater feeds from the surrounding water bodies contribute to the thermal output, although the effects are only shallow. Local topography also has a major influence on the thermal plume geometry. The margins of the field are marked by the electrical resistivity boundary (Fig. 2.4). Given the limitations of a 12-month project, the study of Wairakei-Tauhara is limited to a portion of the Tauhara area (Fig. 2.4).

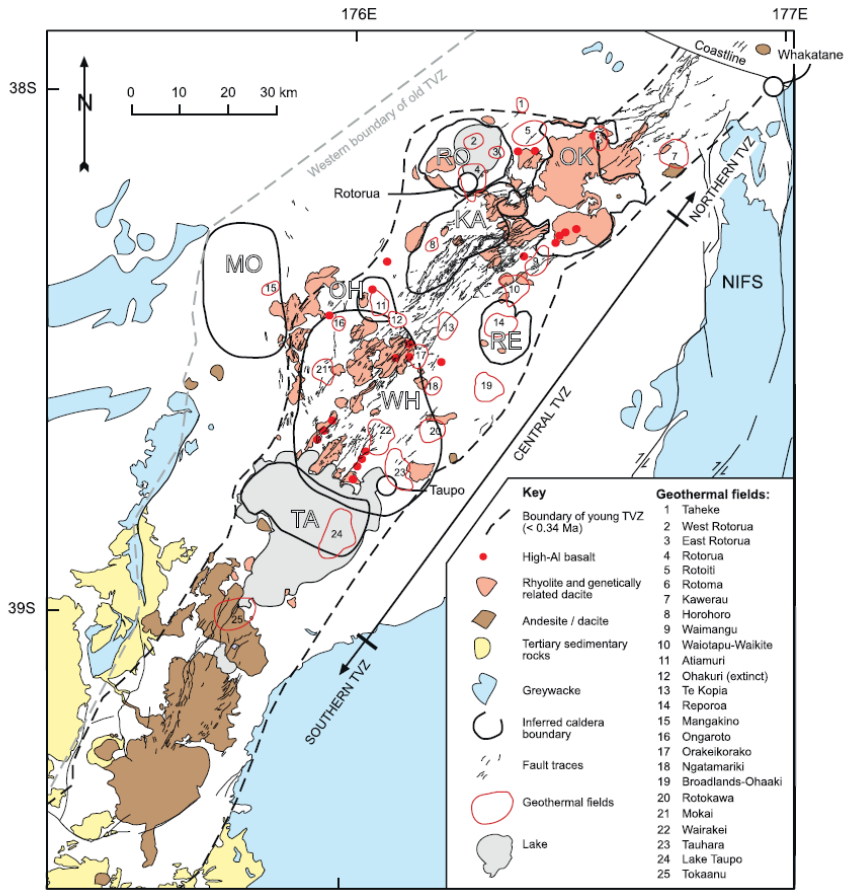

Figure 2.3: The Taupo Volcanic Zone and the associated calderas, faults, geothermal fields, and geology (Wilson & Rowland, 2016).

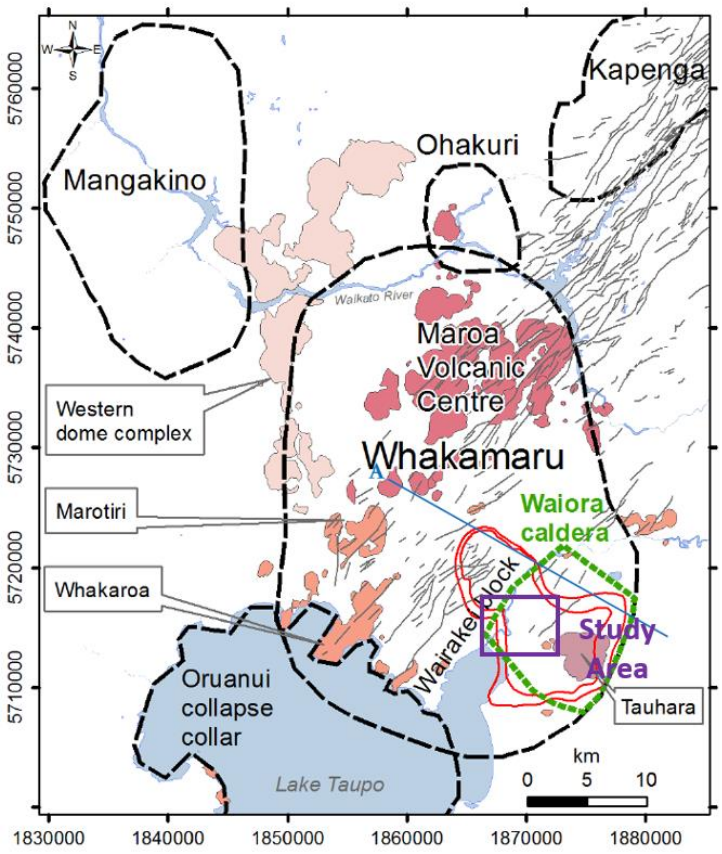

Figure 2.4: The study area (marked in purple). The surrounding red indicates the field's resistivity margins. The Tauhara study area is influenced by the Taupo and Whakamaru calderas. The Taupo caldera is represented as the Oruanui collapse, which is the name given to one event within the Taupo caldera sequence. Likewise, the Waiora caldera is a component of the Whakamaru caldera (2017).

2.1.2 Geology

Extensive drilling in the area means that the stratigraphy of the Tauhara geothermal fields is well known (Bignall et al., 2010; Rosenberg et al., 2009). It comprises a series of predominantly silicic pyroclastic units and lavas which are primarily a result of, and influenced by, Whakamaru and Taupo calderas (Fig. 2.4). This stratigraphy has potentially been affected by caldera margin ring faults and down-sag. An understanding of the geology of the area is important for interpreting the geothermal field. The following unit descriptions (from youngest to oldest) are from Rosenberg et al. (2009) and are summarized in Fig. 2.5 and Table 2.1.

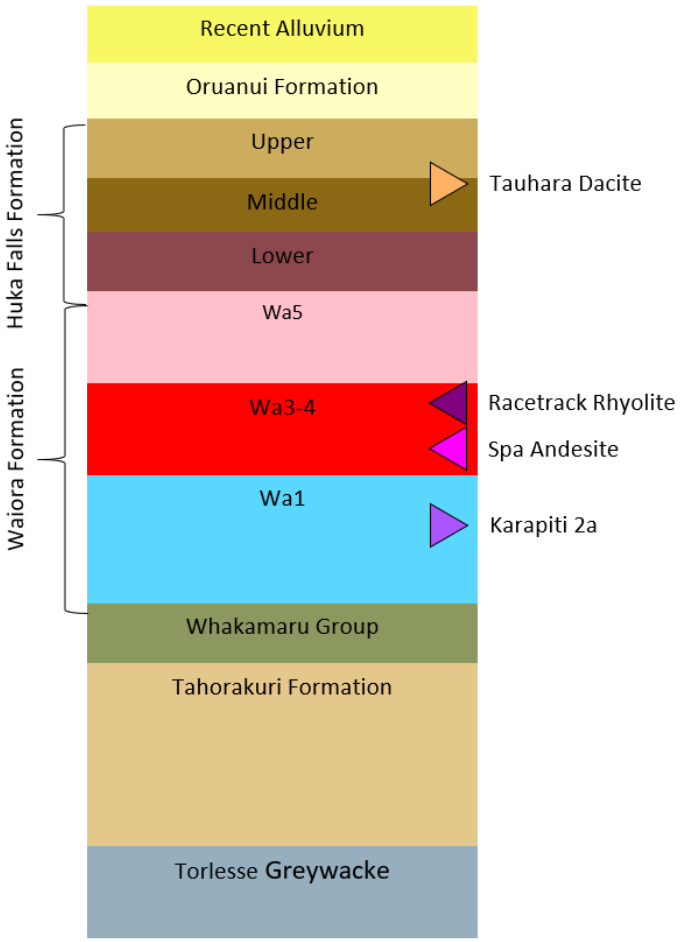

Figure 2.5: Tauhara stratigraphic units. Adapted from Rosenberg et al. (2009).

2.1.2.1 Recent superficial alluvium, tephra & Oruanui Formation

The result of pyroclastic fall, flow, or weathered, older units. The Oruanui Formation and superficial deposits in these areas are up to 60 m thick.

The Oruanui Formation is a single eruption episode from the Oruanui caldera beneath Lake Taupo approximately 26.5 ka. The base is marked by a period of fine ash tuff and accretionary lapilli, followed by pyroclastic density-current deposits interbedded with ash tuff. This formation reaches thicknesses of 120 m in the Tauhara field.

2.1.2.2 Huka Falls Formation

The Huka Falls Formation (HFF) formed in the Huka Falls Lake, approximately 150 ka, before the deposition of the Oruanui. The basin covered 50 km north-east of Taupo, to 20 km southeast of Rotorua, marked by

the Waiotapu geothermal field. The sediments found here are lacustrine and lacustrine-tuffs of variable permeability. Boreholes TH 1, 4, 6, 7, 8 provide some of the best strata and hydrological information on these units. TH 1 and 4 show an absence of the lower layers; showing a quartz-phyric rhyolite breccia instead. Sandstones, siltstones and mudstones make up the upper and lower units of the HFF. These are separated by a variable section of unconsolidated pumice-vitric tuff, pumice pebble conglomerate and reworked ignimbrites. These units thin out toward the south and west. Another control on thickness is the Karapiti rhyolite dome where the sediments are crosscut by the older dome. This dome reaches a shallower depth than these units (Cattell et al., 2016).

The eastern margins of HFF at the Tauhara field contains a volcanic-volcaniclastic sedimentary progression. The units found here are mudstone, muddy sandstones, coarse tuffaceous sandstone, and coarse pumice-lithic breccias. The finer lacustrine sediments are representative of middle and lower HFF, whilst the coarser materials are most like the Waiora Formation, specifically the tuff layers, occuring in layers greater than 350 m thickness.

2.1.2.3 Mt. Tauhara Dacite

Mt. Tauhara dacite is a group of combined composite lava domes, associated breccia, and pyroclastic deposits. The age of these units is uncertain, but they are older than the Huka Falls. Dacites to the north, northwest and south of Mt. Tauhara might provide hydrological pathways for meteoric down flow into geothermal reservoirs or groundwater aquifers.

2.1.2.4 Waiora Formation

The Waiora Formation is a variable sequence of volcanic deposits, interlayered mudstones and sandstones (Cattel, 2015) associated with the Waiora caldera of Rosenberg (2017). There are also several lavas which have their own unit descriptions.

Rosenberg (2017) describes 5 units (Wa1-5) deposited between Wairakei Ignimbrite, and a gradational contact with the overlying HFF. These units are thickest toward the southeast of Tauhara (over 2100 m), and thin to the west of Wairakei (~ 400 m). The five units of the Waiora Formations are not present at every borehole within the Tauhara field. Observations made by Wood (1994) indicate that there is a close petrologic link between the Waiora Formation and the Wairakei Ignimbrites, and that there is also difficulty identifying boundaries between these units.

The Waiora Formation is the key aquifer of the geothermal field. Member 5 ignimbrites contains steam-dominated aquifers, particularly to the northwest of the Wairakei field. The highest temperature fluids are found within the pumiceous breccias within 3 and 4, although the most productive layers are not clear. The siltstones of the member 2 have low permeability and form minor aquicludes. These are most prevalent toward the Wairakei Power Station. An understanding of unit 1 ignimbrites spatial constraints and permeability is limited, but there is a heavy influence of welding on hydrothermal pathways.

There are several rhyolite and andesite units present: Crowbar Rhyolite, Racetrack Rhyolite and the stockyard ignimbrite. These make up from between 1300 to 2100 m of the overall thickness.

2.1.2.5 Wairakei Ignimbrite Formation (Whakamaru Group)

The Wairakei Ignimbrite includes multiple flow units of the Whakamaru Group, and is the name given to the unit within geothermal fields. It is erupted from the Whakamaru caldera. This unit has only been identified in some boreholes in the Tauhara fields. In this thesis the unit is referred to as Whakamaru Group.

Thicknesses and depths vary throughout the area, and the unit does not occur in some places. Some boreholes in this area have drilled through 1100 m of the unit without reaching the bottom contact with the Tahorakuri Formation. Several have drilled up to 2500 m without encountering the Formation at all. South eastern Tauhara wells Whakamaru-type ignimbrites at depths of 1900 m, wells further south reach depths of > 2300 m without making contact. This variability of deposition has been interpreted in several different ways: a fault displaced flat-top pond; a caldera margin; a northwest trending fault; or an east tilted, deeply eroded slab displaced by SW trending Paeroa Fault extension. Drilling indicates a displacement of at least 1500 m in areas that are coincident with the Kaiapo Fault. Other drilling at the Wairakei field confirms that there are major fault structures present. Considering the lack of the unit at areas within Tauhara, it appears that the faulting observed within the two fields may be part of a much larger set of volcano-tectonic structures. New interpretations have been made on local structures. These use well data, geological mapping and seismic data to indicate that there may have been faulting following the Whakamaru Caldera volcanism which would have occurred throughout the deposition of the Waiora Formation.

Permeability is variable within the ignimbrite. However, faulting, fracturing, and other pathways control the flow of hydrothermal fluids. Bixley et al. (2009) observe that flow will follow these structures. The presence of outcropping Whakamaru Group ignimbrites columnar joints in other areas is interpreted to

allow flow along and through this structure. Similar cooling features are predicted to occur within the units at Wairakei-Tauhara.

2.1.2.6 Tahorakuri Formation

Tahorakuri and Waikora Formations are two members of the Reporoa Group (formally named the Ohakuri Group). The Tahorakuri Formation is a ~650 m thick composite of andesitic lava and breccia. There are more layers of this nature in the Tahorakuri Formation than in any other. This formation is strike slip faults, at the Waiora Formation, with sedimentary, volcanic, and volcaniclastic strata. The Waikora Formation is a lithostratigraphic term used to describe a greywacke pebble conglomerate, this is not present at the field.

2.1.2.7 Greywacke Basement (Torlesse terrain) (Inferred)

The Tauhara basement is marked by silicic pyroclastic units intercalated with greywacke sediments and serves as the host of the hydrothermal fluids within the region. This was deposited ~1.8 Ma and is currently at depths of >3 km (Rosenberg, 2017). This unit has undergone strike-slip faulting due to the North Island Shear Belt (NISB) (Cole, 1990). This formation has not been observed in either drill data (up to 2.8km deep) or any outcrops within 30 km of Taupo. Its presence is based on interpretations of seismic refraction and gravity survey data. These also indicate that there are approximately 2.5 km of other units covering this formation.

Table 2.1: Tauhara geological properties. Adapted from Rosenberg (2017).

Units & Formations	Abbreviation	Description	Geothermal Properties	Age (Ma)
Recent Alluvium	R	Quaternary sediments. Some hydrothermal eruption deposits.	n/a	<0.27
Oruanui Formation	OF	Pyroclastic density currents and fall deposits	n/a	
Huka Falls Formation (Upper, Middle, Lower)	HFF	Lower: weakly consolidated silt and sandstone. Middle: Pumice lithics and tuffs. Weak hydrothermal alteration to clay and sericite. Upper: very thinly bedded mudstones and sandstones	Reservoir clay cap	0.22 - 0.025
Te Mihi 4 Intrusive	TM	Weakly altered rhyolitic lava	?	0.31 - 0.35
Racetrack Rhyolite	RT	Rhyolitic fractured coherent lava and breccia	?	0.12 – 0.31
Tauhara Dacite	TD	Superficial Dacite lavas. Highly permeable. Weakly hydrothermally altered.	Meteoric water inflow point	0.25
Karapiti 2a Intrusive	Ka	Highly vesicular top layer. Breccias are associated with highly jointed glassy lava. Lower spherulitic lavas. Denser lavas at the unit base.	?	0.31
Waiora Formation	Wa (1-5)	Pyroclastic flow and fall deposits. Wa5: ignimbrite, highly permeable, pumice breccia, non-welded ignimbrite, tuffs and fine sediments. Wa2-4: pumice breccia, interbedded siltstone Wa1: Course pumice breccia or pumiceous tuff and compact weakly to densely welded ignimbrite.	Reservoir components	0.2 - 0.3
Whakamaru Group	WK	Ignimbrites, andesite lava, strong hydrothermal alteration.	?	0.32 - 0.38
Tahorakuri Formation	THF	Ignimbrite, rhyolitic pyroclastics, tuffs, breccias and andesite lava. Strongly hydrothermally altered. Sediment	Deep Reservoir	0.38 - 1

2.2 Muara Laboh

2.2.1 Regional Setting

Muara Laboh is located on the island of Sumatra, Indonesia, which has a complicated geology, credited to three converging plates: Eurasian (continental; "Sunda"), India-Australian (continental; "Sahul"), and the Pacific-Philippine (Oceanic) plates (Burton et al., 2014). These subduction margins have high rates of subduction, intensive volcanism and intensive seismicity (Hall, 2009). The Muara Laboh geothermal system is in Western Sumatra, where a major control on the geology is the Great Sumatran Fault (GSF). The GSF is a complex NW-SE dextral strike-slip fault (Fig. 2.6), formed between the Indo-Australian and Eurasian plates (Burton et al., 2014). Zones of compression and extension cause horst and graben complexes and are linked to local Quaternary volcanism along the Barisan Mountain Range arc (Mussofan et al., 2018).

Muara Laboh is being developed by Supreme Energy with the intention to become an 80 MW, dual flash geothermal power project (Stimac et.al, 2019). Contacts within the industry have agreed to provide support and available data for us to carry out the investigations necessary to complete this master's thesis.

The Great Sumatran Fault (GSF) is a complex NW-SE dextral strike-slip fault, formed between the Indo-Australian and Eurasian plates Zones of compression and extension create horst and graben complexes and are linked to local Quaternary volcanism along the Barisan Mountain Range arc. The pull-apart basin is located between the Siulak (south) and Suliti (north) Fault segments. The site is interpreted to be under transtension. This is a result of the oblique strike-slip of the GSF combined with normal faulting within the basin. This causes extension and is attributed to local intrusive sequences. The Siulak Fault to the south is associated with the magmatic intrusions that provide the geothermal heat source (Mussofan et al., 2018).

The presence of geothermal activity is indicated at the surface by hot springs, steam, fumaroles and mud pools. Alteration manifests at the system margins as clay caps, there are areas of propylitic and potassic alteration, which along with other mineralogical features, indicate that there have been multiple phases of alteration. Permeability in the Muara Laboh wells is linked to dike intrusions and stock margins (Mussofan et al., 2018; Stimac et. al., 2019; Wisnandary & Alamsyah, 2012).

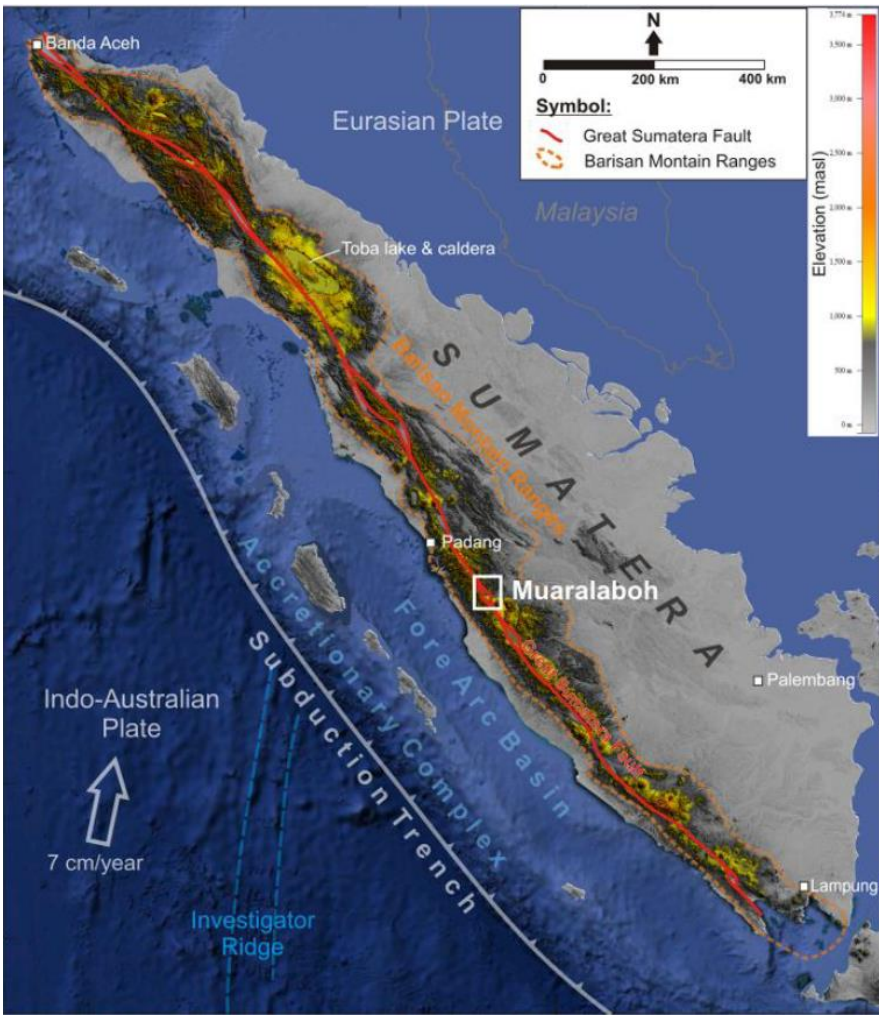

Figure 2.6: Sumatran strike-slip complexes along the Great Sumatran Fault (Mussofan et al., 2018). NB: depending on the literature Sumatra may be spelled Sumatera and Muara Laboh may be spelled Muaralaboh. Sumatra and Muara Laboh have been used in this thesis.

2.2.2 Geology

Surface geology, well data, and geophysical testing have been used to identify the key geological features in the area (Fig. 2.7). Two asymmetric grabens exist to the east and west. The older granites in the area are overlain by andesitic lava and silicic lavas & tuffs. Radio-carbon dating gives an age to the upper sequence of 34 to 41 ka. There may also be some degree of sector collapse and debris flow from the local volcanoes. The geothermal fluids are understood to be related to these volcanic centers (Hochstein et al., 2008; Mussofan et al., 2018).

2.2.2.1 Quaternary Alluvium

Clays, silts and sands formed within the river plains and valleys (Qal). These serve as the reservoir clay cap.

2.2.2.2 Quaternary Volcanic Complexes

The youngest of the Quaternary andesitic igneous units are sourced from Mt. Kerinci, Mt. Kapur, Mt. Anak Patah Sembilan, Mt. Patah Sembilan, and Mt. Banko. These volcanic complexes are andesitic; containing lavas, breccias and tuffs. Quaternary silicic volcanics are predominantly dacitic to rhyolitic tuffs but contain lavas and other volcaniclastic units. The oldest andesitic volcanic sequences are mostly lavas. They also contain pyroclastic materials, volcanic sediments and other sediments. These volcanic units contain the reservoir cap, and host the shallow and intermediate depths of the reservoir.

2.2.2.3 Tertiary Silicic Volcanic Complexes and related intrusions

This formation includes granite (Tgr), granodiorite (Tgdr) and Painan Formation (Tomp). Tgr and Tgdr units are granite and granodiorites intruded into the Horst and Graben faulting which was initiated during the GSF in the Miocene (~13 ma). The Painan formation is made up of andesitic to silicic volcanic units, as well as shale and sandstone sediments. These complexes mark the deepest areas of the reservoir.

2.2.2.4 Mesozoic Granites and Sediments

Mesozoic granites (Kgr) and Siguntur quartzite (Ps). Kgr units are granites which have intruded into the underlying Paleozoic formations. The Siguntur formation is comprised of intra-continent metasedimentary rocks, which have been partially metamorphosed into quartzite. These formations occur within, what is interpreted as, the last period of stability before the activation of the GSF. These exist beyond the margins of the geothermal reservoir.

2.2.2.5 Paleozoic Sediments

Comprised of the offshore Bukit Barisan Formation (Pb, Pbl). Pb describes the phyllite, slate and metagraywacke component, Pbl is a limestone component of the same formation.

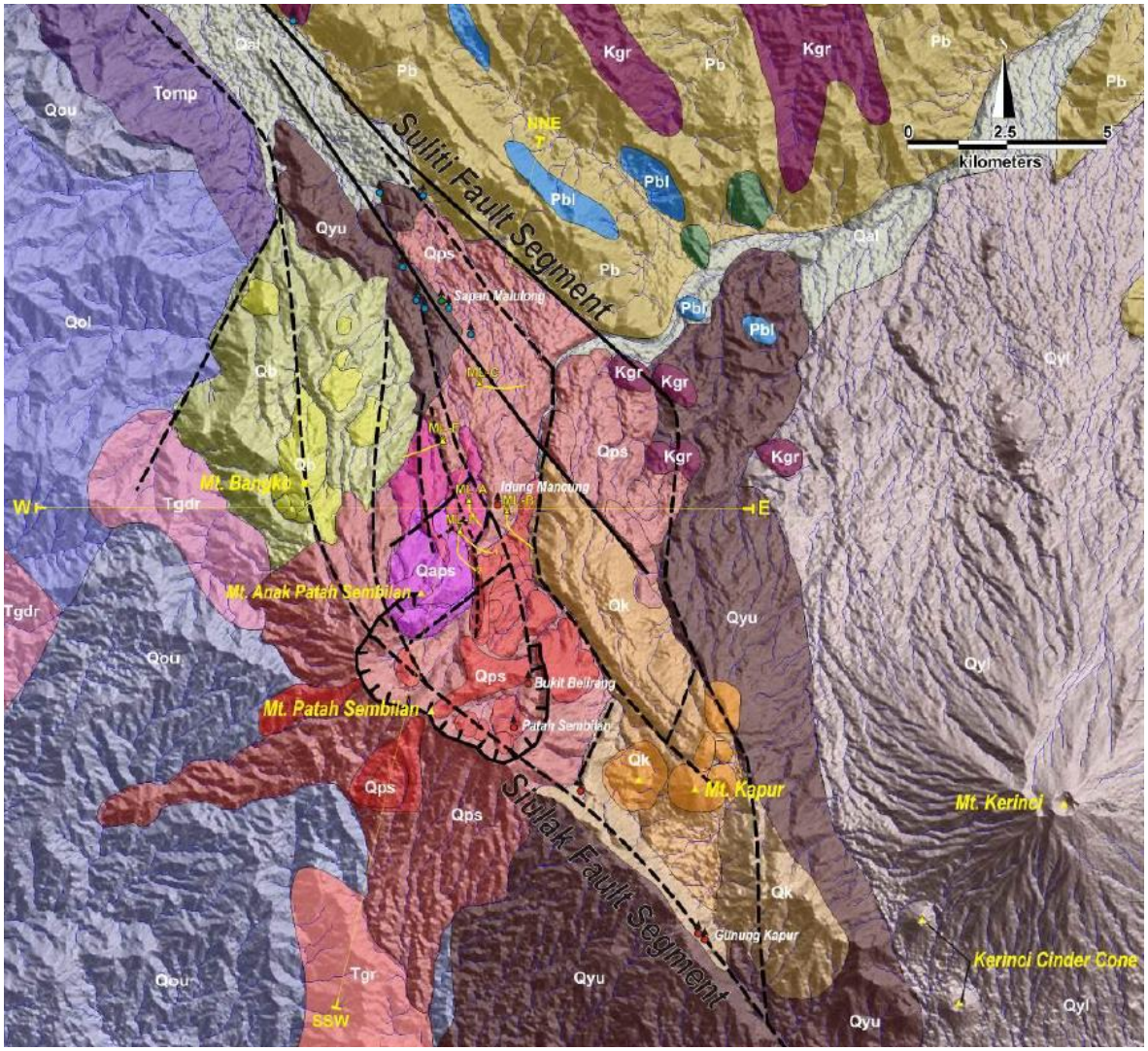

Figure 2.7: Muara Laboh proposed target area. Adapted from Mussofan (2018). Abbreviation references can be found in Table 2.2.

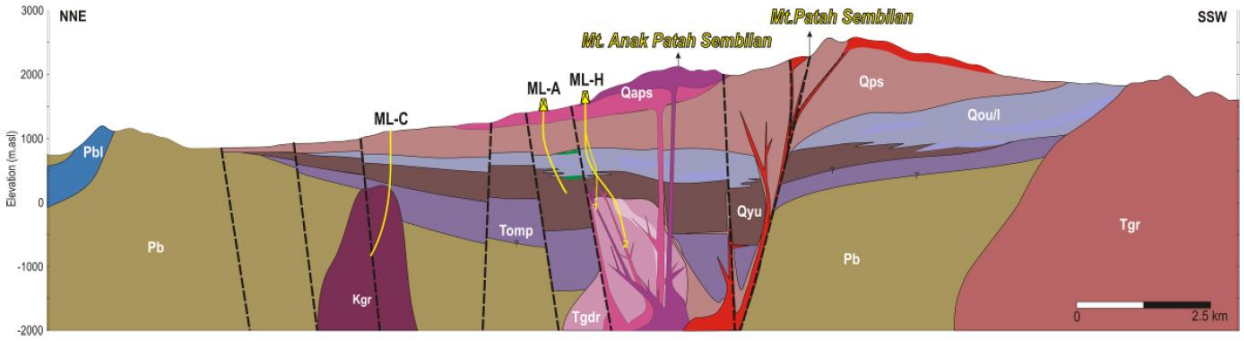

Figure 2.8: NNE-SSW cross section of the Muara Laboh basin. The NNE and SSW points are marked in Fig. 2.7, the unit abbreviation references are available in Table 2.2.

Table 2.2: Muara Laboh Geological units and properties summary. Adapted from Massofan (2018).

Units & Formations	Abbreviation	Properties	Geothermal Properties	Age (Ma)
Mt. Patah Sembilan Volcanics	Qps	Andesite tuffs breccias and lava	Reservoir clay cap	<1.8
Silicic Sequence	Qou/l	Dacite/rhyolite tuffs, lavas and volcaniclastics	Shallow Reservoir/ Intermediate Zone	
Andesitic Volcanic Sequence	Qyu	Mostly lavas, pyroclastics and volcanic sediments. Intercalated with Silicic Sequence	Intermediate Zone	
Intrusive Sequence	Tgdr	Granite and Granodiorite. Intrudes into horst-graben structures.	Deep Reservoir	33 - 5.3
Painan Formation	Tomp	Andesitic and silicic volcanics and shale to sandstone sediments	Deep Reservoir	
Intrusive Granite	Kgr	Intrudes into the Bukit Barisan	Outside reservoir	144
Bukit Barisan Formation	Pb	Phyllite, slate, limestone, metagreywacke	Outside Reservoir	248

3 Methods

Struthers (2017) provided a basic knowledge of the steps involved in a Leapfrog Works modelling project and the techniques used are cross-compatible with the Leapfrog Geothermal processes used in this thesis. The same Leapfrog Geothermal 3.7 tutorial (now 3.9) is used to develop technical modelling skills – how to create specific models and the steps required.

Case-studies and background reading provide an understanding of the general steps involved in the data processing but have limitations. The same applies to understanding which aspects investigated are important and what may not be relevant to completing the goals of the thesis.

Other studies do not always exactly translate to each step of the project, potentially leading to steps that are not necessary or do not provide enough detail of steps that are. This can be addressed with the help of others with experience in these types of project. Individuals with higher levels of relevant educational and/or technical competency are a valuable resource, perhaps the most important; especially their understanding of the "bigger picture", whether it be of the field geology, processes, or a greater fluency in the software. These individuals and parties have been used in this project to make sure that the workflow has been kept on track - specifically in the right direction.

3.1 Leapfrog Geothermal Software

Leapfrog is a 3D modelling software developed by Seequent. Leapfrog *Geothermal* has been developed for the geothermal industry to produce models from a combination of field data and specialist interpretation, including to model sections of the Taupo Volcanic Zone geothermal fields (Alcatraz et al., 2011, Rosenberg, 2018). Models assist engineers and geoscientists to understand the subsurface conditions for long-term field management or continued field development.

The Leapfrog software requires data from surface and subsurface to develop a model. It principally interpolates between data points, but the 3D model provides more accurate representation than previous 2D methods (Alcatraz et al., 2011; Milicich et al., 2014). The input data points may be complex and irregular, but Leapfrog allows users to optimize smooth interpolation surfaces representing key geological features.

Whilst Leapfrog is primarily used to model continuous surfaces, it can also be used to model individual features, lava bodies, intrusions, and other closed surfaces, as well as representing features such as faults, fractured zones, feed zones, and temperature (Alcatraz et al., 2011). These models are then used to

interpret rock mass permeability, and hydrothermal alteration pathways, essential to the development of geothermal modelling. This method of three-dimensional software is gaining momentum as an industry standard.

An advantage of using Leapfrog is the ability to manipulate the model in 3D. Changing the orientation or slicing through the model are easy ways for the operator to interpret the complex geology in geothermal systems. The software can also be used to easily make calculations in any chosen direction (Milicich et al., 2014) and makes the outputs more consistent and representative than two-dimensional analysis. This chapter will describe the tools, data and workflows used in this study.

3.2 Leapfrog Geothermal Model Types

- *Geology Model* – These are created using the Geology Model tool to create a 3D space with set spatial boundaries and fills this space with volumes containing certain attributes. The resulting model represents different attributes, but many attributes share some of the same techniques used to build them. This means that attributes other than geology can be modelled using this process. In this thesis "GM" refers to the tool used to create a model, rather than a model which just represents geology. All GM model figures used in this thesis have 1:1 vertical exaggeration. The GM tool is used to build:
    - Geology models (representing the lithologies, not to be confused with the name of the tool used to make it).
    - Feed zone models (each of the feed zone classes are treated as though they are lithologies using the GM tool).
- *Numeric Model* – Represents how numeric attributes change through space.
    - Temperature models (how temperature changes through space).
    - Distance offset models (establishing distance buffers from given features within a model).
- *Combined Model* – These take a number of geology and numeric model isosurfaces to create a new *combined model*. Up to four models can be combined to create these. These are useful for assessing the geometries or volumes of a target feature, where there are known controls on where that target feature occurs. The controls in this project are temperature, fault offset, and known feed zone occurrence. The target feature is geology i.e. understanding which lithologies occur within the feed zones, a specified temperature isosurface, and a specified fault offset. There are forms of combined model that can be made for each area in this project:

    - Actual models: These are based on feed zone models i.e. where recorded feed zones occur. These feed zone models indicate areas of permeability but are limited by the density and spacing of well measurements.
    - Potential models: These are based on the features that feed zones are hypothesised to occur within. These constraints are used to develop a predictive model of where feed zones could occur.
- *Block Model* – These compare and calculate relationships between many different geology and numeric models. This technique can be used to achieve the same as the combined models but has the benefit of being able to automatically calculate the statistics of any feature against another (restricted to categorical data vs. categorical data, and numeric vs. numeric), including a *resource estimate*. The statistic outputs include:
    - *Table of statistics:* Compares categorical features.
    - *Scatter plot:* Compares two numeric features.
    - *Q-Q plot:* A quantile-quantile figure which compares two numeric features or one feature with two filters.
    - *Box plot:* Compares categories for single numeric features
    - *Resource Report:* Typically used in the mining industry, this tool is used to find the relationships between categories and numeric data within a target resource's geometry/volume
- *Refined Models –* The difference between a *combined model* and a *refined combined model* is the fault offset data that they use, the refined model uses values calculated using the block model tool and has equivalent potential and actual models.

3.3 Data

The many types of data used in this project are from different sources and are in different formats (Table 3.1). Literature was collated at the start of the project to complete the initial objective of the project. This step is important to understand current knowledge about the areas studied and provides a significant component of input data, usually in the form of interpretive data such as maps and cross-sections. In addition to literature, developer and operator data were also obtained. Well data is the most common, provided as tables (.CSV files) and provides coordinate, survey, interval, or point data. The coordinate data describes the locations of key features - typically well collars or well trajectory. Orientation data describes

the dip and dip direction of the well. Interval data describes categories such as geological units, alteration types, and feed zone intensity, from one depth to another along the well. Point Data describes numeric features at certain points along a well e.g. temperature data. Well locations and maximum depth measurements are available in appendix A.

*Table 3.1: A summary of required data types for modelling. Adapted from Alcaraz et al. 2010. * = Manually created during the modelling process*

Data Type	Data
Imagery	• Maps (including geology and structural) • Structural mapping (faults) • Georeferencing • Projection systems • Geology cross-sections
Borehole data	• Collar • Survey • Intervals (geology, alteration, etc.) • Alteration & geological descriptions
GIS data (points*, polylines*, structural disks*)	• Surface Geology • Geothermal surface expressions • Fault orientation • Points of interest • DEM data
Numeric data	• Temperature

3.4 Input Models

There are different tools and features within Leapfrog that create the input models required to create the result models and other outputs which are used to answer the thesis objectives (Fig. 3.1). Primary models are those which are based solely on the input data. Secondary models are comprised of additional input data, combined with primary input models.

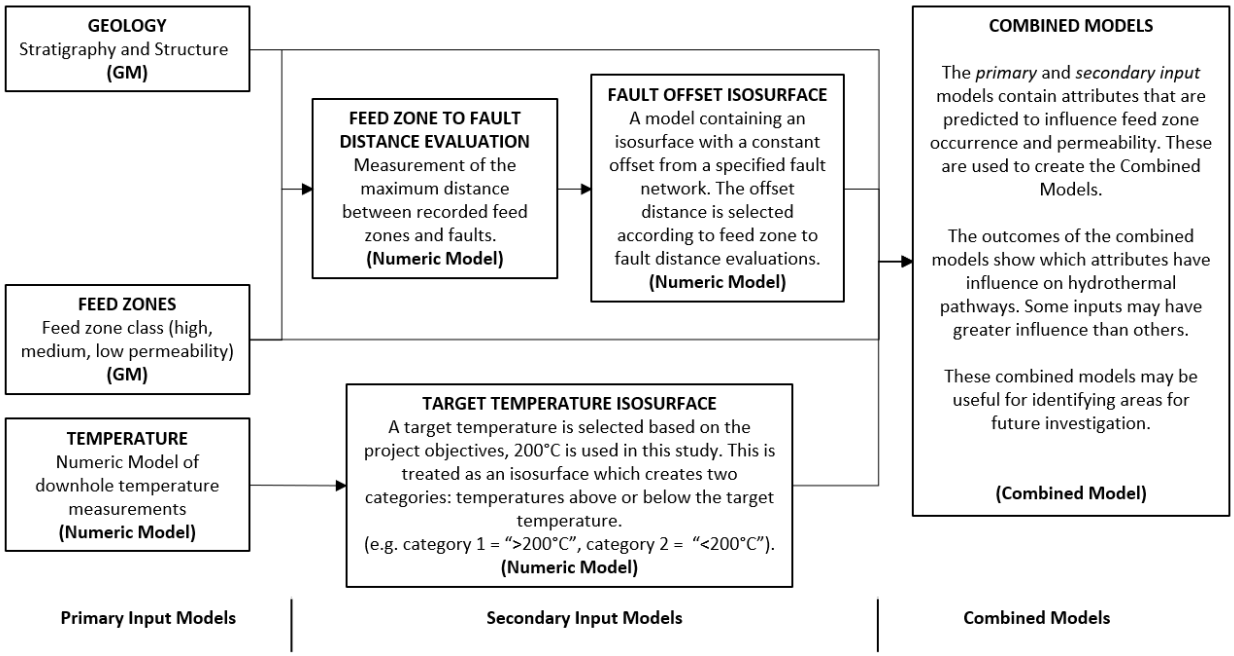

Figure 3.1: The assessment process from start to finish. Primary input models are those based on raw data: well logs, figures, temperature measurements. Secondary models are those that are based on some type of assessment/processing of the primary models. The result models are used to understand the nature of feed zones and permeability within the target area. GM, Numeric Model, and Combined Model refers to the tool used for each respective step

3.5 Geology

An initial geology model serves as the basis for later modelling. Unfiltered well geology interval data is selected as the base geology for the geology model, with the model extents set vertically and horizontally to include and extend partially beyond the well data. Having set the model boundaries, the features within it are introduced. In Leapfrog, geology is introduced as surfaces between units, as opposed to as individual units. This requires an understanding of how the units form and their relationships with surrounding units. Much of this information is found within literature or apparent from the unit's appearance in well logs.

The original description and rock type columns in the well logs were interpreted by using a dedicated naming scheme to create a "default stratigraphy" column (Table 3.2, Fig. 3.2). Some of the lithologies described in this column did not provide enough resolution for the purpose of this project and were subdivided or joined by assessing the rock type and descriptions to make more suitable classifications that were consistently applied to each well log ("revised stratigraphy" column; Table 3.2, Fig. 3.2). The Interval Selection tool can then be used to select segments along a well and assign the interval to an existing or new lithology category.

Table 3.2: The left-hand side of this table show all the geological description data that is available (i.e. Default Stratigraphy). These are used to make the unit interpretations on the right-hand side (i.e. Revised Stratigraphy).

From (m)	To (m)	Description	Rock Type	Default Stratigraphy	Revised Stratigraphy
0	20	-	No returns	No returns	Recent Alluvium
20	46	-	Alluvium and tephra	Superficial alluvium and tephra	Recent Alluvium
46	116	-	Pumice-lithic-crystal tuff	Oruanui Formation	Oruanui
116	228	-	Sandstone and siltstone	Huka Falls Formation	Huka Falls Formation (Upper)
228	290	Pumiceous tuffs and minor siltstones	Tuff	Huka Falls Formation	Huka Falls Formation (Middle)
290	382	Rhyolite breccia and rubble	Lava and breccia	Rhyolite Breccia	Waiora Formation (Wa5)
382	500	Complex mix of muddy tuffs, silicified mudstone and rhyolitic debris	undifferentiated volcano-clastic deposits	Waiora Formation	Waiora Formation (Wa5)
500	560	Rhyolite lava interbedded with pumice breccia at 544 m	Lava and breccia	Karapiti 2a Rhyolite	Karapiti 2a Rhyolite
560	600	Tuffaceous muddy sandstone	Sandstone	Waiora Formation	Waiora Formation (Wa5)
600	750	Predominantly fine-grained muddy sediments	Siltstone	Waiora Formation	Waiora Formation (Wa2-4)
750	924	Variable bedded tuffs of ignimbrite origin mixed with coarse sediments (including breccia-conglomerate)	Undifferentiated. volcano-clastic deposits	Waiora Formation	Waiora Formation (Wa2-4)
924	1207	Pumice-crystal-vitric tuffs. Ignimbrites (more than one flow sheet)	Ignimbrite	Waiora Formation (Wa1)	Waiora Formation (Wa1)

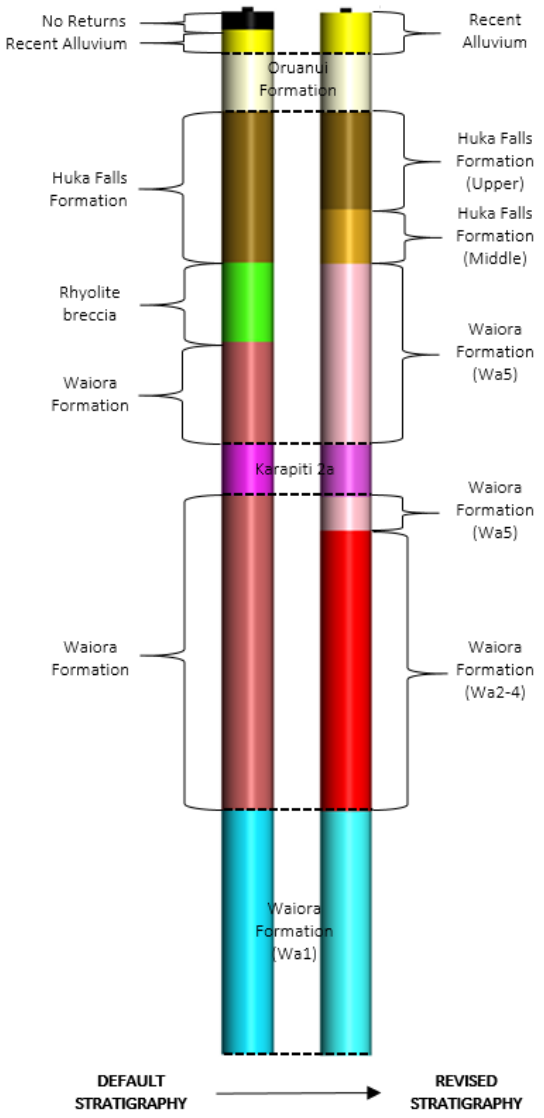

Figure 3.2: The default and revised well nomenclature for TH02 at Tauhara geothermal field. This process was used for each well to ensure consistent nomenclature across the field.

Once the well lithology data was input into the geology model, imagery data (mostly geological maps and cross sections) were imported as *maps* to improve the model representation. These were manually georeferenced using six points, three on the image to be imported, and three corresponding points on the model. This process gives these points specific XYZ coordinates (X&Z are the lateral coordinates, Z represents elevation). The further apart the points are from one another the more accurate the georeferencing will be. This works for horizontal maps but does not apply to cross-sections.

Cross-sections were imported using the *cross-section* feature built into the software. This process follows the same six–point technique as the surface mapping. Georeferencing relies on knowing two points at the

surface that can be identified top-down on previously imported maps, and as a third point at a known depth. Identifying the top two points can be difficult but faults provide reliable reference points. A third point needed to be identified at depth below one of the first two points (i.e. the same XY coordinates) are the same as one of the surfaces. In cases where it is unclear which selectable start and end locations to use, approximate points are used initially based on orientation, geology and surface features. Improvements are then made by comparing the topography in the Leapfrog model and the topography of the cross section with manual adjustments to the selected points to align the two topographies.

Having imported well logs, maps, and cross sections, multi-dimensional constraints are formed, and the contact surfaces between the lithologies developed. The best results are obtained when the surfaces are assigned either oldest to youngest or vice versa – ensuring that they are in the right sequence within the s*tratigraphic sequence* section. Each contact surface represents a relationship between two or more lithologies, making it important to understand the nature of these contacts – either from reading literature or from an interpretation of the well logs. By default, the surfaces are created using only the well data. For the context of this project, the type of contact impacts more than the geometries. There are three main contact surface types; the following descriptions are of the default outputs, all of which can be modified using the tools and techniques described (Fig. 3.3):

Depositional – The surface will not cut younger contact surfaces and will tend to create more linear surfaces.

Erosional – The surface will cut any older contact surfaces. These will also tend to create more linear surfaces.

Intrusive – The surface will ignore (cut) any older contact surfaces. These will create more spherical geometries.

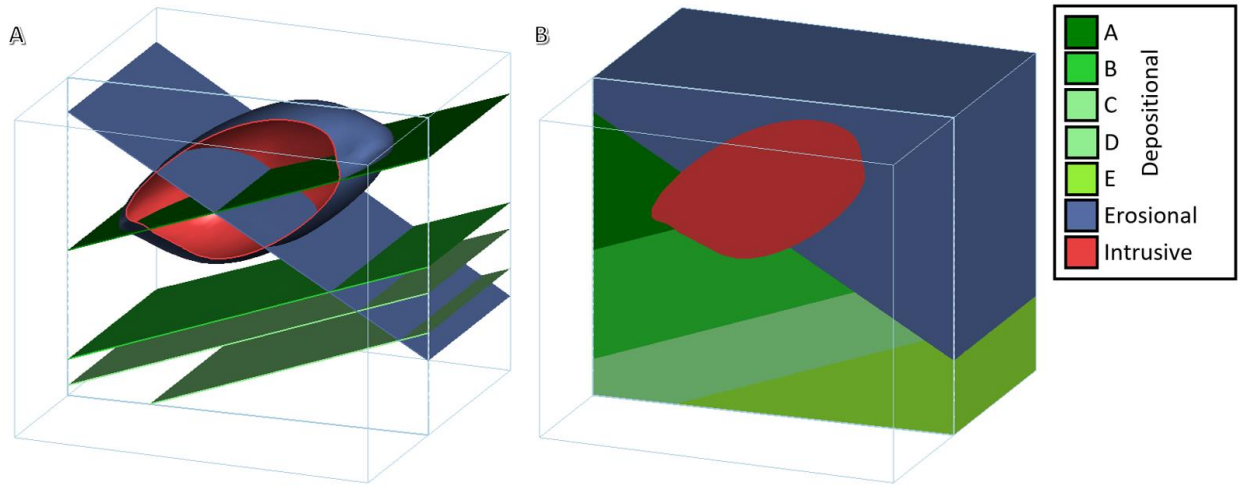

Figure 3.3: Schematic of the different types of contact surfaces used in this project (adapted from the Leapfrog Geo tutorial, Seequent). The planes in A represent contact surfaces between all the units. In this example the green units are a depositional sequence and are emplaced one on top of another, leaving each of the previous units intact. These are crosscut by the erosional surface (blue). These have all subsequently been intruded into by the intrusive unit (red). B shows the resulting volumes of each of the units once the surfaces have been "activated".

Once a basic geological model has been completed the faults are added. Muara Laboh is used to demonstrate the fault modelling process. The first step requires geological maps, which include fault traces, to be draped over the topography (Fig. 3.4). Polylines are drawn on the geological model along the fault traces. The term polyline describes a continuous line made up of connected line-segments. This automatically generates a fault plane for each fault, but these are inactive and do not yet affect the geology.

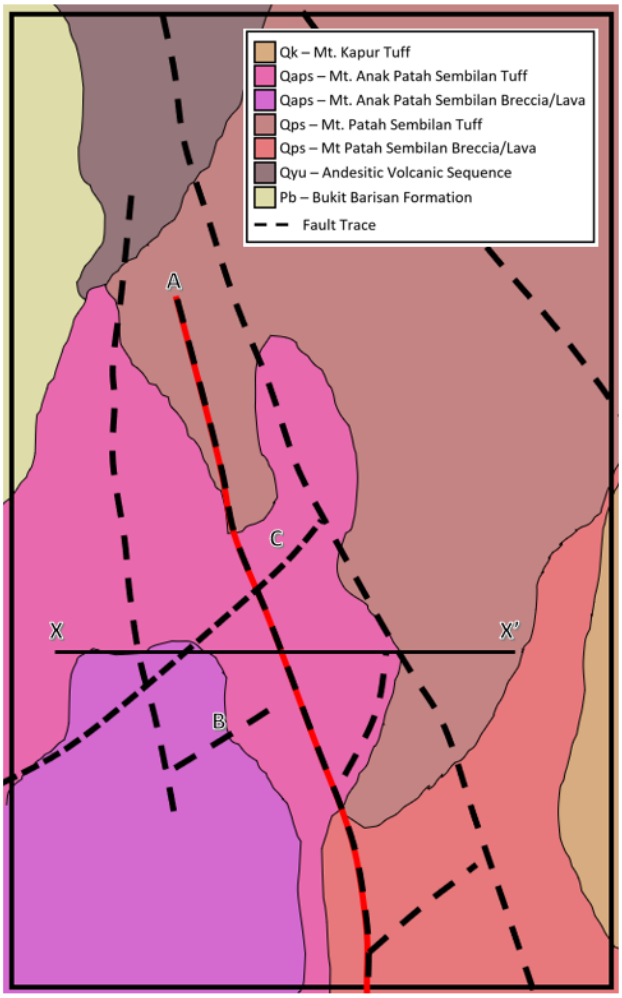

Figure 3.4: Geological map of the Muara Laboh site. The map is overlaid on the topography and polylines are drawn over the top of the fault traces (red line for fault "A"). A, B & C are references to faults in Fig. 3.6.

There can be inaccuracies in the newly generated fault planes, as there is no data to define their dip and dip directions. The most effective method to edit these is using cross sections and structural data. Structural data represents points within the geology model with orientation and dip. Points of structural data are added to influence the nature of surfaces (e.g. geological contacts or fault planes). These data include Easting, Northing, Elevation, Dip and Dip Direction. These points and their properties are represented by a structural disk (Fig. 3.5). When modelling fault plane orientation, the structural disks for each fault can be drawn on cross sections. Note that the scene view when drawing these should be parallel to the direction of the surface fault trace polyline as it intersects the cross section. This makes sure that the structural disk has the right orientation.

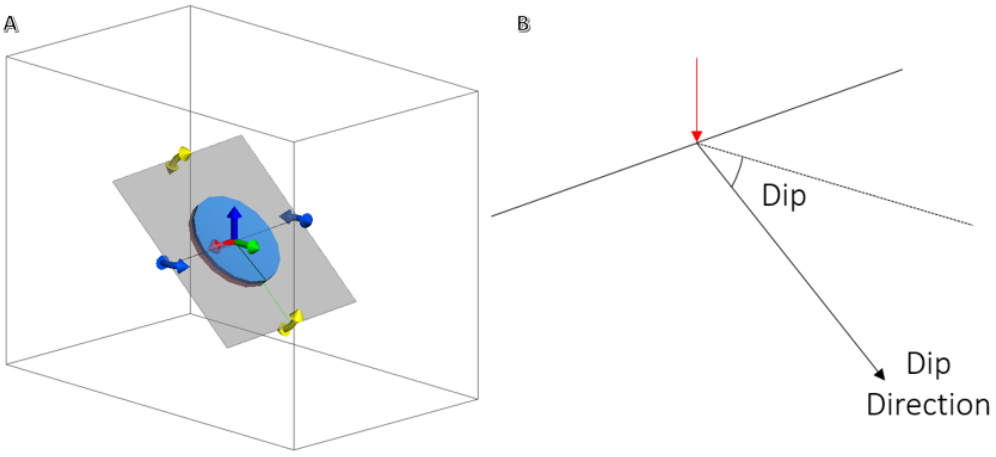

Figure 3.5: The structural disk. A) Represents how the disk is drawn. The black box represents the geology model extents and the disk size has been exaggerated for this example. The arrows indicate how the disk can be moved and adjusted. The disk forms a surface with one attribute category on one side, another on the other. The close, top half of the disk is blue, the other half is red. The disk will indicate which category will appear on which side using the red and blue halves. B). the red arrow indicates the point where the structural data is recorded.

There are two situations where an informed guess is necessary when drawing structural disks: distant faults and non-linear faults. Inaccurate or unrealistic fault planes may occur at distances away from the cross section, where the structural disks have little effect on the fault plane dip/dip direction. In such cases, the general properties of the fault orientation can be replicated at these distances, provided that there is no drastic change in the surface fault trace direction. With non-linear faults, the dip observed at the cross section can be repeated underneath the surface fault trace further away. The dip will remain the same, but the dip direction will change to the orientation of a right angle through the surface fault trace.

Faults are ordered by age from surface mapping (Fig. 3.6). Younger faults terminate against older faults. Older faults can also extend through younger faults. This can be tested by visually assessing the fault planes and their relationships before activating the faults.

Activating the faults results in the software interpreting the fault relationships (Fig. 3.7) and uses them to create *fault blocks*. In some cases, the surfaces defined in the basic geology model do not provide enough information to create each fault block. This is because the reference points for each of the geological surfaces are not dense enough to fall in each fault block. For example, a surface created using only one well will only provide one reference point (e.g. the contact point between unit X and unit Y). This means that

fault blocks that do not include that well data will have no available reference points and will result in the fault blocks having “unknown” volumes.

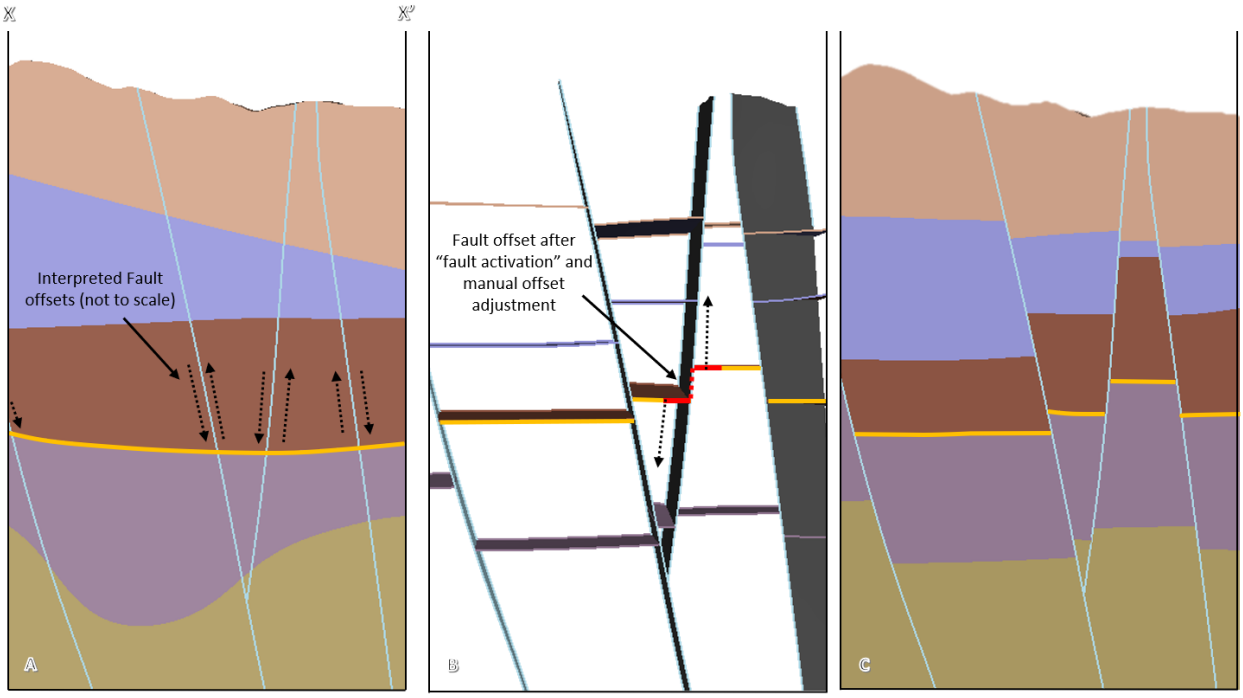

Figure 3.6: Application of faults and fault offsets to the geology model. A) Shows the original geological model with faults overlaid in light blue. The dotted arrows indicate offsets based on surface mapping, cross sections, and descriptions of regional geology. The orange line emphasizes how a single contact surface changes during this process. B) “Fault activation” in the geological model allows faulted surfaces to be manually adjusted for each fault block. C) Activating the “stratigraphy” in the geological model fills the spaces between each of the contact surfaces with the relevant units. X-X’ refers to Figure 3-4

There are several ways to fix this issue: through adjustment of boundary filters and the addition of manual data points (polylines and structural data, Fig. 3.7A and 3.7B respectively). The “boundary filter” setting controls how much/which information the software can reference to shape the contact surfaces on either side of a fault. By default, the new surface-fault relationship boundary filters are set to “all-data”, meaning no information from an adjacent fault block is passed to another (discussed earlier as the source of the unknown volume error). An example of the all-data boundary filter application is shown in Fig. 3.7, where each of the surfaces (1, 2 & 3) represent the same geological contact surface, but due to faulting, belong to three separate fault blocks. The well intercepts surfaces 1 and 2, giving these a reference point, but not surface 3. This means that surface 3 has needed to be inserted manually using structural disks. Additionally, surface 1 is large and only has one reference point at its margin which causes the surface to skew, so a polyline has been added to make this surface more representative of the geology. For surfaces that are

unaffected by a specific fault (i.e. the unit/surfaces have been formed post-faulting), the boundary filter can be set to “off”. This means that the software can use the surfaces of faults blocks adjacent to them to recreate the selected surface in the new fault block.

For units that are affected by faults, the contacts needed to be adjusted manually within each block using polylines and structural data. These adjustments are based on well data and cross section information. This process starts with well blocks which are interpreted as having the highest level of accuracy i.e. those with wells adjacent to cross-section information. Blocks with no internal data are progressively modelled outward from these, with an understanding that the further away from the more accurate blocks, the less accurate these would be. The main consideration when making these changes is the fault relationships (i.e. hanging wall vs footwall) and regional geology. Structural disks are used in this step (Fig. 3.8C) as they are more time efficient but result in a simplification of the unit relationships, which can be considered as acceptable given the scale, timeframe, and uncertainty of these surfaces.

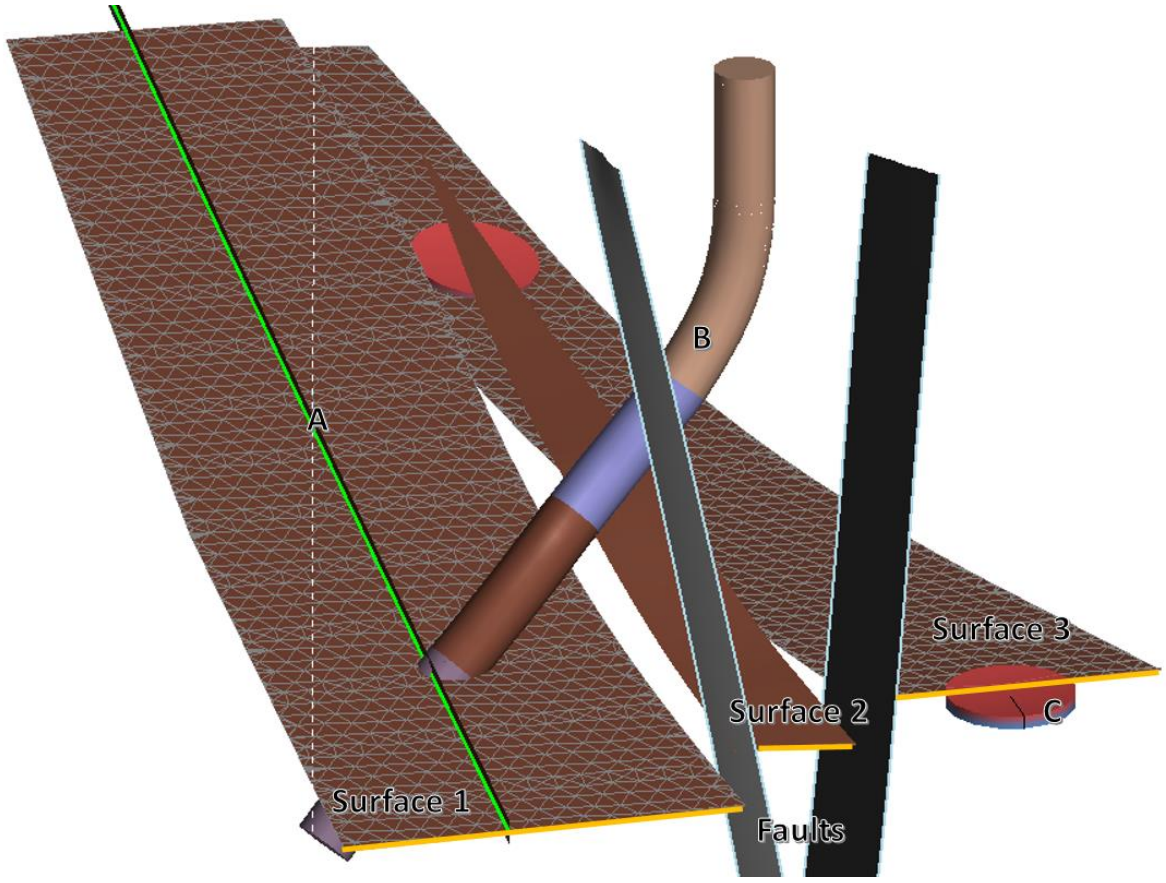

Figure 3.7: The orange line relates to the same coloured surface in Fig. 3.6. Mesh polygons have been added to surface 1 and surface 3 to help distinguish them from one another. A: Polylines (green line), B: well data and C: structural disks (red/blue circles) represent the 3 types of data used to build surface 1 (which uses A+B), surface 2 (which uses B) and surface 3 (which uses C).

3.6 Temperature

The number of data points affects how long Leapfrog takes to develop models. At Tauhara, the temperature resolution is 20 metres between points and poses no problem for modelling. At Muara Laboh however, the data resolution is at 0.1 metre intervals which is too close for the available processing speed. This was changed to 1m resolution by filtering temperature measurements. Isosurfaces are created using the *numeric model* tool which uses Radial Basis Function (RBF) computation to generate surfaces which represent specific temperatures. Leapfrog interpolates between the recorded well temperatures to create sections of the isosurfaces where there are no data, and because the RFB models do not take thermodynamic laws into account, sparse data will result in anomalous results. An extreme example might include the generation of a 200°C surface intersecting the topography, which is not realistic at either of the studied fields. These errors are attributed to geometry of the available wells combined with the software not considering the nature of a geothermal gradient. A minor example of an incorrect interpolation includes the temperature model of Tauhara where the numeric model only considers well data, not the field's reservoir boundary measurements. Both types of errors/inaccuracies can be fixed using points and polylines to best represent the temperatures provided both in well data and literature.

Some of the data points are not used in the models as they are unrealistically hot at shallow depths, as found at Muara Laboh. Several wells start from the same well collar (e.g. ML-H1, H2, H3, & H4). ML-H3 is much hotter than the other nearby wells so it appeared unlikely that this could occur naturally; this may be as a result of the well not being logged when in equilibrium with the natural formation temperatures. This is addressed by comparing wells with each other, to test and examine whether there are geological or thermodynamic features that could cause this type of anomaly. If there are none, the outlying data points(s) are omitted.

The steps described to this point generate a default temperature model based on software interpolation of well log temperature data. The representativeness of a temperature model is restricted by how well distributed the data is throughout the field, there are options for manually editing temperature gradients where this is the case, and there are similar options where there are known features that effect temperature but are also not recorded in well data. Model adjustments can be made using the RBF *edit with polyline* tool. Fig. 3.8 and 3.9 indicate how this has been carried out at Tauhara where there is little temperature data and the reservoir is known to be influenced by a resistivity boundary. Resistivity mapping provided by GNS (Rosenberg, 2017) was imported and georeferenced, and polylines were drawn to

represent the inner and outer margins of the reservoir boundary. Note that there are two types of polylines discussed here, (1) those that are drawn on the map to establish the inner and outside margins of the reservoir (the red lines in Fig 3.8 and 3.9), these are used as a reference for the second type of polyline, (2) those that are used to modify the geometry of the 200°C isotherm (the green lines in fig. 3.8 and 3.9). The 200°C isotherm is edited because this is the isosurface used in the combined model analysis. The resistivity boundary is interpreted as a clay or some other low permeability layer that prevents the flow of hot fluids. This modelling process also assumes that the resistivity boundary projects vertically to depth. There is little information on quantitative changes that the resistivity boundary has on the temperature, so an approximate, straight-line temperature vs. depth relationship is modelled, this type of interpretation may introduce inaccuracies but provides reasonable guidance for the temperature model.

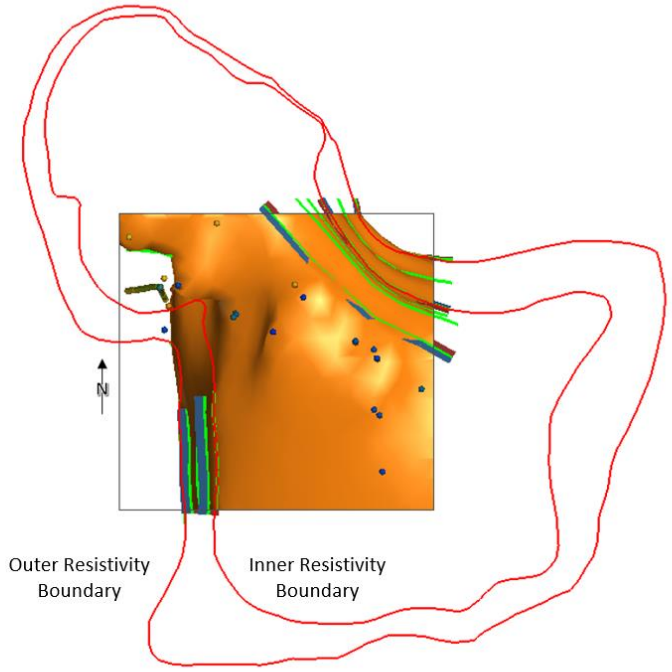

Figure 3.8: Top view of the Tauhara temperature numeric model. The red lines indicate the resistivity server boundaries.

Edits to the lateral temperature model boundaries were carried out with the Leapfrog scene view looking directly downward (Fig. 3.8). The hottest point expected to occur at the outer resistivity margin is at the base of the model, so, a polyline (green) was drawn by projecting the outer resistivity margin marked by mapping (red) onto the base of the temperature model margins (the black box) shown by the left-hand

black arrow (Fig. 3.9). The inner resistivity margin was assumed to be the coldest point of temperature at shallower depths of the reservoir, so the same projection technique was used, but instead, was used to intercept the default temperature model shown as the right-hand blue arrow. Polylines were drawn in between the two new green polylines in order to achieve a straight-line relationship from the outer resistivity margin at the base of the model to the inner resistivity margins at the top. The resulting surfaces can be too abrupt, these can be smoothed using more polylines.

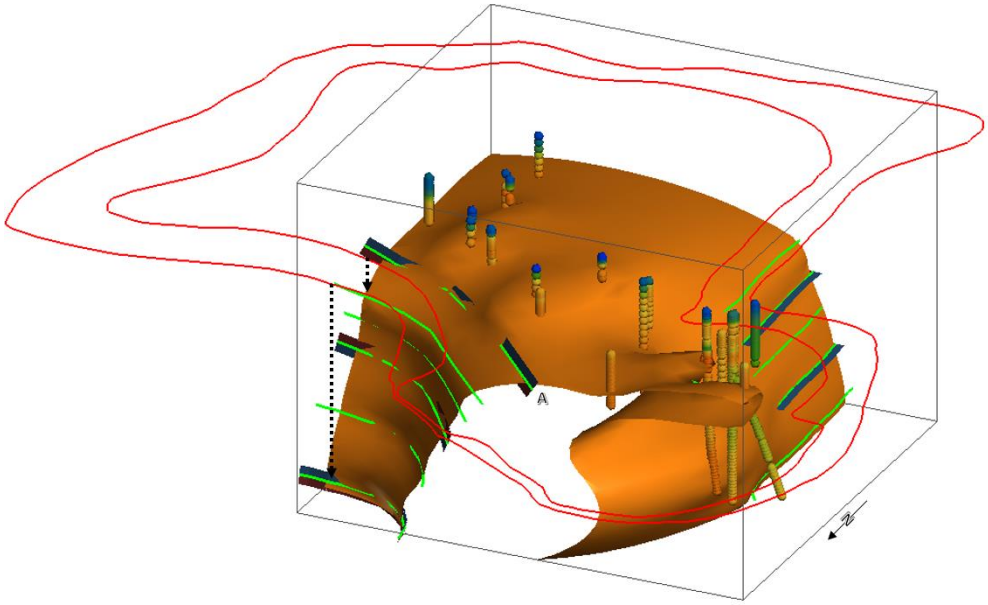

Figure 3.9: The green polylines control the form of the isosurface, A represents a line used to smooth the temperature gradient. The black arrows indicate the projections from the inside and outside of the resistivity survey margins.

3.7 Feed Zones

The feed zone data represent the degree of flow into or out of a well. For this project these can be related to permeability. Feed zones are provided as both interval and point data and classified as high, medium and low at both sites. A feed zone described as high flow is treated as though it is an area of high permeability, a low feed zone is represented as a point of low permeability, etc. Throughout the project these descriptors do not change, but the terms 'feed zone' and 'permeability' are used interchangeably (although there are cases where permeability does not relate to fluid flow).

Both interval and point data are needed for the feed zone modelling. Interval data is used with the GM tool to create a geology model where the feed zone intervals are treated as if they are lithologies (Fig. 10). This

means that the feed zone model gives approximate geometries and volumes of the different feed zone types. The point data is used for numeric calculations.

Both point and interval datasets are required, but in some situations only one or the other is provided. If only point data is provided then each point is treated as the centre of a feed zone, with 4 m added on either side. A 4 m thick feed zone is much larger than a typical natural feed zone, but this thickness was selected to make the point visible on the model and has minimal effect on the results. If only interval data is provided, the centre point between the top and bottom of the interval is extracted to build a point dataset.

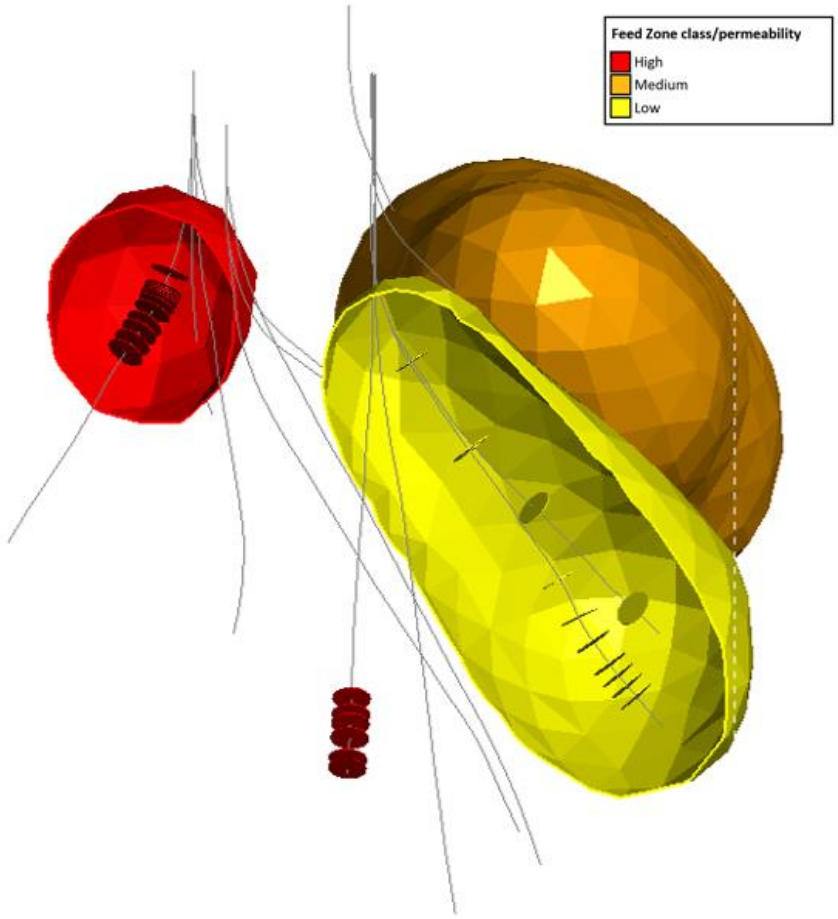

Figure 3.10: The disks represent feed zone intervals recorded in the wells. The spheroidal shapes are the software's interpolation of the available well data.

3.8 Model Processing

3.8.1 Temperature Isotherm-Isosurfaces

A temperature of 200°C is chosen as the target temperature isotherm because it is the low end of geothermal production temperature. This isotherm is taken from the original temperature *numeric model* as an isosurface and used for feed zone assessment (Fig. 3.11). In the context of this project, the feed zones of importance are those which could be used for production i.e. fall within the >200°C zone. This means that feed zones outside the >200°C zone can be ignored. A *mesh* is made of this surface to create temperature geology models used in creating block models for the Feed zone assessment.

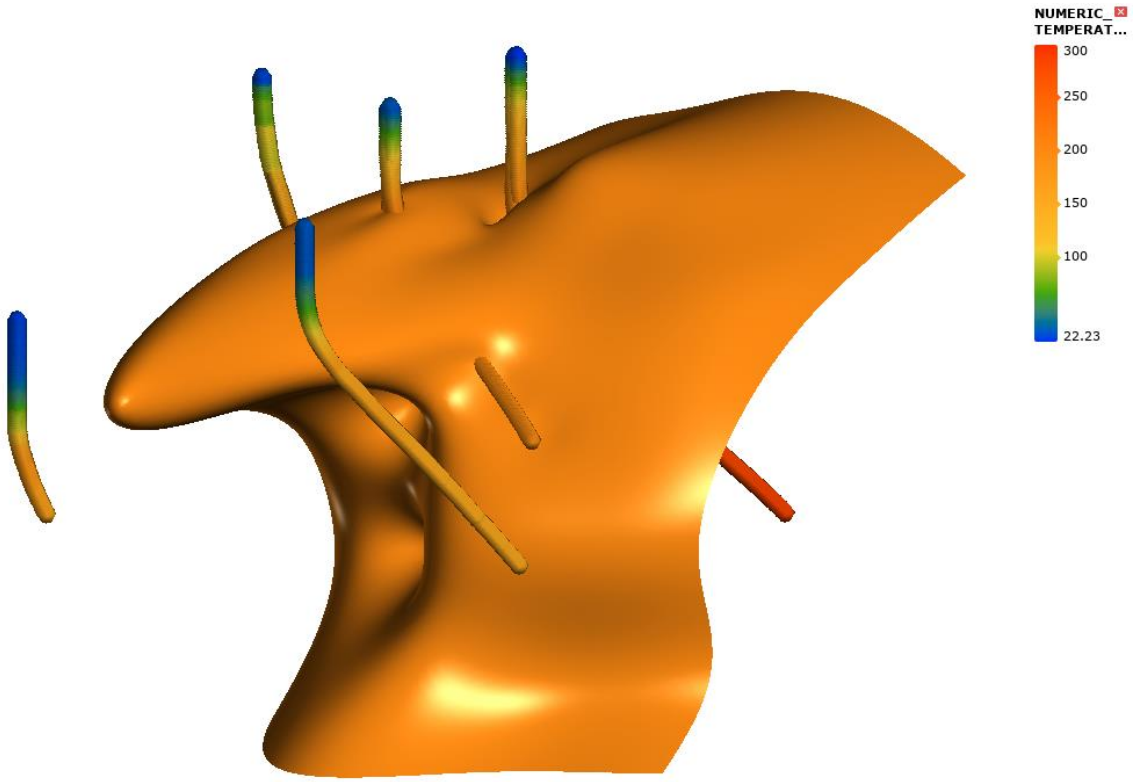

Figure 3.11: An isotherm-isosurface with an overlaid distance to well trace numeric function. This provides insight into the density of data.

3.8.2 Distance Evaluation and Fault Offset Isosurfaces

Distance based modelling is used to measure key features in the models, and to isolate areas of interest which are either understood or hypothesized to influence fluid flow. There are two ways that this feature can be used to make these assessments: using numeric distance functions to create contours of distance

and manual offset measurement using the measurement tool. Both techniques are useful and can be compared to assess the reliability of the measurements. The measurements made using these techniques are the ones used in the combined models.

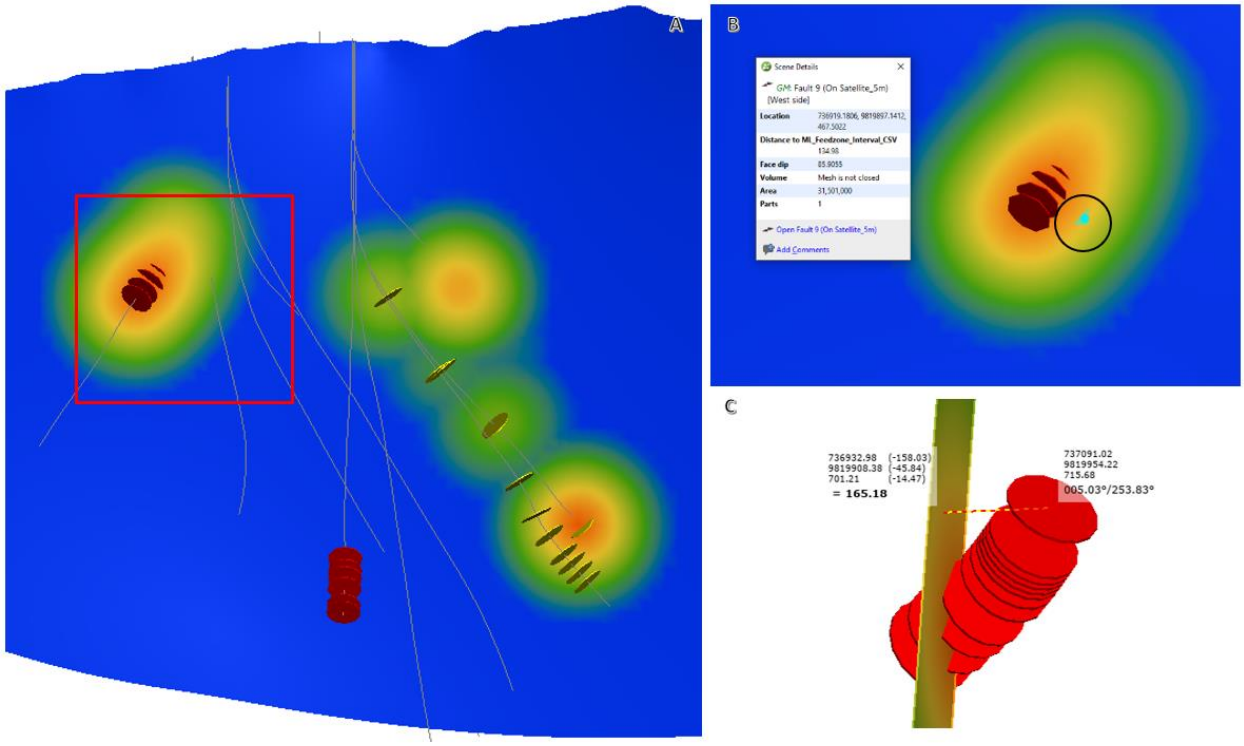

Figure 3.12: Different fault offset measurement techniques. The red disks are high permeability well data measurements, interpreted as feed zones. A) Fault surface contoured according to feed zone distance with well traces and feed zones overlaid. B) Inset from A) showing offset measurement of the farthest feed zone to its projection on the fault plane (turquoise point) using the distance function. The distance shown in the white window is 135 m C). Represents the use of the ruler tool to measure from the furthest field zone data point to the fault. In this case the distance is 165 m.

The distance function technique uses a distance offset numeric model overlaid onto fault planes. This model generates a proximity-based contour heat map where hotter areas indicate areas along the fault plane that are closest to the feed zones (Fig. 3.12A). This model shows the distance of every point along the fault plane to the nearest feed zone.

It is also possible to determine the farthest distance of any feed zone from a particular fault. This requires identifying a feed zone which appears to be the furthest away from any fault. By orienting the scene view in the same plane as the fault, clicking on the fault plane directly behind the feed zone will give the distance from that zone to the fault. In Fig. 3.12B, the projection of the farthest feed zone on the fault plane is the turquoise mark, highlighted by the black circle, which is at a distance of 144.98 m from the fault.

The measurement tool measures the linear distance between two points by clicking on one object and then clicking on another. As for the numeric model overlay, the measurement tool requires finding a feed zone which appears to be the furthest away from a fault. In this case the two objects to be clicked are the farthest feed zone and the fault (Fig. 3.12C).

Other uses for this feature include assessment of a chosen model feature with respect to well data e.g. comparing the distance between isotherms and well locations: which provides insight into the degree of extrapolation being made in the model outputs. Or simply, a basic visual representation of feed zone trends and orientations.

3.8.3 Combined Models

Combined models provide comparisons between key features. The outputs are easy to generate but it is important to understand the goals of the combined mode. One of the aims of this project is to develop a way to understand what controls how and where fluid flow occurs i.e. feed zones. The reservoir characteristics, or controls, that contain these feed zones are established using the initial and secondary model methods. Combined modelling takes these parameters and uses them to create a model with a volume which fulfils all these controls and can then use to estimate other areas that may contain feed zones.

Summary of Initial and Secondary Input Models:

- Fault Isosurface: A continuous surface at a specific offset from all the selected faults temperature generated with the numeric model tool
- Temperature Isosurface: A continuous surface that represents a target temperature generated with the numeric model tool
- Feed Zone Model: a volumetric representation of where feed zones have been recorded generated with the GM tool.
- Geology Model: A model that represents the lithological and contact features generated with the GM tool.

3.8.4 Block Model

The *Block Model* tool was added to the Leapfrog Geothermal toolbox late in the life cycle of the thesis project. The tool takes blocks of a specified dimension (i.e. resolution) and simplifies the contents so that

each block represents a single attribute depending on the type of model. These models can then be used to compare relationships between categories and numeric data.

Many of the block model outputs are automatic, all that is required is to select the parameters that need to be compared. The “statistics” tool is used to create a table of statistics, scatter plot, Q-Q plots, and box plots. There is another feature called a “resource report” which uses the same statistics to make volumetric assessments of any given features.

4 Results

4.1 Geology

4.1.1 Tauhara

The amount of well data within the Tauhara site is limited (Fig. 4.1, 4.2). The well collars tend to be located from the northwest to the southeast, with a large cluster of wells to the northwest. The areas at the northeast and to the southwest are therefore inferred. The depths that some of these wells reach over 3 km (e.g. WK408, 3012m), however some of the wells are nearly as shallow as 400m (e.g. TH16, 403m). Some units are only observed in a few wells which means a greater degree of interpretation is necessary.

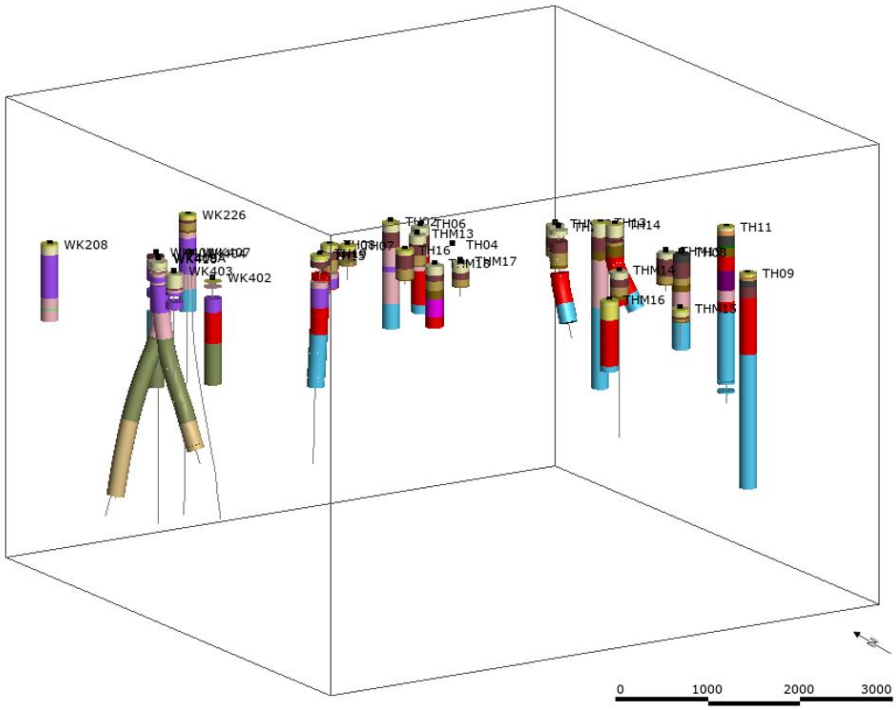

Figure 4.1: Well log data distribution at the Tauhara study area (scale shown in this and subsequent figures in metres).

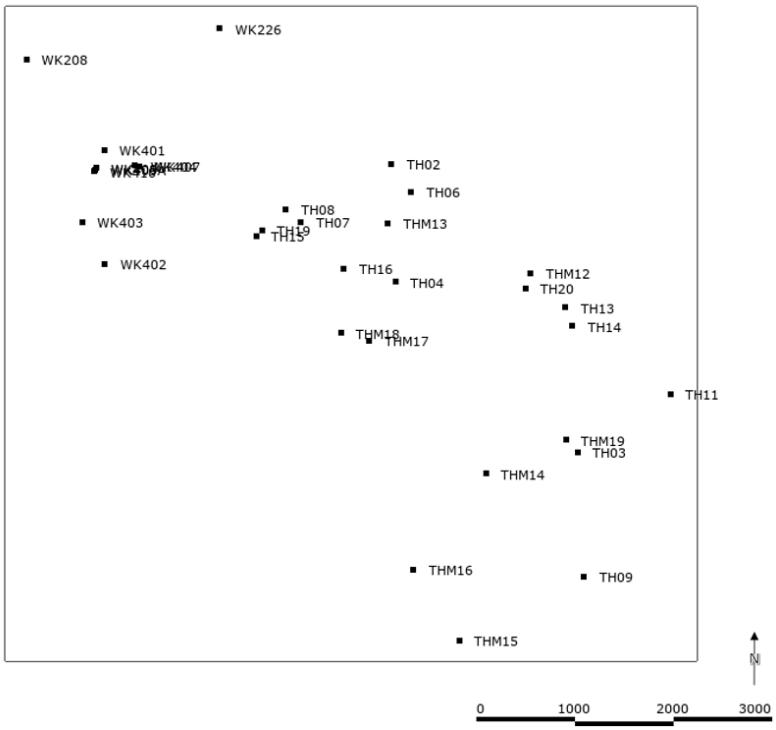

Figure 4.2: Horizontal well log locations. Well collar references included in the appendices.

In the well logs there are several parts of some wells labelled "core lost". This is interpreted differently depending on the depth that the measurements were made. For example, if these were recorded close to the surface, it is safe to assume that this was a component of the alluvium deposits/Oruanui Formation, due to their high permeability and poor induration. Core loss observations made deeper in the well have been allocated to the unit that the measurement occurred within. If the measurement occurred in between two units, it is allocated on an assessment of the strength properties of the two units: i.e. which unit would be more likely to be lost during drilling. If this was unclear, then the no core data was omitted when building the geological model.

The oldest unit observed in the well log is the Tahorakuri Formation (Fig. 4.3). This unit is limited to two wells to the northwest and does not appear in wells of similar depths to the southeast. It is inferred that this unit deepens to the south and is below maximum well depth. Above the Tahorakuri Formation is the Whakamaru Group. This unit is limited to a small part of the study area in the northwest, where it appears to be restrained by faulting. It is observed within 4 wells which show high fault offsets. The Waiora Formation (Wa1) is thin towards the north of the study area, but greatly increases in thickness and depth

toward the south (Fig. 4.4). There is no contact seen in the well logs with the Tahorakuri Formation to the south. Waiora Wa5 and Wa3-4 share the same horizontal bottom and top contacts, contacting Wa1 and the Lower Huka Falls Formation respectively. Thicknesses of each unit vary despite the shared space: Wa3-4 is more prevalent to the southeast and Wa5 is more prevalent to the northwest. Rosenberg (2017) indicates that the fault offset in these units is relatively small compared to the scale of the model so have been left un-faulted in the geological model. The units exhibit similar geothermal properties when modelled at this scale.

There are lava units within the Waiora Formation, including Karapiti 2a, Spa Andesite and the Racetrack Rhyolite. Karapiti 2a is horizontally expansive and is recorded in 10 different well logs to the northwest whereas the Spa Andesite and Racetrack Rhyolite are only recorded in one. There is no indication where the feeder pipes may occur, so these have not been included in the models. The Huka Falls Formation (upper, middle and lower) are relatively thin layers of similar thicknesses. They are thickest to the east and are thinnest to the north and northwest, proximate the Waikato River. The Trig 9471 Rhyolite, like the recent alluvium and Oruanui Formation, is superficial and very thin when compared to the scale of the model. The thinness makes these units difficult and time consuming to model. In many areas these units have not been differentiated as they will have little influence on the geothermal properties of the model. The distribution of the Mt Tauhara Dacite is based on surface mapping. There are only two records of this unit in the well logs which makes it difficult to constrain the feeder system at depth.

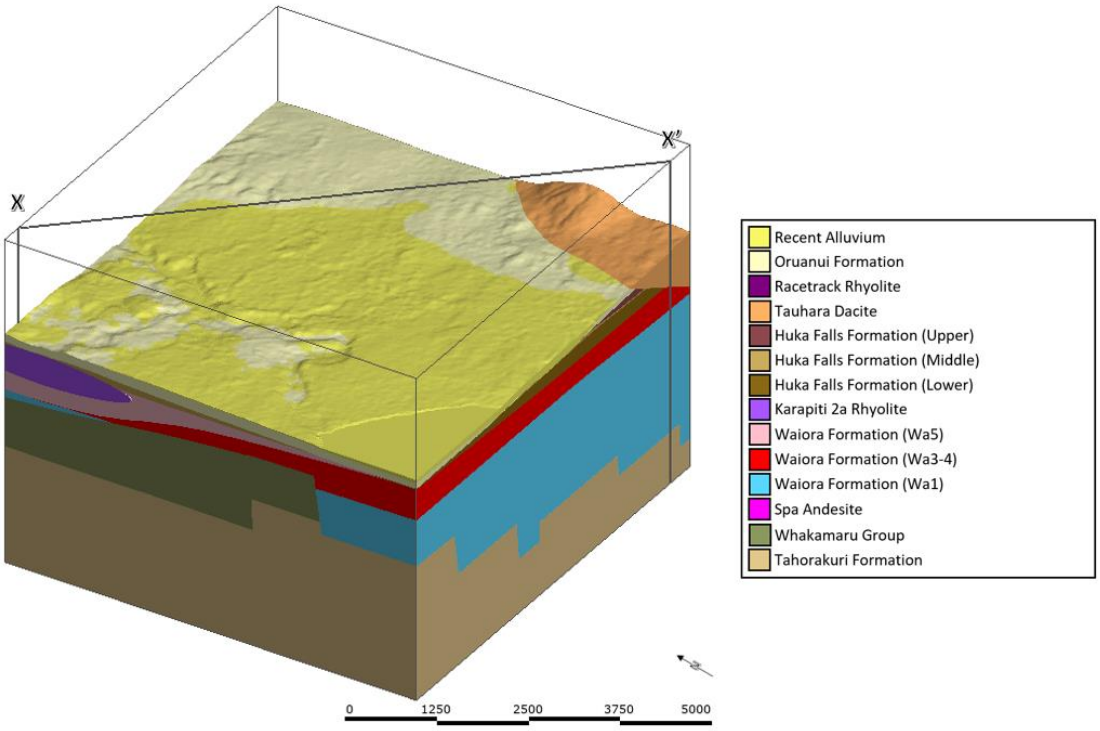

Figure 4.3: Oblique view of the Tauhara geological model.

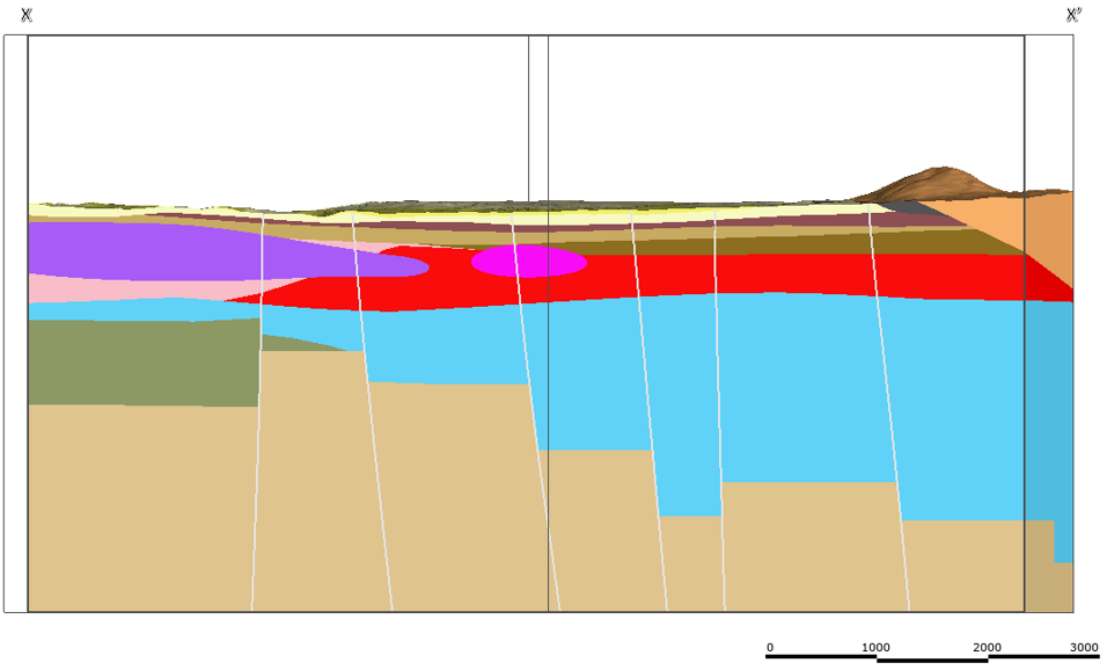

Figure 4.4: NE-SW Geological model cross section. Faults are shown in white.

Faulting in the Tauhara study area is mostly oriented from the southwest to the northeast (Fig. 4.5), with a minor component that runs approximately north to south. Most of southwest-northeast faults are parallel with the occasional intersection from a north-south fault. The most complex area is to the northwest, where there are a large cluster of intersections between the two dominant fault orientations. The measurement techniques found a maximum distance of approximately 310m between high feed zones and faults.

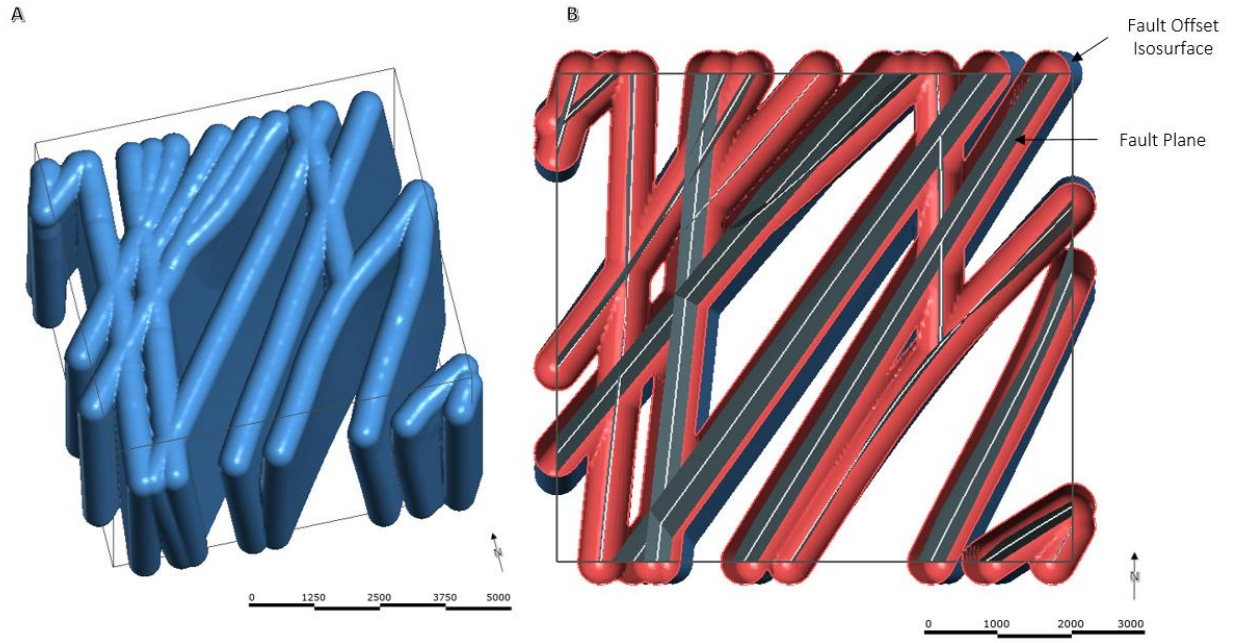

Figure 4.5: A) Oblique view of the Tauhara fault network B) Downward view of the Tauhara Fault network, horizontally truncated. The Fault planes/network is generated while building the geological model, the Fault offset isosurface is generated using the numeric model tool.

4.1.2 Muara Laboh

Muara Laboh has several different data types available for modelling. In terms of well logs, the site has wells concentrated above areas that are interpreted as more complicated geology (i.e. above the heavily faulted areas to the south of the field and along major faults). There is typically more than one well at each well collar and these are oriented in different directions. There is a reasonably comprehensive dispersion of geological data over the site, however some of the wells, particularly to the south, do not have detail on geological unit logs, but will take other measurements such as temperature or pressure. These wells range in depth from 966m to 3100m.

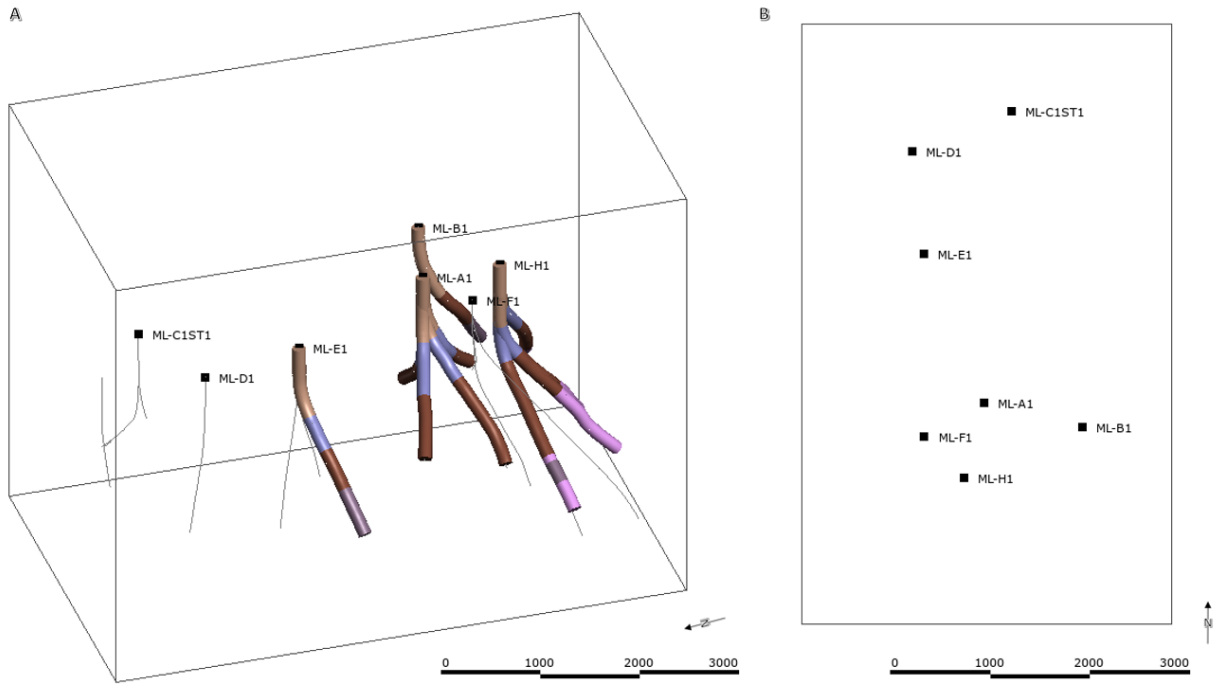

Figure 4.6: Well log data distribution at the Muara Laboh study area

Following the deposition of the Bukhit Barisan basement Formation the great Sumatran fault became active. This results in tensional pull-apart basin faults with numerous fault blocks, creating complicated horst-graben in the basement rock and subsequent units i.e. the Panian Formation., intercalated Dacite & Andesite Formation, and the undifferentiated Silicic Formation. These units are thickest to the southeast (Fig. 4.6, 4.7), which is the southern depicentre of the pull apart basin. The top contact between these units and the basement rock becomes shallower to the north and northeast, where these units pinch out and are overlaid by the PS Andesite Fm. The reduction in depth of the top surface of the basement rock is a result of the shallowing of the pull-apart basin.

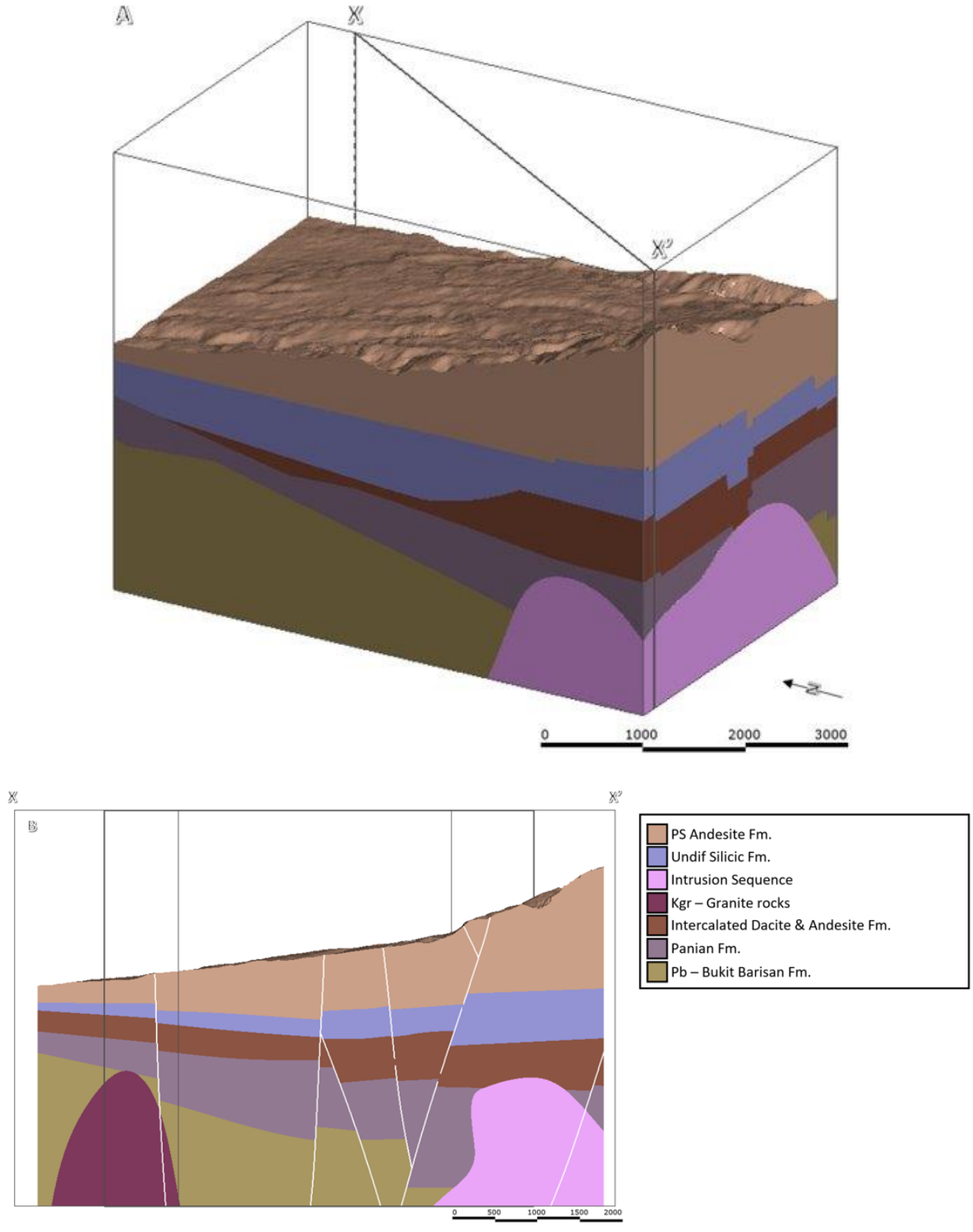

Figure 4.7: A) Oblique view of the Muara Laboh geological model B). Cross section at Muara Laboh. Faulting is indicated in white. Vertical lines in cross section indicate long and short edges of the block.

The youngest of the units, PS Andesite formation, is comprised of the Mt Patah Sembilan and Mt Anak Patah Sembilan sequences which have a source just south of the study area. This unit is thickest at the southern margin of the field and thins out to the south, pinching out beyond the extents of the study area, where the basement rock is exposed.

Faulting at Muara Laboh is typical of a pull-apart basin (Fig. 4.8), with a SE-NW central cross basin strike-slip fault, several sub parallel en echelon faults and a number of younger faults which crosscut these at approximate right angles (SW-NE), there is also one N-S to NNE-SSW fault. The younger faults are only present in the southern half of the study area. An offset distance of approximately 200m was identified as the maximum offset that a feed zone occurs from a fault.

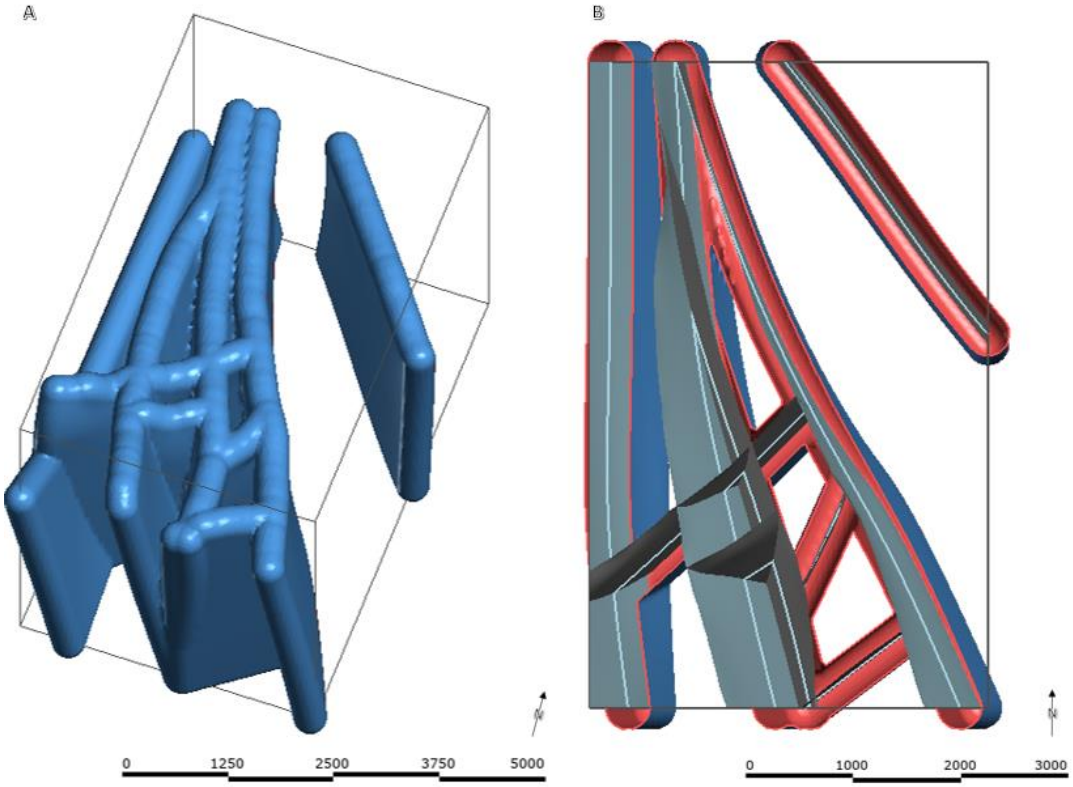

Figure 4.8: A) Oblique view of the Muara Laboh fault network offset model B) Downward view, horizontally truncated.

4.2 Temperature

4.2.1 Tauhara

Temperature varies throughout the Tauhara site. There are high temperatures at relatively shallow depths, from the northwest to the southeast, reaching temperatures of 75°C within 100m of the surface and 225°C within 500m of the surface. The hottest areas occur at depth to the southeast, close to Mt. Tauhara. Changes in temperature are gradual in most areas at Tauhara. However, to the northwest there is a shallow lobe of high temperature which sits above an area of cold fluid infiltration (Fig. 4.9, 4.10).

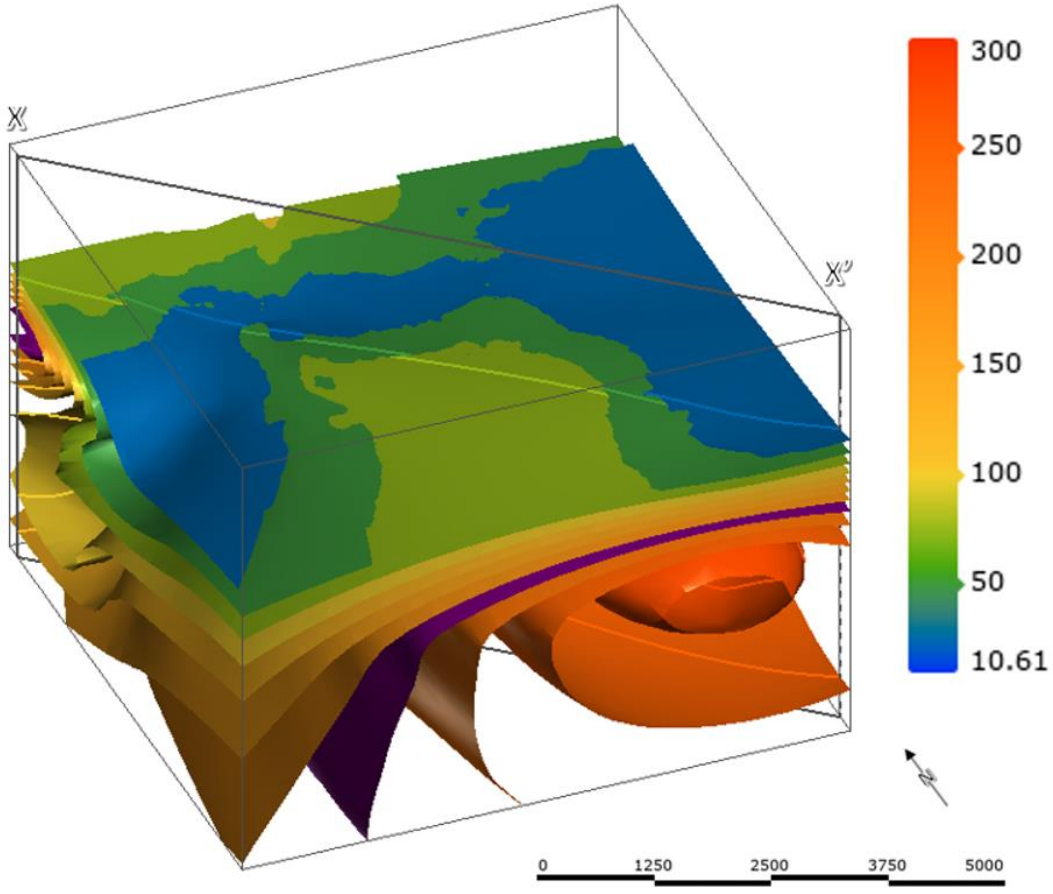

Figure 4.9: Tauhara Temperature model. Isotherms/isosurfaces are at 25°C increments.

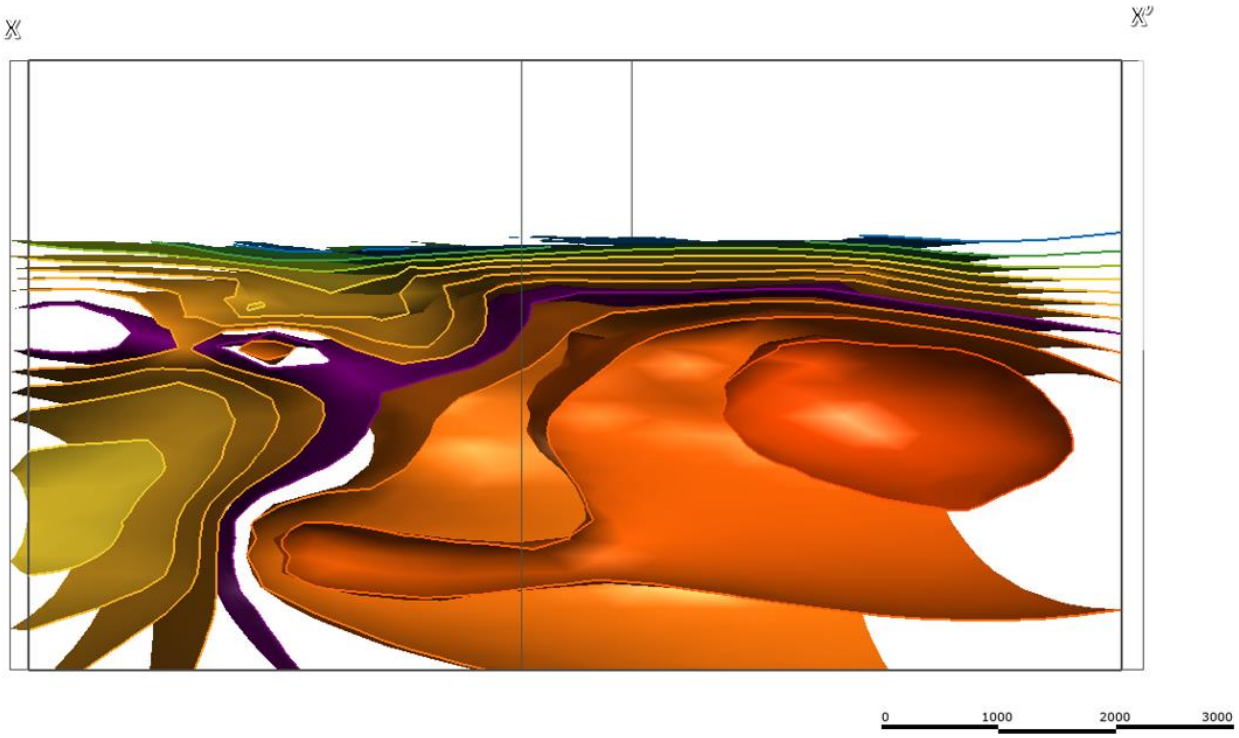

Figure 4.10: Cross section of the Tauhara temperature gradient. X-X' shown in Fig. 4.9 The 200°C isotherm is shown in purple.

The temperatures cool rapidly towards the surface at this location, and a temperature inversion occurs, where upper areas of the model are hotter than those below. These variations in temperature occur directly underneath the Waikato River. Other areas where cooling occurs are to the northeast and southwest at the reservoir margins, this cooling is more rapid on the south western side.

The 200°C isotherm at each site (Fig. 4.11) represents the transition point where hydrothermal production becomes viable. The 200°C surface is characteristic of the other heating and cooling patterns observed at Tauhara.

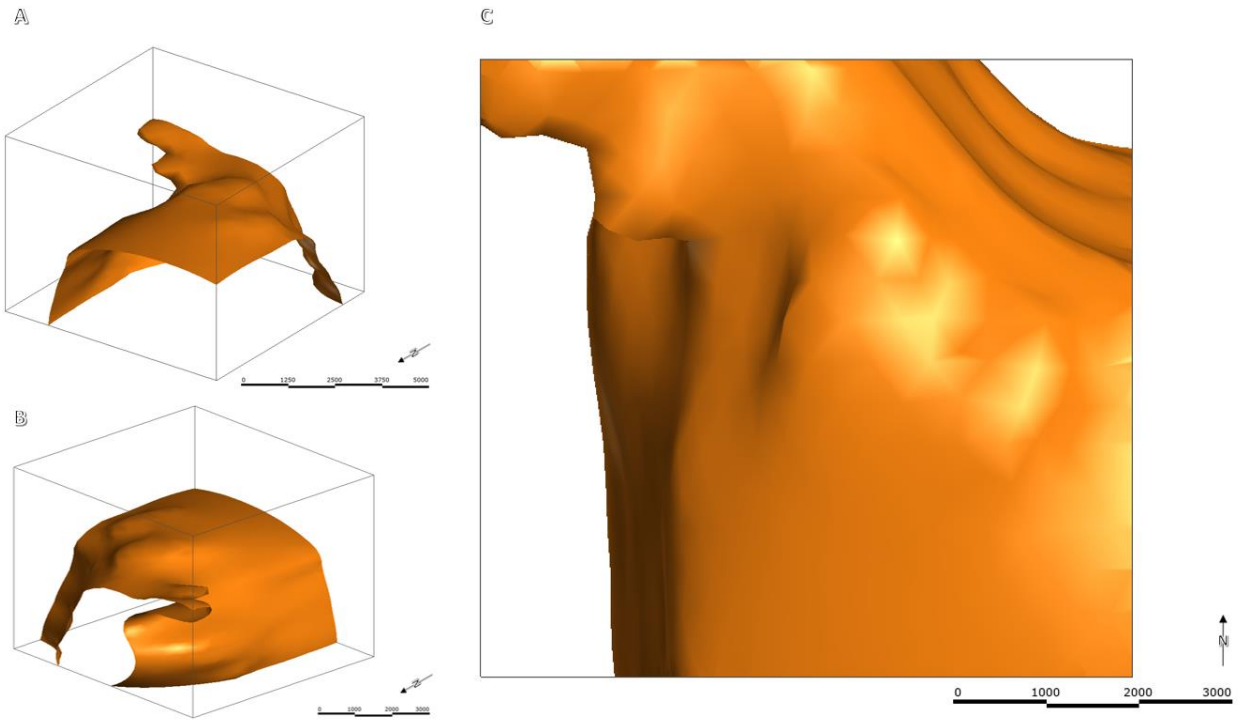

Figure 4.11: The 200° isosurfaces at Tauhara. A) Northwest perspective B) Southeast perspective C) Downward perspective.

4.2.2 Muara Laboh

At Muara Laboh temperature variation has a strong north-south orientation (Fig. 4.12; 4.13). The hottest areas are at the southern margin. High temperatures extend northeast as a giant lobe with a temperature inversion below it. Higher surface temperatures are observed along ridgelines, while the areas of depression remain cold. The temperature of the lobe decreases to temperatures of <175°C by the northern end of the study area. Again, the 200°C surface (Fig. 4.14) is used for assessment.

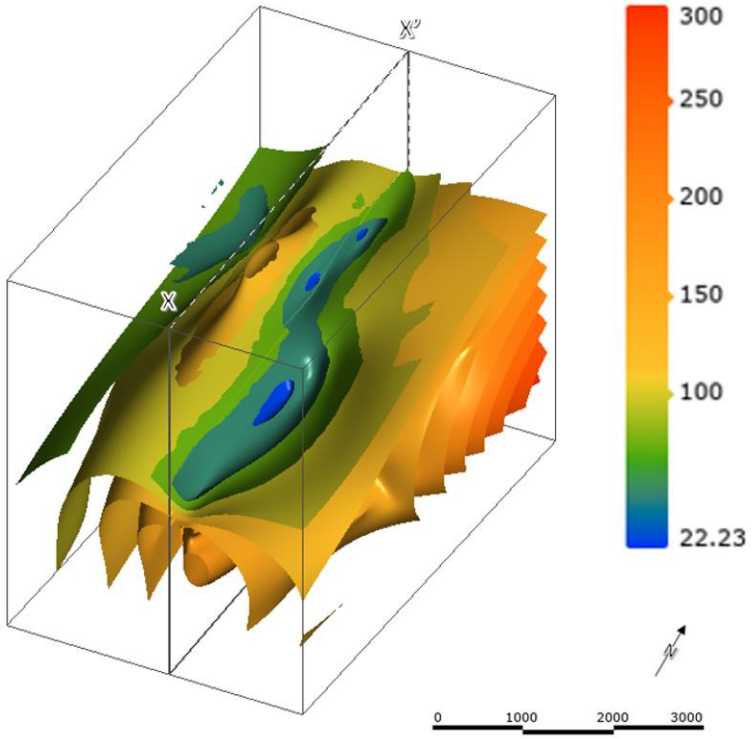

Figure 4.12: Muara Laboh temperature model. Isosurfaces are at 25°C increments.

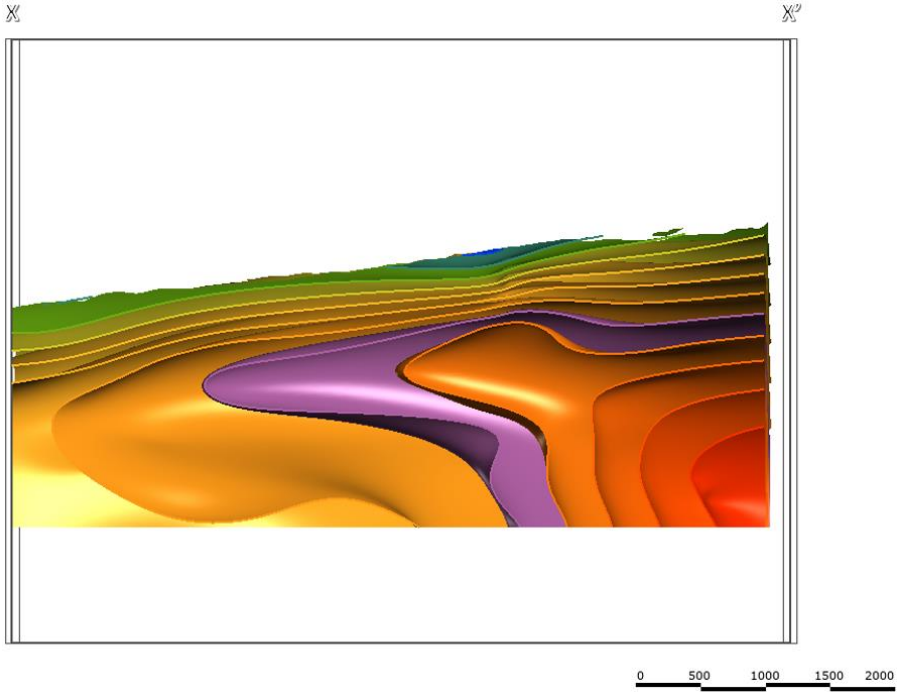

Figure 4.13: Cross section of the Muara Laboh geothermal gradient. X-X' references Fig. 4.12. The 200°C isotherm is marked in purple.

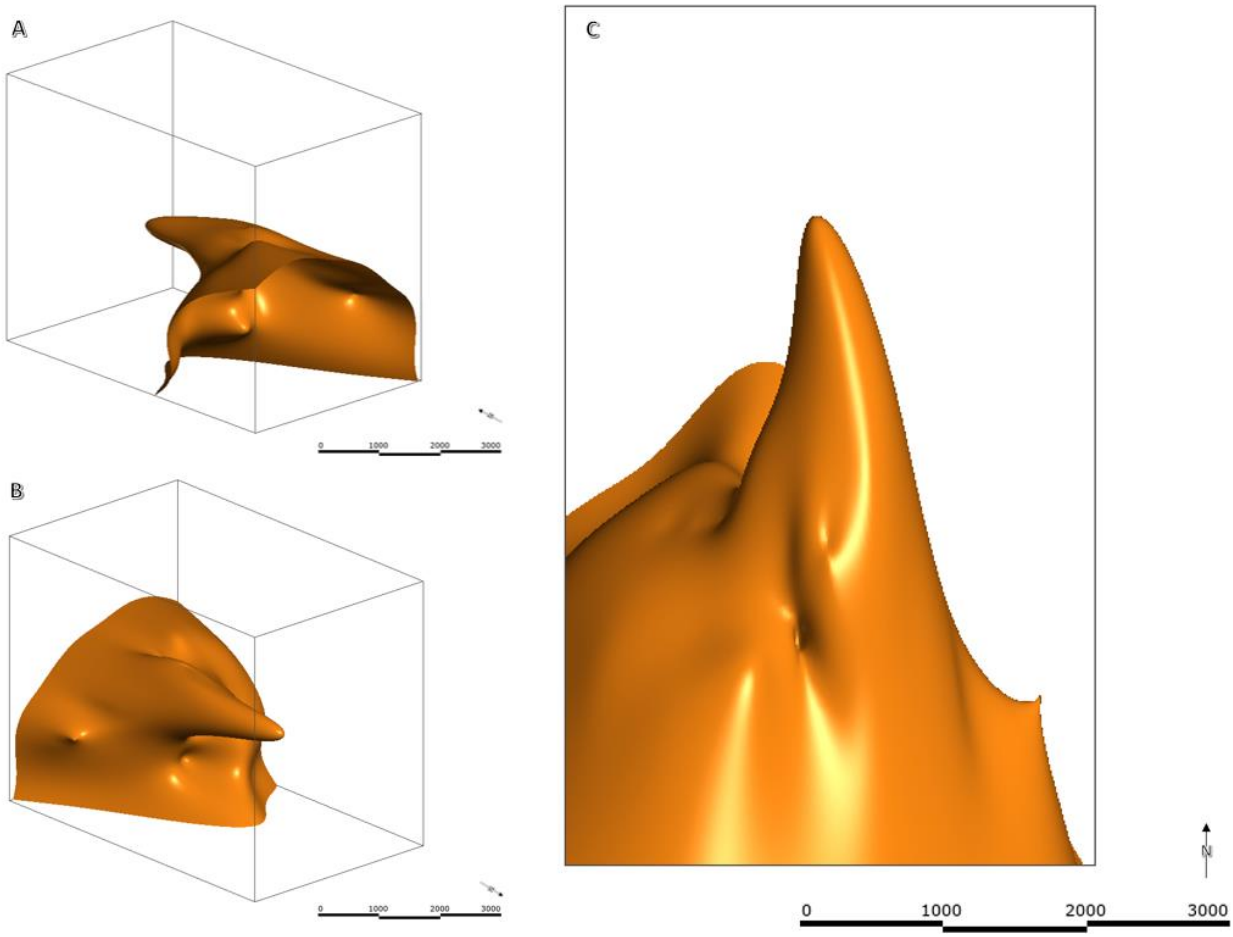

Figure 4.14: The 200° isosurfaces at Muara Laboh. A) Northwest perspective B). Southeast perspective C). Downward perspective.

4.3 Feed Zones

Feed zones are a measure of the inflow or outflow measured at wells. The terms high, medium and low indicate the degree of permeability. Inflow and outflow measurements have been combined in these results, for simplicity.

When modelling the feed zones, it is important to 'interpret' the data as little as possible, in order to create an unbiased, objective model. For this purpose, the feed zones models are agnostic of any features (e.g. geologic or structural fabric) other than the raw feed zone data. The interpolant is to create spheroidal/lensed feed zone representations which keep the surface extents localized. The base range is set to 500m for the same reason. The base range represents how far the software can radiate around a

data point in order to connect to a nearby well point. Typically, the base range is approximately double the average distance between wells, but this distance was unrealistic.

The data from Tauhara provided describes increments of very high, high, medium, low, and very low for permeability magnitude. These categories have been simplified to high, medium and low during feed zone modelling to match the categories used at Muara Laboh. They are classified relative to each well.

4.3.1 Tauhara

Feed zone modelling at Tauhara is limited by the distribution of wells. This means that the feed zone models here are limited to a band spanning from the northwest to the southeast. At either end of the drilled area deeper wells help to identify different trends in permeability, while data in the center has limited depth.

It is difficult to identify any strong trends of any of the units at the site looking solely at the feed zone model (Fig 4.15). Low permeability is prevalent throughout the area and tends to appear closest to the surface. However, it is not limited to shallow depths. Similarly, the medium and high feed zones do not have any strong trends although there is a slight clustering of both to the northwestern corner up to about 2.5 km depth.

There are many areas of low permeability which are prevalent throughout the model.

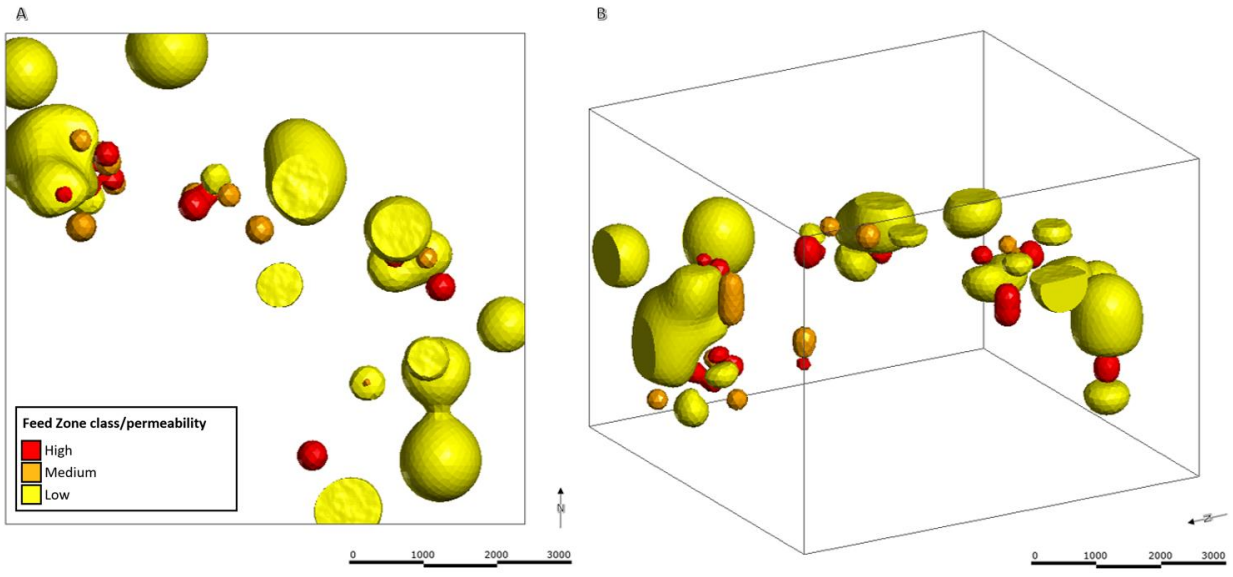

Figure 4.15: Feed zone records at Tauhara. A) downward view B) oblique view.

4.3.2 Muara Laboh

Permeability at Muara Laboh is interpreted from Borehole Image Log (BIL) fracture characterization (Baroek et al., 2018) (Fig. 4.16) and PTS logs. BIL fracture characterization provides information on where fractures occur, the properties of the fracture, and its orientation (Fig 4.17). Effective fracture feed zones are the classification used to model the feed zones in this project. Being effective feed zones means that they are associated with feed zones based on injection losses or productivity. Of the 4900 fractures assessed with BILs only 286 appear to be related to permeability zones. Only small numbers of open faults and fractures found at Muara Laboh are hydraulically connected to the reservoir.

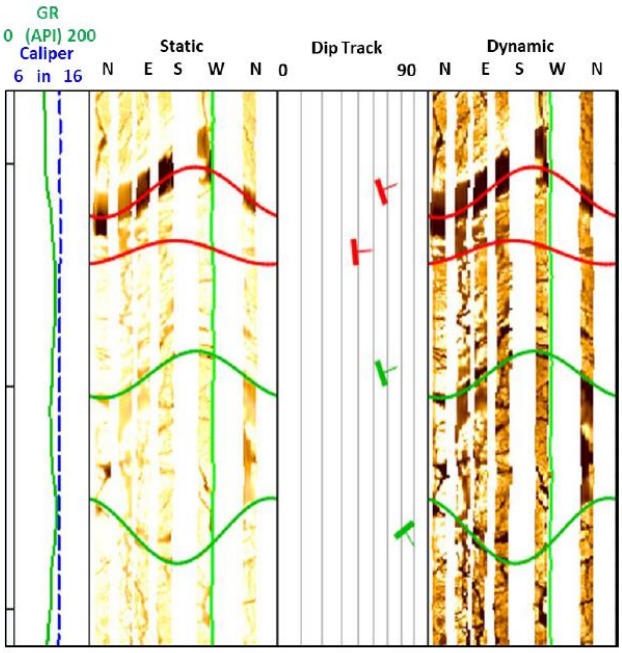

Figure 4.16: An example Borehole Image Log. The red lines indicate open fractures, the green indicate partially conductive fractures. (Baroek et al. 2018).

Compiling the BIL logs from each well onto stereonets gives the effective fracture orientation (Fig. 4.17). The size of the stereonets indicate the relative magnitude of permeability. In this same figure, N represents the number of effective fractures measured in the well, but note that the number of recorded fractures does not translate to higher permeability (Baroek et al. 2018).

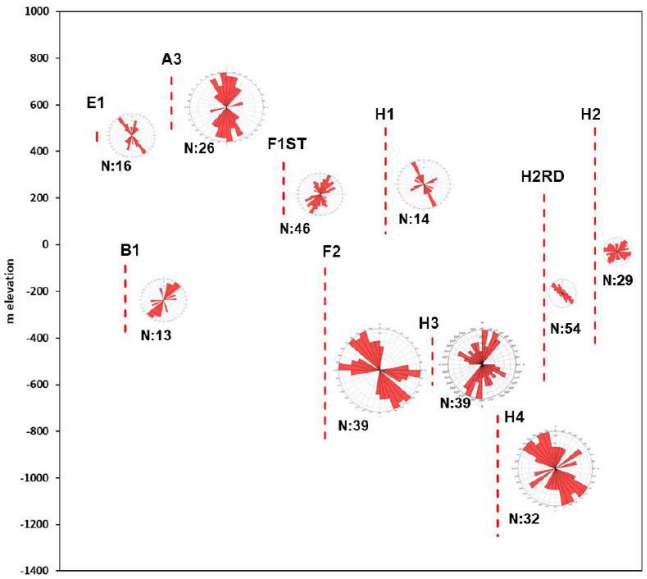

Figure 4.17: Effective fracture orientation. Size approximately represents permeability magnitude. N = fracture count. (Baroek et al. 2018).

The stereonets for each available well were split into three groups: high, medium, and low – based on the size of the stereonet. These groups were grouped as: [F2>H4>A3>H3>H1] > [B1=F1ST=E1] > [H2=H2RD], where [High] > [Medium] > [Low]. Note this data was not available for each well in the area. Relative permeability, along with PTS details are summarized in Table 4.1.

Table 4.1: Summary of the well permeability (i.e. feed zone) data at Muara Laboh. PTS = Pressure Temperature Spinner

Well ID	Interpreted Permeability	PTS (Production/Injection)
A3	High	Production + Injection
B1	Medium	Injection + Shut-in
E1	Medium	Injection
F1ST	Medium	Not provided
F2	High	Not provided
H1	Medium	Production
H2	Low	Injection
H2RD	Low	Injection
H3	High	Injection
H4	High	Not provided

The resulting feed zone GM is much simpler than that of Tauhara (Fig. 4.18). There are also fewer data points. The feed zones are all located to the south/southeast, which is known from the geological models to be the area with the highest fault density, as well as one of the deepest points of the basin. The areas of low permeability are clustered, the medium and high permeability volumes are separated.

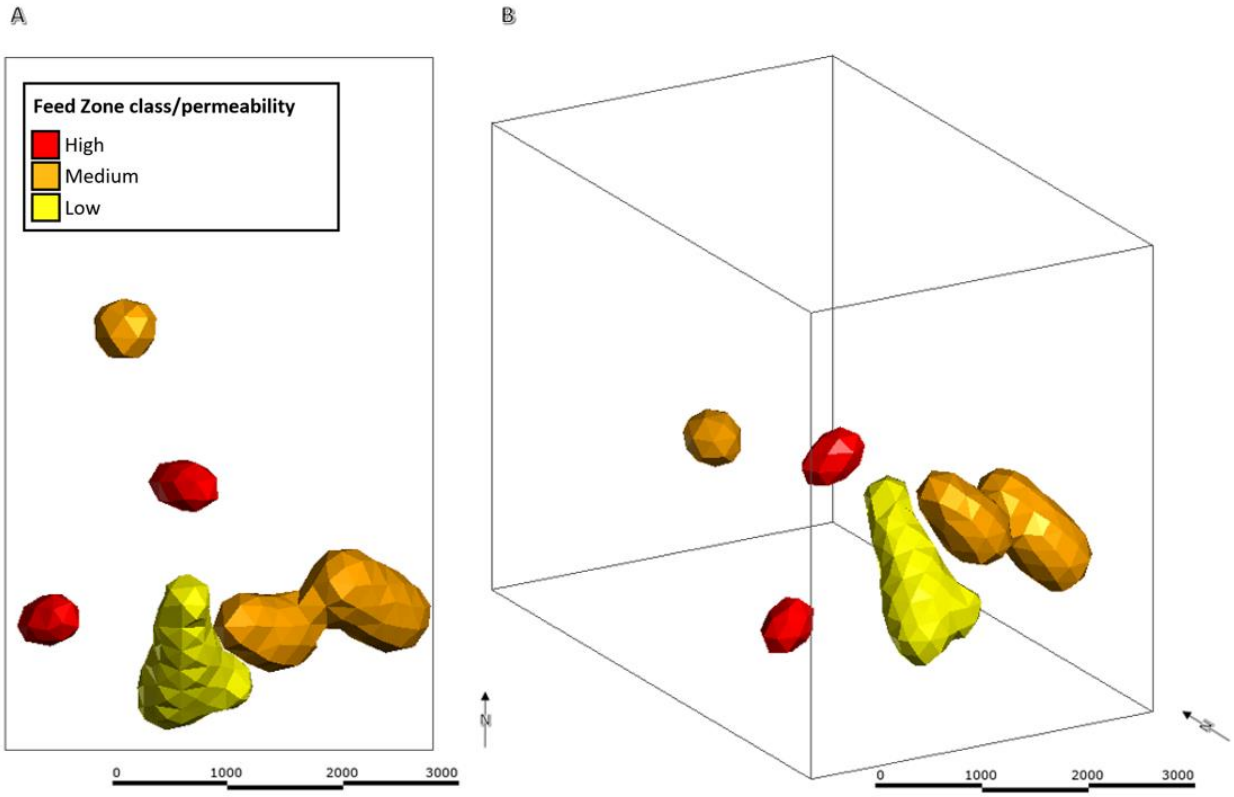

Figure 4.18: Feed zone records at Muara Laboh. A) Downward view B) Oblique view.

4.4 Combined Models

There are two types of combined models that can be created: a *potential* and *actual* model.

The *potential* model uses fault offset and temperature control isosurfaces, creating the internal volume (i.e. an area which contains all the variables being tested for feed zone influence). The inclusion of geology in this model combines the geometries of the units within the offset and temperature parameters but does not distinguish whether the feed zones are limited to specific geologies.

The *actual* model is most useful for outlining which geologies are present. The constraints of the actual model are based on the feed zone models as well as the temperature and fault offset restrictions

established in the potential model. The constraints of temperature are the same as those applied in the potential model

By comparing the potential and actual model it is possible to understand the volumes where a feed zone may occur, as well as the geology that it occurs within. This can be represented by creating a copy of the potential model and removing the units which are identified as missing in the actual model.

The following results target the high feed zones, to find areas of optimal productivity. A summary of this data is available in appendix C.

4.4.1 Tauhara

The combined model controls applied at Tauhara use a >200°C temperature boundary and a <310m fault offset boundary (Fig. 4.19, 4.20). The Tauhara potential model indicates that there is a large area of potential productivity at the site. The high temperatures at shallow depth means most of the area from northwest to southeast is included within the potential combined model. In addition to this, faults within the field are common and are approximately evenly distributed, other than the northwestern clustering. This distribution means that any given point within the model is never very far from a fault. This means that the fault offset constraint includes most of the combined model.

The Tauhara *actual* model (Fig. 4.21) properties indicate that feeds zones at Tauhara are limited to the Waiora Formation, the Tahorakuri Formation, and a minor portion of the Whakamaru Group. The Tahorakuri and Wa1 appear to host most of this reservoir. The lithologies present in both the potential and actual model are summarized in Table 4.2, where the given volumes are calculated from the potential model. This gives the maximum prospective reservoir volumes but excludes lithologies that are not recorded within feed zones.

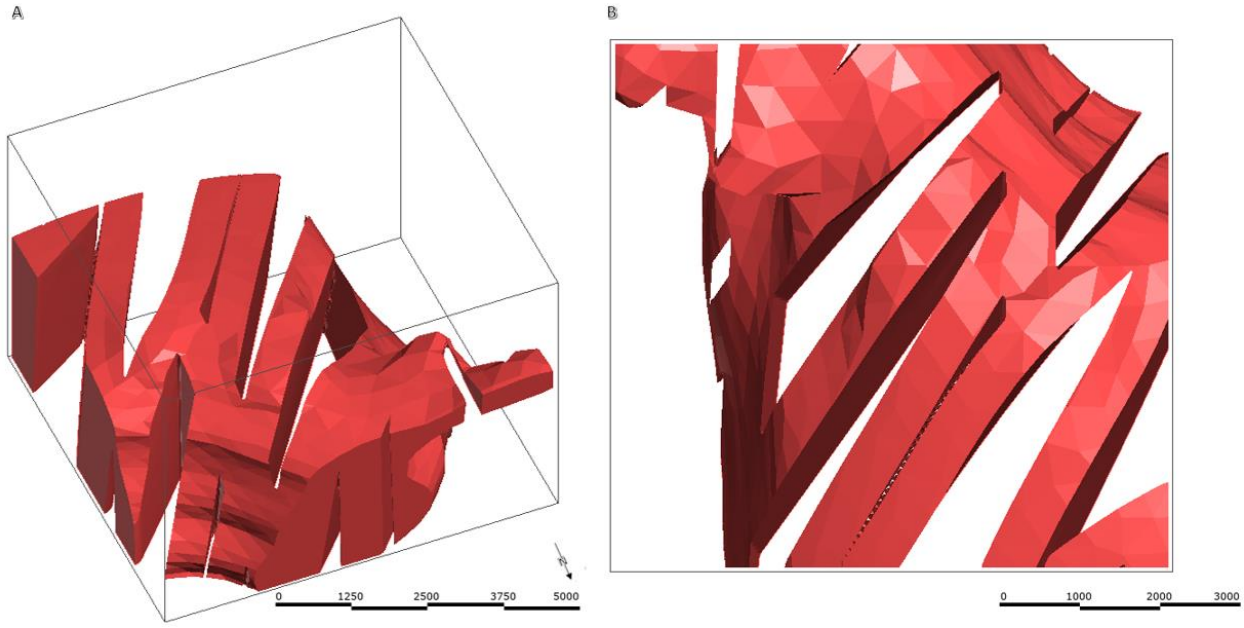

Figure 4.19: "Tauhara potential constraint model" - a combined model showing the constraints required to build a potential model i.e. the fault offset and temperature constraints identified at Tauhara. The red volume represents the area greater than 200°C which is within 310m of the nearest fault A) Oblique view B) Downward view.

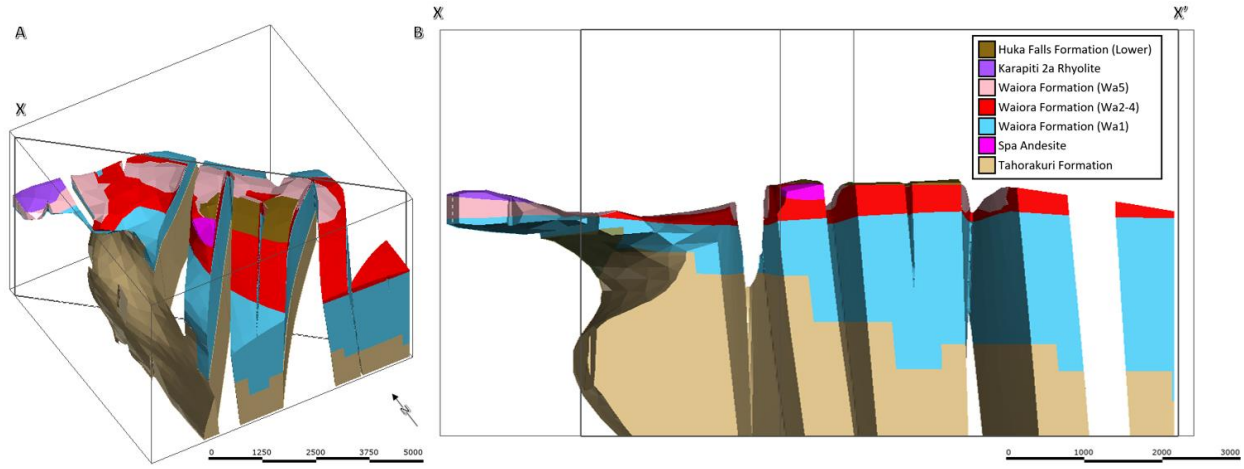

Figure 4.20: Application of the potential constraint model to the Tauhara geology model. A) Oblique view. B) Cross section.

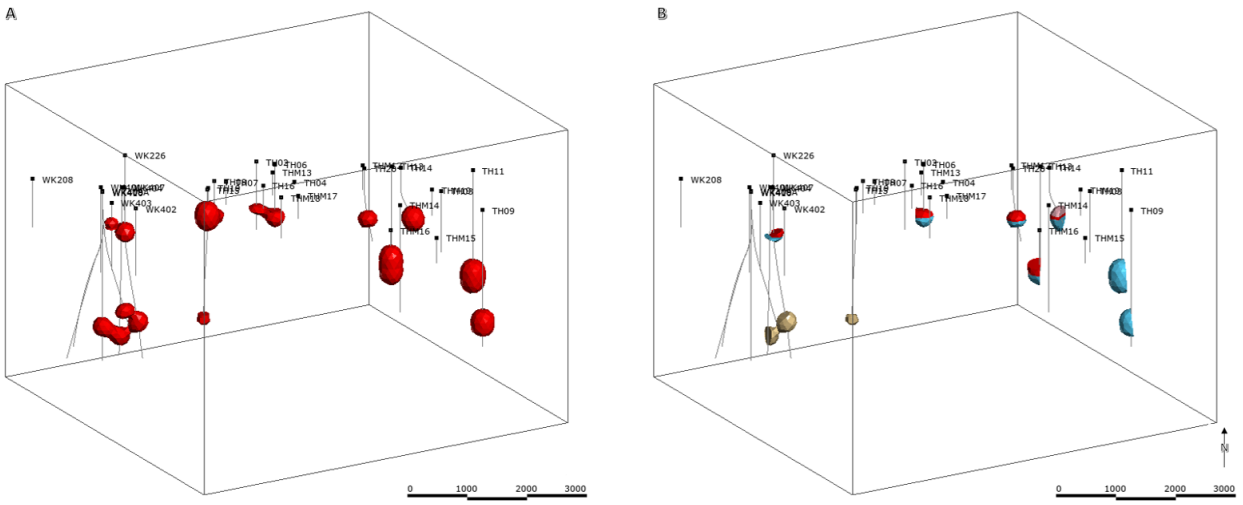

Figure 4.21: A) "Tauhara actual constraint model" which incorporates temperature, fault offset and feed zone margins B) Application of the actual constraint model to the Tauhara geology model.

Table 4.2: Lithologies present in both the Tauhara potential and actual combined models. The volumes of the missing units are removed from the potential combined model.

Lithology	Volume (m^3)
Waiora Formation (Wa5)	701,540,000
Waiora Formation (Wa3-4)	2,781,100,000
Waiora Formation (Wa1)	25,120,000,000
Tahorakuri Formation	33,979,000,000
Whakamaru Group (Wairakei Ignimbrite)	138,940,000
Total	**62,720,580,000**

4.4.2 Muara Laboh

The combined model controls applied at Tauhara used a >200°C temperature boundary and a <200m fault offset boundary (Fig. 4.22, 4.23). The Muara Laboh potential model (Fig 4.22) indicates that the area of potential productivity is restricted to the south/southwestern section of the study area. It has high temperatures close to the surface which increase with depth but to a southward temperature inversion forces the model into a lobe which is also oriented to the north.

Investigation of the properties of the actual model (Fig 4.24) indicate that all units, except the basement rock (the Bukit Barisan Formation), act as conduits for hydrothermal fluids, but this is most prevalent in the

intrusive sequence. There is some evidence of permeability within the PS Andesite Formation, but in much smaller proportions than the other lithologies (Table 4.3).

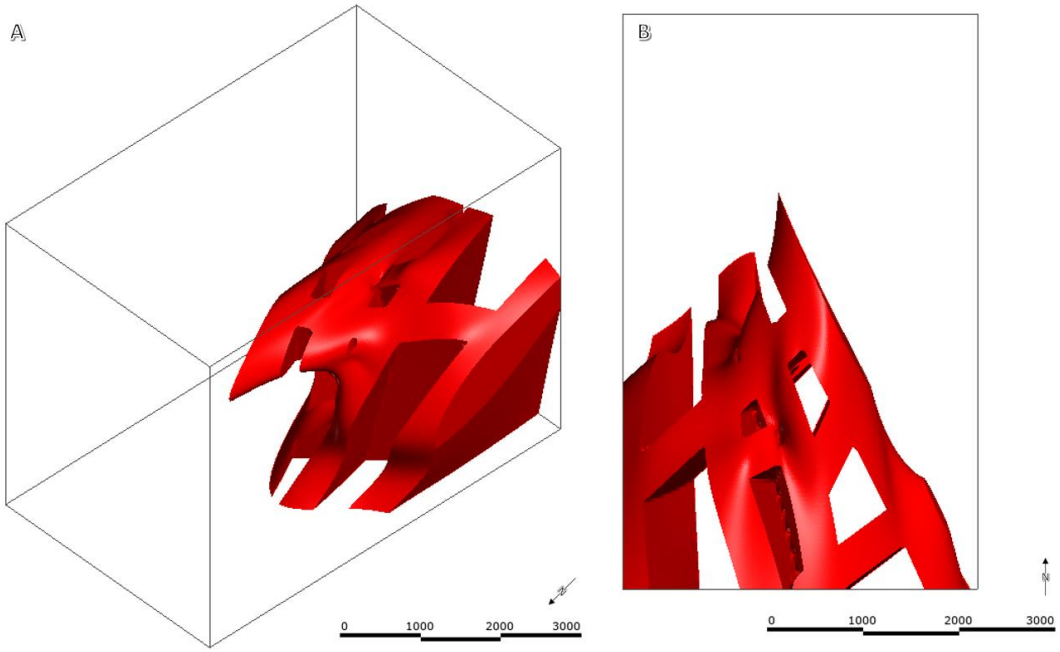

Figure 4.22: Muara Laboh potential constraint model A) Oblique View B) downward view.

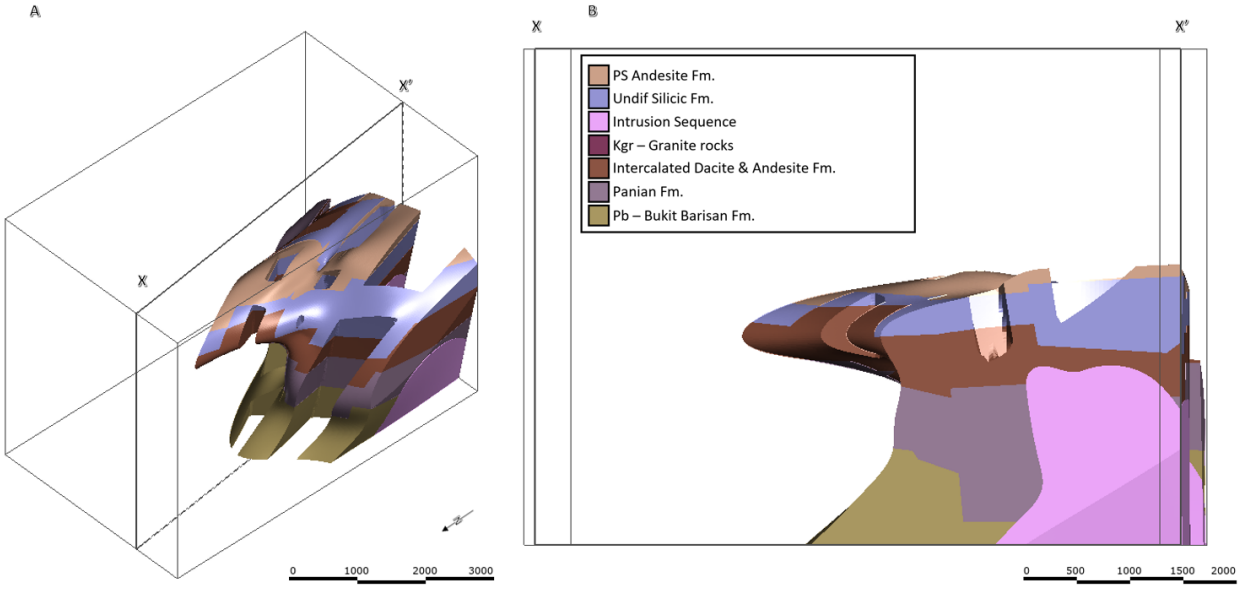

Figure 4.23: Application of the Muara Laboh potential constraint model to the Muara Laboh geology model. A) Oblique view. B) Cross section.

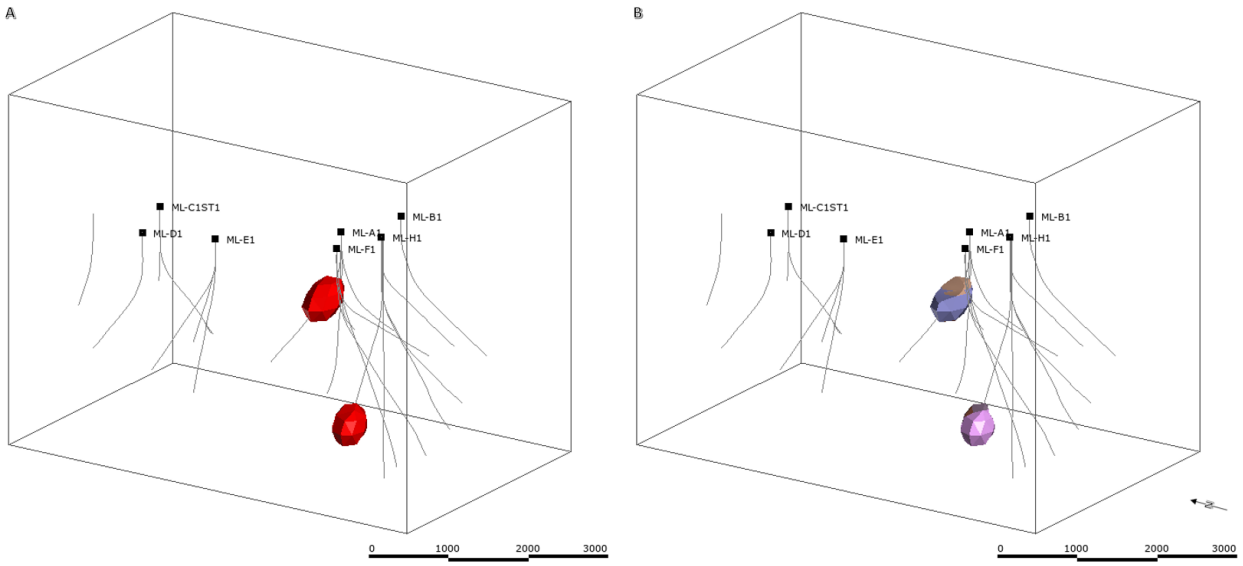

Figure 4.24: Muara Laboh actual constraint model B) Application of the Muara Laboh actual constraint model to the Muara Laboh geology model.

Table 4.3: Lithologies present in both the Muara Laboh potential and current combined models.

Lithology	Volume (m^3)
PS Andesite Fm	275,230,000
Undifferentiated Silicic Fm	1,545,100,000
Intercalated Dacite & Andesite Fm.	2,165,900,000
Painan Fm.	1,931,800,000
Intrusion Sequence	3,376,200,000
Total	**9,294,230,000**

4.5 Block Models

The block modelling process can be used to compare different numerical and categorical data against one another. This was used to find the volumetric and temperature properties of each of the units within the target offset and temperature zones at Tauhara (Table 4.4) and Muara Laboh (Table 4.5). The block modelling calculation process is different to the combined modelling process and uses “resource reports” to assess the relationships of chosen attributes.

4.5.1 Tauhara

The block model calculations at Tauhara show that the Tahorakuri Formation and the Waiora 1 are the largest contributors to the reservoir. The Waiora 1 also contains the highest average temperature fluids, despite being higher in the stratigraphy than the Tahorakuri Formation. Based on the work carried out during the combined model process the Karapiti 2a Rhyolite, Lower Huka Falls Formation and the Spa Andesite may cap the reservoir.

Table 4.4: Summary of the volumetric and temperature properties of the Tauhara reservoir potential model.

Lithology	Volume (m^3)	Average Temperature (°C)
Karapiti 2a Rhyolite	54,20,000	208.36
Lower Huka Falls Formation	79,500,000	208.47
Spa Andesite	33,625,000	210.72
Tahorakuri Formation	34,117,750,000	228.40
Waiora Formation (Wa1)	24,215,875,000	247.43
Waiora Formation (Wa3-4)	278,750,000	229.03
Waiora Formation (Wa5)	684,250,000	218.99
Whakamaru Group (Wairakei Ignimbrite)	138,250,000	206.94
Total	**69,092,250,000**	**235.65**

4.5.2 Muara Laboh

The block model calculations at Muara Laboh indicate that the intrusion sequence makes up approximately one-third of the total reservoir volume.

Table 4.5: Summary of the volumetric and temperature properties of the Muara Laboh reservoir potential model.

Lithology	Volume (m^3)	Average Temperature (°C)
Bukit Barisan Fm	1,099,500,000	228.77
Intercalated Dacite & Andesite Fm.	2,160,500,000	238.57
Intrusion Sequence	3,258,375,000	279.96
Painan Fm.	1,920,000,000	232.53

PS Andesite Fm	263,375,000	210.58
Undif Silicic Fm	1,542,875,000	229.08
Total	**10,249,625,000**	**247.38**

4.6 Refined Models

The completion of the block models introduced new statistics into the combined model and block model processes. The only constraint that these new statistics change, is the feed zone to fault offset distance, but this affects volumetric and temperature data in the block model resource report outputs.

Refined models contained enough detail to test the average and maximum values for the distribution of potential feed zones. Previous testing had only allowed for testing at the distance that was measured manually (measuring the maximum feed zone occurrence offset distance). These were applied to the combined models that are used to describe the constraints, as well as the combined models that incorporated the actual feed zone volumes.

Offset distance was the only value changed in the combined model refinement, and the results were predictable: a change in thickness on either side of the fault margin of the combined model. These new surfaces could undergo the same processes described in the methods to be imported into a block model and be analyzed using a resource report. A summary of this data is available in appendix C.

4.6.1 Tauhara

The initial maximum feed zone to fault offset distance measured was 310m, this distance was measured manually. The block model calculates this same maximum value of 536.49m, but this is too large to be of any use to predicting feed zones at Tauhara, as this would result in most of the model being included within the feed zone potential model. The average offset distance along with the standard deviation (229.77 ± 119.52 m, where 119.52 m = one standard deviation) gives a better indication of the distribution of feed zones from a fault, Fig. 4.25 gives a representation of this distribution. This graph indicated that fracture intensity does not necessarily increase with proximate to faults.

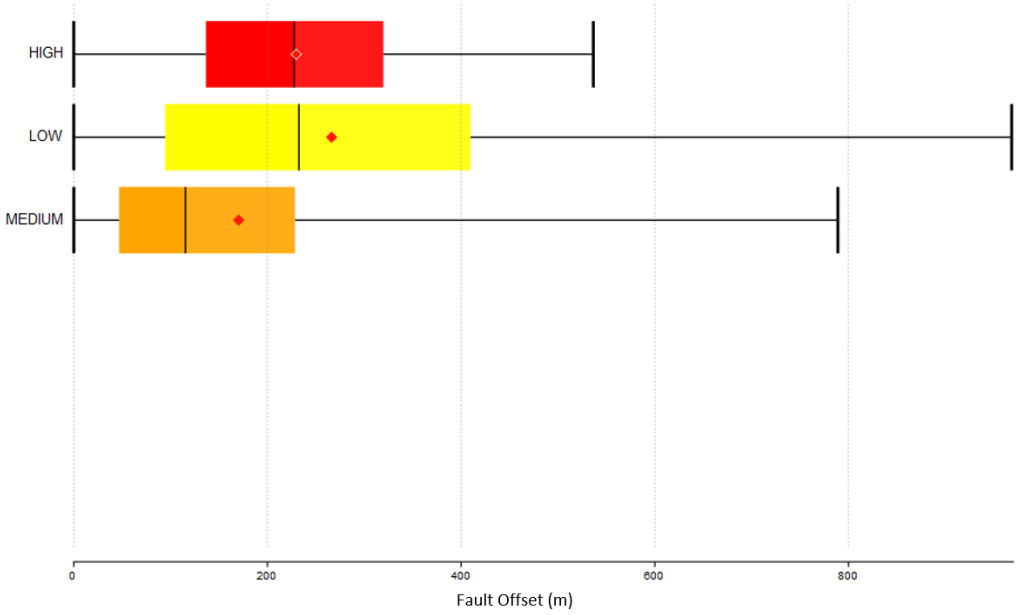

Figure 4.25: Box plot of each feed zone category compared to offset distance at Tauhara.

The new average feed zone to fault offset values were used to create a new combined model i.e. a refined model (Fig. 4.26). The same processes as the previous combined models were applied; creating a potential model, an actual model, and then eliminating geologies from the potential model based on those that are not present in the actual model. This is summarized in Table 4.6 which indicates that many of the relationships, in terms of proportions, are similar as those found using the initial combined model process e.g. Tahorakuri Formation and Waiora 1 are still the dominant reservoir hosts, although the Whakamaru Group has been removed.

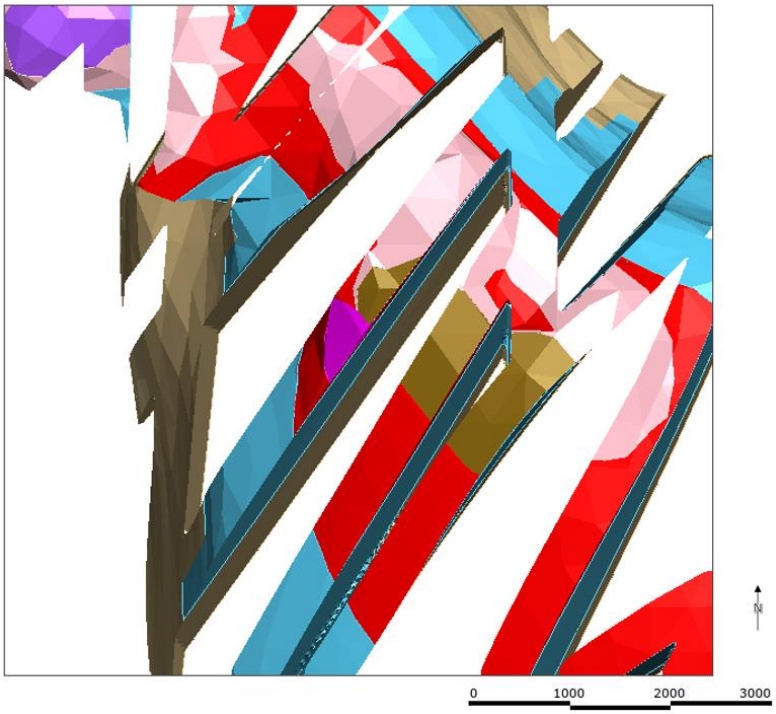

Figure 4.26: Refined offset distance values applied to the potential combined model at Tauhara (229.77m offset).

Table 4.6: Results of the Tauhara refined combined model.

Lithology	Volume (m^3)	Average Temperature (°C)
Tahorakuri Formation	26,736,500,000	228.18
Waiora Formation (Wa1)	18,747,250,000	246.85
Waiora Formation (Wa3-4)	2,128,625,000	228.92
Waiora Formation (Wa5)	530,875,000	218.86
Total	**48,143,250,000**	**230.70**

4.6.2 Muara Laboh

The initial offset measurements used were 200m for high feed zones from faults, the new refined average value used was 84.35 m (± 119 m) with a maximum of 303m. The distribution of this is shown in Fig. 4.27. Assessment of the refined combined model made using these new statistics (Fig. 4.28) shows that there is a much more equal distribution of feed zone distribution between the Intercalated Andesite Dacite Formation, Intrusion Sequence, and Panian Formation (Table 4.7).

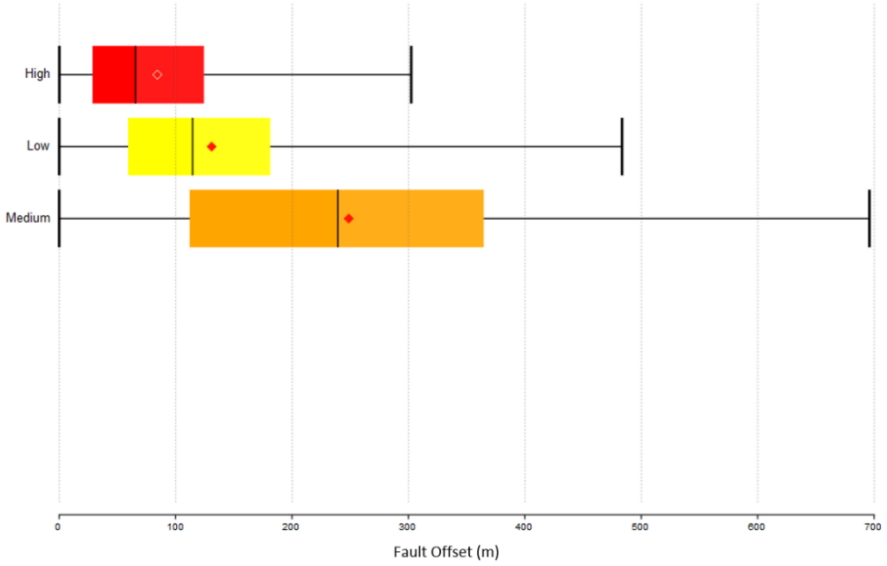

Figure 4.27: Box plot of each feed zone category compared to offset distance at Muara Laboh

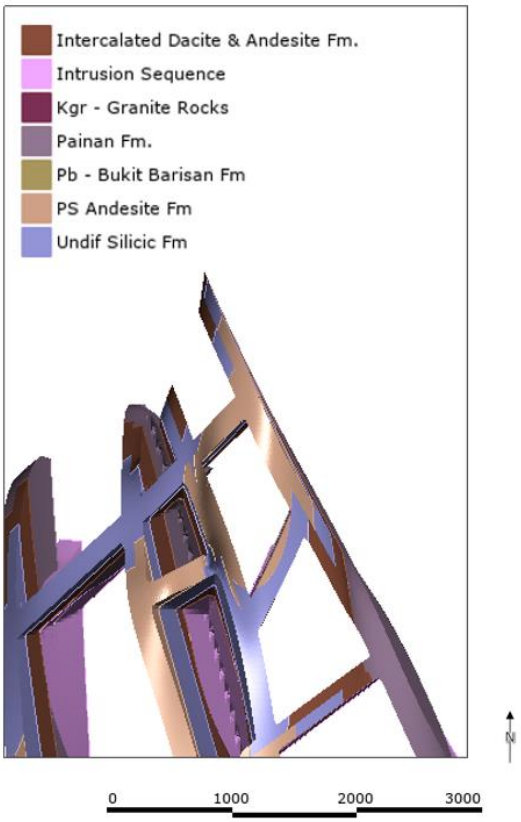

Figure 4.28: Refined offset distance values applied to the potential combined model at Muara Laboh (84.35.m offset).

Table 4.7: Results of the Muara Laboh refined combined model

Lithology	Volume (m^3)	Average Temperature (°C)
Intercalated Dacite & Andesite Fm.	1,060,500,000	237.95
Intrusion Sequence	1,559,250,000	282.68
Painan Fm.	1,010,875,000	230.09
PS Andesite Fm	124,375,000	210.38
Undif Silicic Fm	727,250,000	227.75
Total	**4,482,250,000**	**237.77**

5 Discussion

Datasets from the literature and fieldwork has been used to investigate, create and assess the geothermal parameters, and compare the properties of the Tauhara and Muara Laboh field. This makes temperature measurements, modelling and interpretation the most important aspects of understanding the critical features the geothermal systems. Fluids will be hottest within and adjacent to their source (e.g. fluids associated with an intrusive dike). Convective hot fluids will travel through permeable features, creating areas that are hotter than a typical temperature gradient at the same depth, therefore temperature can also be used as a proxy for permeability. Geology (stratigraphy and structure) is the feature of both sites that have been examined with relation to temperature. This testing has been supplemented by feed zone measurements and feed zone modelling, which indicate where feed zones (areas of increased permeability) have already been measured, as well as their capacity to act as a conduit (high, medium, or low permeability). The processes used in this study have applications in modelling and resource assessment in the geological field, despite there being limitations in the scope of this project.

5.1 Tauhara Geothermal System

5.1.1 System Properties

Tauhara geothermal system occurs within an extensional back-arc basin, a result of subduction of the Pacific plate below the Australian plate, as discussed in chapter 2. The basement rock is hypothesized to have undergone strike-slip faulting; this unit not been recorded in wells at the Tauhara field, but is found in the Wairakei field (Rosenberg, 2017). The younger units are a result of volcanic and caldera eruption events and have undergone primarily normal faulting. Combining back-arc basin extension with the en echelon dextral strike-slip fault overlap will cause a transtensional structure (Seebeck et al., 2014; Wu et al., 2009) (Fig. 5.1). This type of structure would explain the oblique relationship between the faults, the TVZ margins and the basins to the east. These structural relationships can lead to caldera formation and eruptive events (Cole, 1990). There is also commonly a strong inter-relationship between regional faults and caldera-related faults, and the combination of these provide pathways for the hydrothermal fluids which are the essential component of geothermal fields (Sepúlveda et al., 2012).

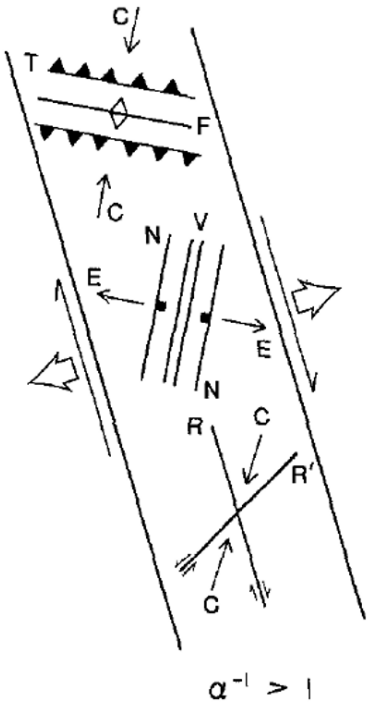

Figure 5.1: Fault and fold orientation under transtension. C, compression axis; E, extension axis; N, normal faults; T, thrust faults, R, Riedel shear/strike-slip; V, extensional fractures (Cole, 1990).

Structure is a fundamental control on geothermal locations within the TVZ (Rosenberg, 2017). The Tauhara geothermal field structural properties are partially attributed to the Whakamaru, Taupo and Waiora Calderas (Rosenberg, 2017; Wood & Browne, 2000) (See Fig. 2.2 and 2.3). High versus low permeability controls the dissipation of heat, whether it happens quickly via convection or slowly by conduction respectively (Rosenberg, 2017). The basement Torlesse rock low permeability makes it a poor conduit, but the fractures within the unit can act as pathways for hydrothermal fluids (Rosenberg, 2017). Active faults result in surrounding permeability within the deep reservoir of the field. At shallower levels in the field these hot fluids disperse, circulate, and mix with meteoric water, mostly within the field's volcanic units (Rosenberg, 2017). These results in high permeability zones occur in porous rock: tuff, volcanic breccia and sandstones, although, there is often variability within these units (Rosenberg, 2017; Rosenberg et al., 2009a).

5.1.2 Modelling Interpretation

The Tauhara field has higher temperatures to the southeast, approximately under Mt. Tauhara. Here the field is closest to the margins of the Whakamaru caldera, which could relate to a higher level of fracturing

and permeability (Milicich et al., 2018). There are also basement faults which are poorly represented in the model due to the model extents. High temperatures occur at this location and predominantly flow through the Waiora 1 unit and the Tahorakuri Formation (Wood & Browne, 2000). The temperatures decrease toward the northeastern section of the Tahorakuri, below the Whakamaru Group. The Whakamaru Group contains the most rapid reduction in temperature. This could be interpreted as a reduction in permeability, or inflowing cold temperatures. The Waiora 3-4 and 5 also show high temperatures but the geothermal gradient decreases in temperature closest to the Huka Falls Formation. There are also drops in temperature in the Karapiti 2a Rhyolite, Spa Andesite and Racetrack Rhyolite (Fig. 5.4 – 5.7).

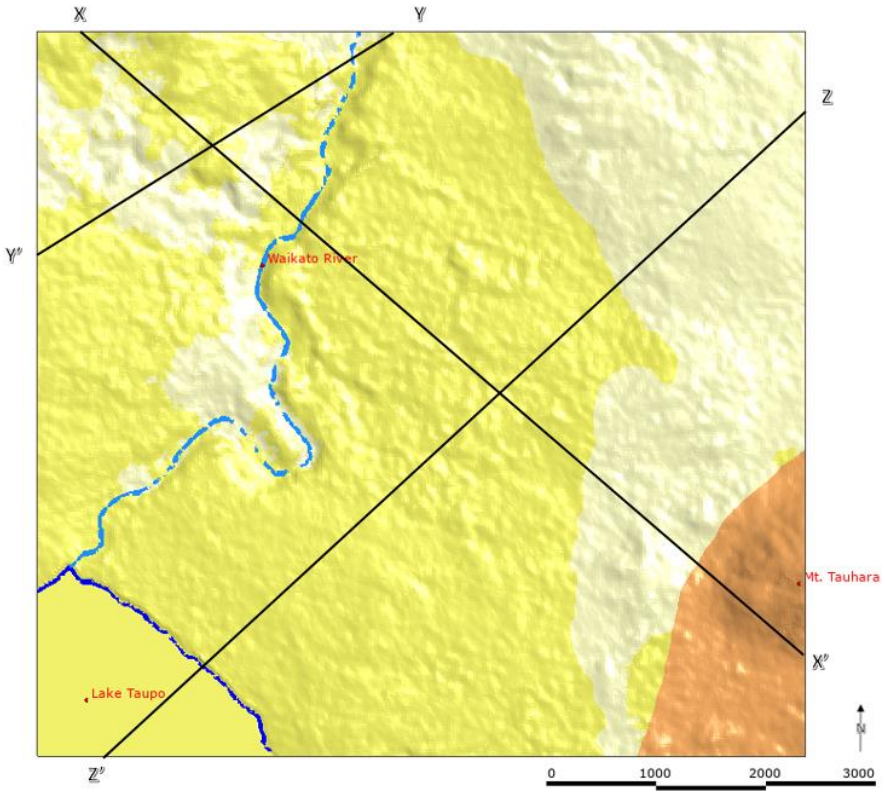

Figure 5.2: Downward view of the Tauhara Field, showing locations of cross sections shown in Figs 5.3-5.5.

During the modelling process, the deeper temperature areas were not adjusted manually due to a lack of temperature data at these depths. Given the nature of upwelling in the area, the temperature isotherm could be adjusted so that the higher temperatures extend downward to better illustrate upwelling around faulting, and within the Tahorakuri and Waiora Formations.

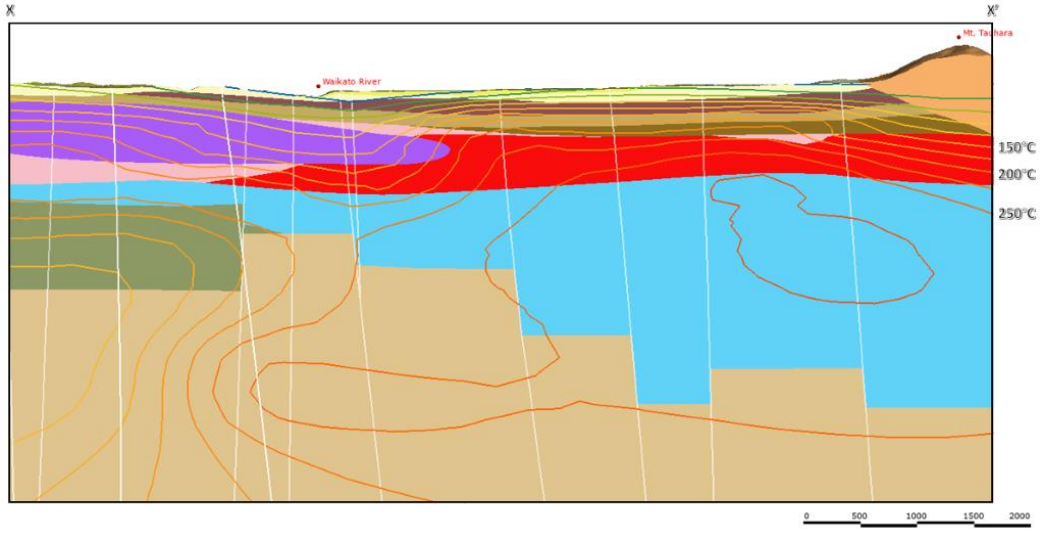

Figure 5.3: NW-SE cross section showing geology and temperature isotherms.

The edge of the modelled field is at the geographical transition between the Tauhara and Wairakei fields, which has a strong relationship between the two fields (Rosenberg, 2017). The model developed in this thesis suggests this relationship is through the shallowest parts of the Waiora Formation to the NW, constrained by the Whakamaru Group, below, and the Karapiti Rhyolite above. Shown as a high temperature (approximately >200°C) bulb at about 1500m below Tauhara (Fig. 5.3, 5.4).

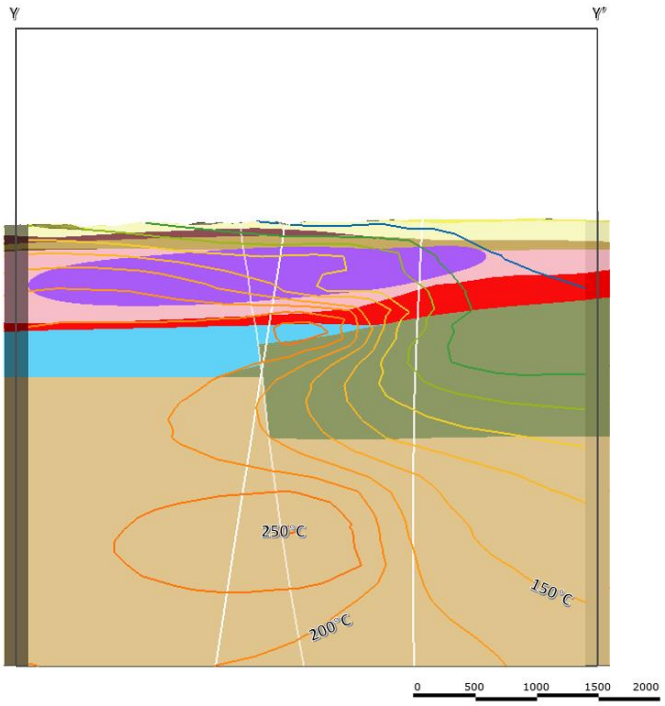

Figure 5.4: NE-SW at NW end of area. Showing geology and temperature isotherms.

Horizontal cross section (Fig. 5.7) of the temperature profile indicates that temperature flow at the field has an NNW-SSE orientation, approximately parallel to the basement faulting. The point at which this differs is around the Whakamaru Group. Upwards the temperature isotherms begin to align more closely with the younger extensional faulting. This is evidence for an association between transtensional structures and permeability, resulting in a change in the orientation of preferential fluid pathways.

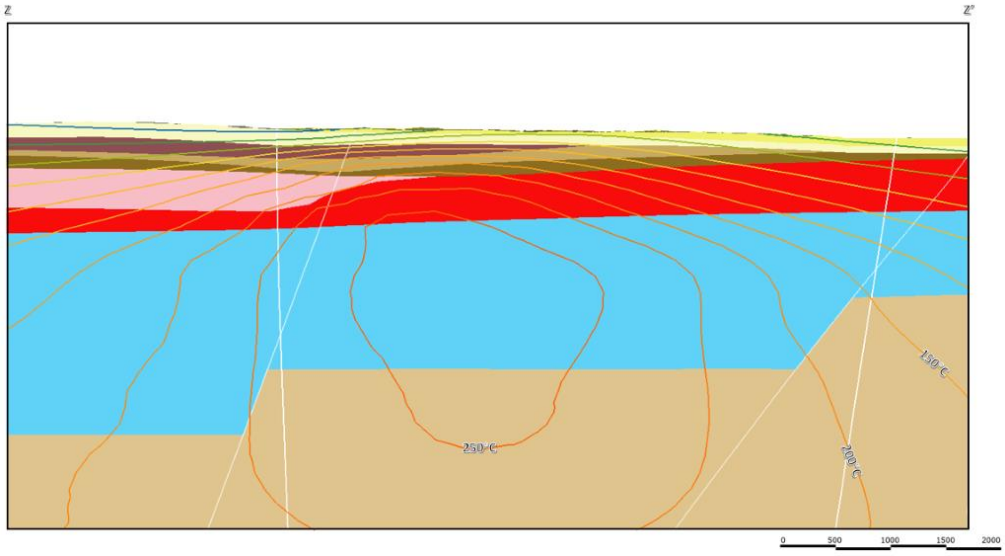

Figure 5.5: NE-SW cross section of the temperature isotherms, faulting (white) and geology.

Feed zone arrangement is difficult to understand in the field. There is an alignment of wells from NE to SW which may cause a bias interpretation of where feed zones occur. There is also a difference in well depth distribution which causes a similar bias. Regardless, the Whakamaru Group to the northwest implies that this is an area with the highest concentration of feed zones. The same occurs in the south east below Mt Tauhara. The same problem arises when examining the relationship of the other observed feed zones and their relationship to faults. The faulting in the area is typical of the extensional normal faults which are relatively evenly dispersed throughout the area, and it appears that wells have been drilled either proximate to, or crossing, these faults.

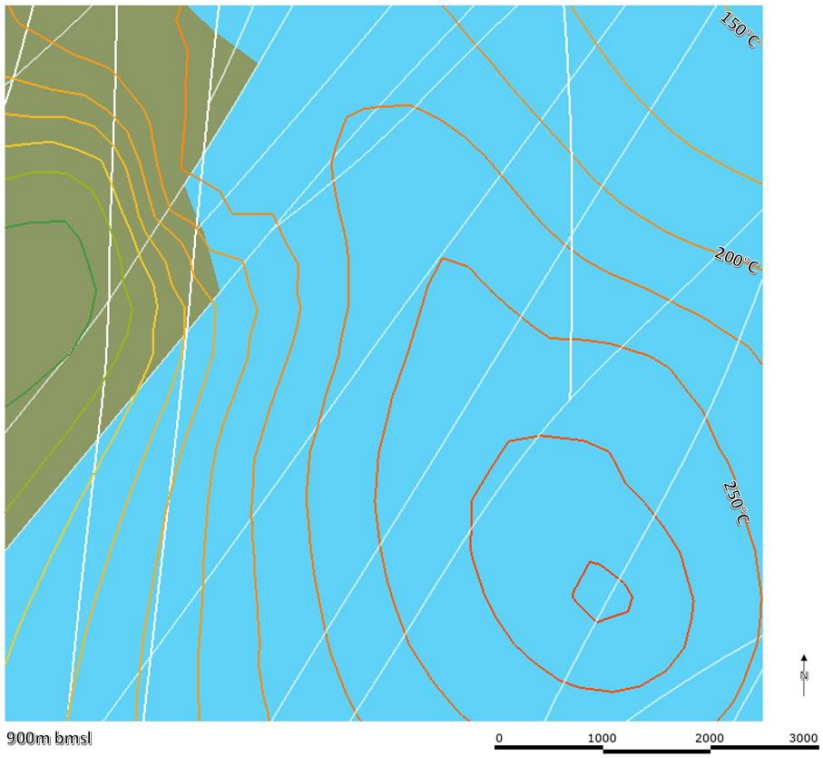

Figure 5.6: Horizontal cross section at 900 MBSL showing geology and temperature isotherms

There is an important distinction to be made between the temperatures observed between feed zones; with those to the northwest of lower temperature than the ones to the south. This suggests that heat source flows from the southeast to the northwest, from a source below either below Mt Tauhara or further south. The areas to the northwest of the field contains the most feed zone measurements but also contains the lowest temperatures in the field (Fig.5.7). This may be linked to interaction between the high permeability and the Waikato River, causing an infiltration of meteoric water.

The use of the refined combined model gives a similar result to the geological, structural, and temperature models, despite being limited to areas that are above 200°C. It shows that the potential resource of the area is largely limited to the Tahorakuri formation and Waiora 1, with some of the resource attributed to the wa3-4 and wa1 (Rosenberg et al., 2009a; Rosenberg, et al., 2009b Wilson & Browne, 2000) (Fig. 4.20). The values provided by this can give useful resource estimates.

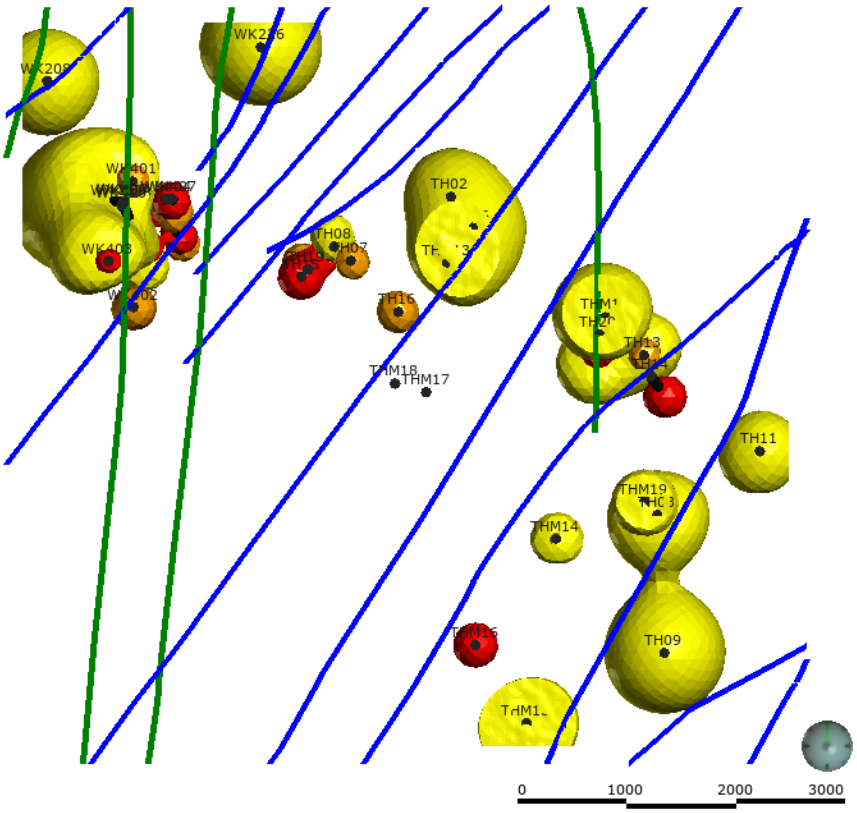

Figure 5.7: Downward view of feed zones at Tauhara.

The temperature flows are at right angles/oblique to the extensional normal faulting and are more closely related to inferred strike-slip faults of the basement or the Waiora Formation, which is thickest in this direction, as the Tahorakuri increases in depth in well measurements.

5.2 Muara Laboh Geothermal System

5.2.1 System Properties

The Great Sumatran Fault (GSF) is a result of oblique subduction of the Indo-Australian plate beneath the Eurasian plate (See Fig. 2.5 and 2.6). The Muara Laboh geothermal system is in a pull-apart basin: a result of the Suliti (north) and Siulak (south) fault segments of the GSF (Fig. 2.6) and represent the basin sidewall faults. There are two main grabens in the basin: one is to the east and is shallow and wide, the other to the west is narrower and deeper. Faulting in the basin is a result of transtension, extensional oblique strike-slip and normal faults with approximately 60-80° dipping. These faults accommodate magmatic intrusions which provide the heat source for the system (Dyaksa et al., 2016; Baroek et al., 2018; Mussofan et al., 2018). The key faults within the basin are (Mussofan et al., 2018):

- N-S: Step over fault. Extension fracture attributed to the development of the pull apart basement horst graben structures.
- NE-SW: Shear fracture (R). These are antithetic to the GSF, both shallow and deep measurements of NE-SW striking features indicate that this is a recently formed structural feature.
- NW-SE: Shear Fracture (R'). These are associated with the GSF, that are observed deeper in the well logs. These have the same fracture orientation as those found at the extremities of the basin i.e. along the Suliti and Siulak faults.

Volcanism shows NW to SE lateral migration of dikes, sills and stocks which extend upwards from depths greater than 4 km. The intrusive complex is a pluton with multiple stages of intrusion. Dikes associated with this complex are interpreted to intrude existing faults and fractures. The reservoir is capped by the Patah Sembilan complex, the transition between the bottom of this unit and the underling silicic volcanics is the most permeable (Mussofan et al., 2018).

Samples tested from the site indicate that most of the sites permeability is a result of fracturing and/or alteration as opposed to the nature of the stratigraphy (Baroek et al., 2018). This does not mean that geology has no influence on permeability, however, extension in brittle lithologies (lava flows, breccia, devitrified tuff) is one of the main causes of permeability in the N and NE. Disparities between modern temperatures and types of alteration and their associated formation temperatures indicate that different hydrothermal systems have been active within the area (Baroek et al., 2018)

Baroek et al. (2018) tested porosity and the relationship of porosity and permeability. This found that there was not a strong relationship between the two and that there was a high variability in the porosity measurements in plug samples of each individual units. Porosity analysis on plug samples are difficult to carry out without incurring samples that are fractured. In most cases lava-breccia and tuff samples had higher porosity, with an exception of a sample ML3-A1 core 2, and lavas and intrusive samples had the lowest porosities. This investigation did find that porosity increases with fracturing, brecciation and dissolution.

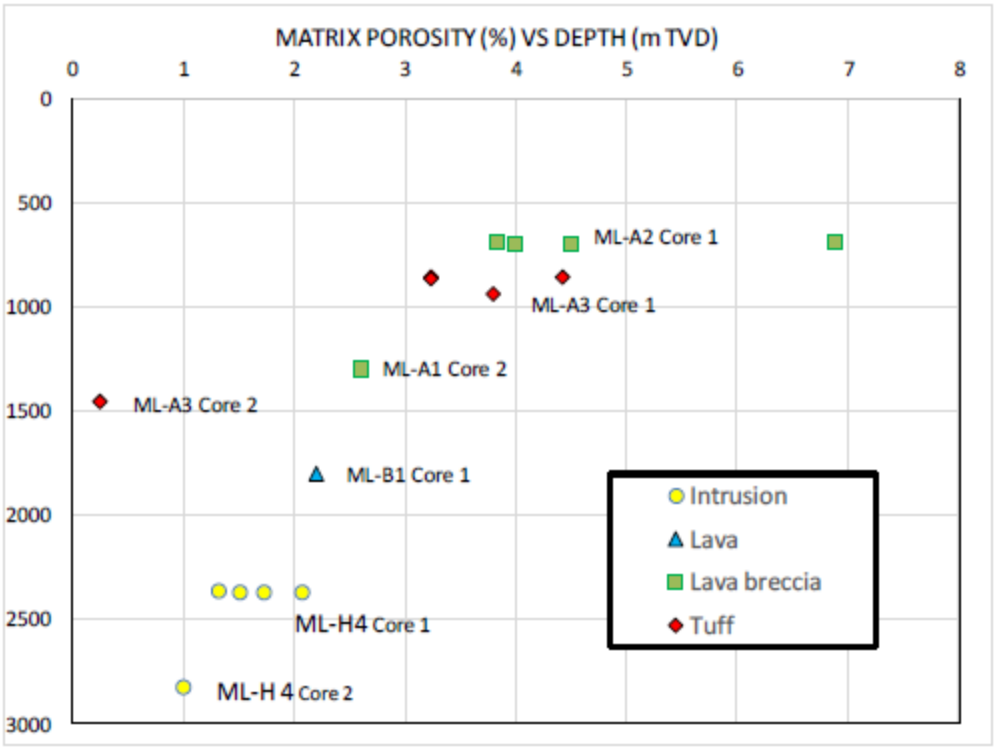

Figure 5.8: Matrix porosity vs. depth at Muara Laboh. Results are based on plug sample testing.

The relationship between faulting and permeability at Muara Laboh is complex. Drilling and BIL logs indicate that a fault may act as a barrier or a conduit at different depths. This is varies based on the stratigraphy, geometry, and how recently the fault was active (Baroek et al., 2018). They key faults identified at Muara Laboh all have associated effective fractures (NW-SE, N-S, NE-SW), although Mussofan et al. 2018 suggest that the N-S fault is the main contributor to fluid flow, permeability and discharge. Fractures provide the main controls on reservoir permeability; relying on fracture dilation and shear. Of these fractures, those that support fluid flow are approximately oriented the same as faulting and in-situ stress. Fracturing is also caused due to hydraulic pressures and exacerbated by dissolution.

Intrusive contacts are associated with deep permeability within the field to the SW, based on fractures analysis. Most dykes follow the GSF trend, but N/NE dikes and fractures are also found in wells. Shallow NE permeability is related to formation contacts. Mineral deposition causes permeability losses in some fractures, especially in areas to the southwest. (Baroek et al., 2018; Mussofan et al., 2018; Stimac, 2019). Temperature modelling carried out by Dyaksa et al. (2018) suggests that the high temperature fluids are sourced from the deep southwest of the reservoir and travels parallel to the NW-SE

faults until passing the Idung Mancung fumarole where is flows parallel to the NE-SW faulting (Situmorang et al,. 2016).

5.2.2 Model Interpretation

Temperature is hottest at the south, isotherms indicate that this heat travels to the north, cooling as it does so (Fig. 5.10). The highest temperatures are measured in and adjacent to the intrusive sequence. This sequence is a series of dikes that are associated with the extensional faulting of the basin and are hypothesized to be the source of upwelling geothermal fluids (Fig. 5.10, 5.11).

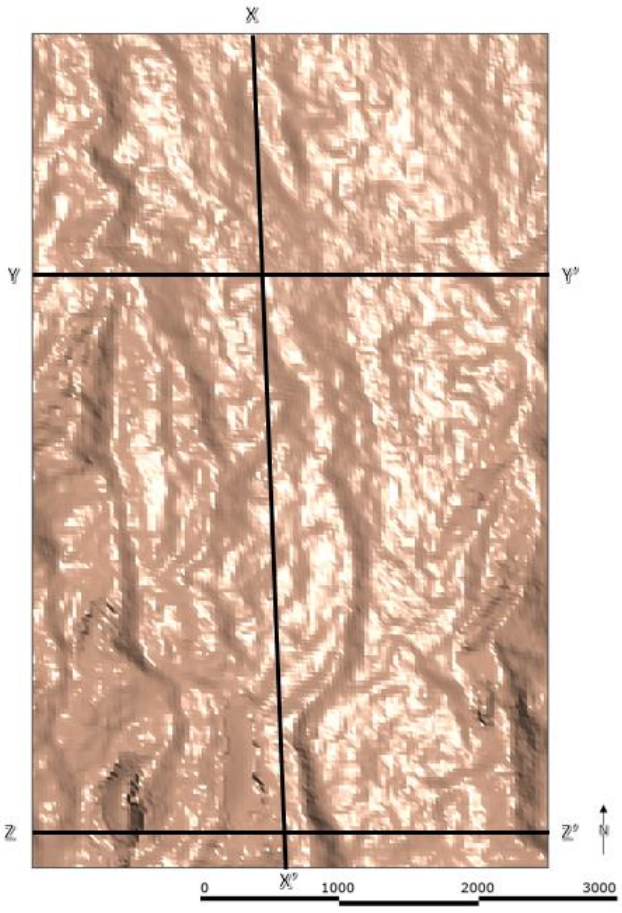

Figure 5.9: Downward view of the Muara Laboh site showing cross section references.

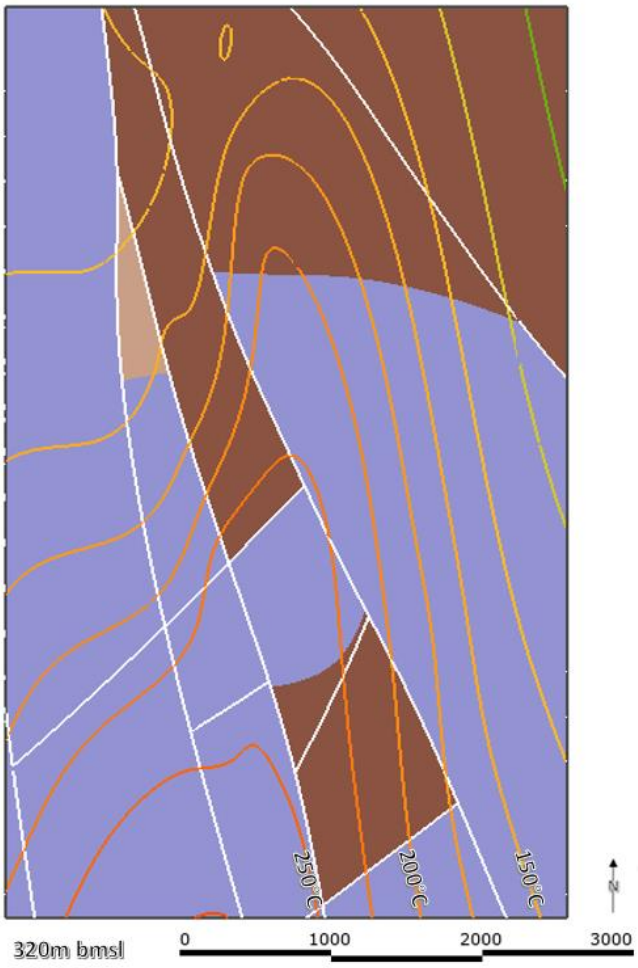

Figure 5.10: Downward view of the Muara Laboh field, sliced at z = -320m. Faults are marked in white. Isotherms occur in 25°C intervals. This cross section has been taken at the depth where the 200°C isotherm reaches the furthest to the south (i.e. away from the heat source).

The temperatures cool toward the north, which is the same direction as the basin decreases in depth. This may be related to a shallowing of the Bukit Barisan Formation, which, even adjacent to the intrusive units, is where there the lowest temperatures are modelled.

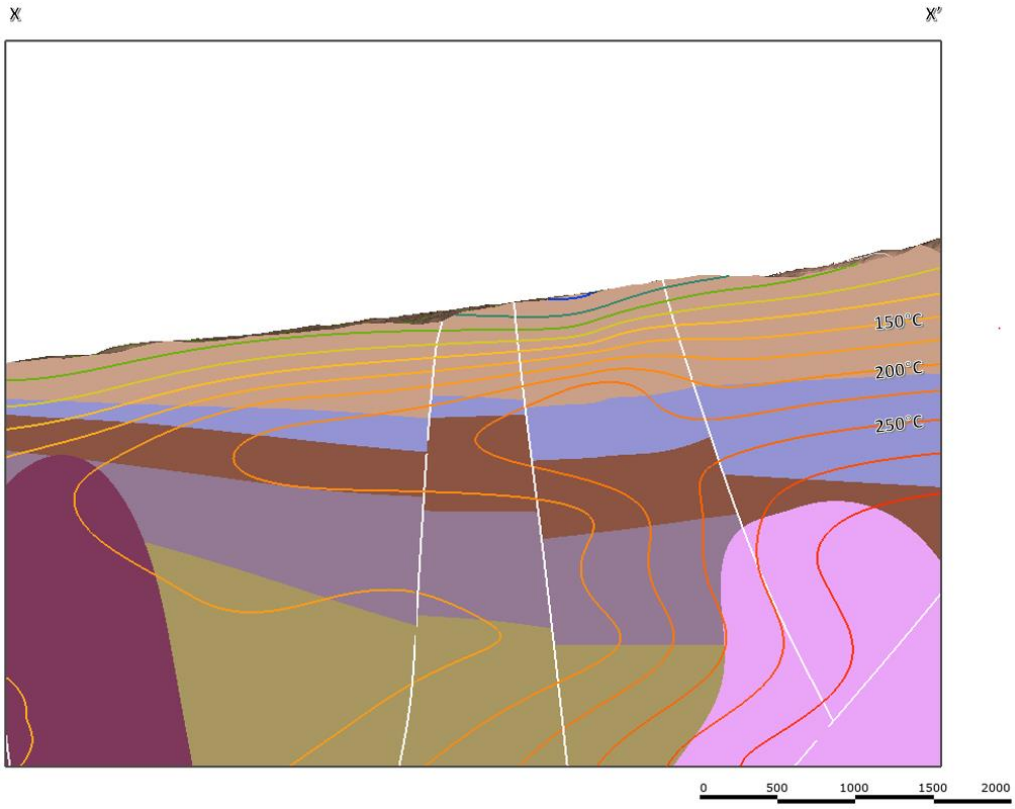

Figure 5.11: NS cross section of the Muara Laboh field. Faults are marked in white. Isotherms occur in 25°C intervals.

The temperature increases in the Painan formation, but there is a decrease in temperature at the contact between this unit and the Bukit Barisan Formation (inferred) (Fig. 5.11). The top surface of the Bukit Barisan has undergone periods of uplift and faulting which the Painan formation infills unconformably (Mussofan, 2018). The Painan Formation is comprised of sedimentary and volcanic materials which by nature have variable permeability. These are not specified in well logs which limit any ability to contribute this decrease in permeability to any feature within the Formation. A unit associated with the upper layers within the Bukit Barisan is the Bakit Barisan limestone (Pb/l) (Mussofan, 2018) This unit is of marbleized, compact and crystalline limestone and is inferred to be of low permeability. It is not identified in well logs or cross sections within the model constraints but is present outside the model. Any links between this unit and the decrease in permeability at this contact have some uncertainty, but this is one possible interpretation. Extensional faulting is known to cause extensional fracture in brittle material (REF), possible in both the Bakit Barisan Formation and the Barisan Limestone. This gives an explanation as to why points of lowest temperatures at this contact are the centre of fault blocks where there are no faults present. Another interpretation may be related to the general decrease in porosity with depth at the site (Baroek et al., 2016, Stimac et al, 2019)

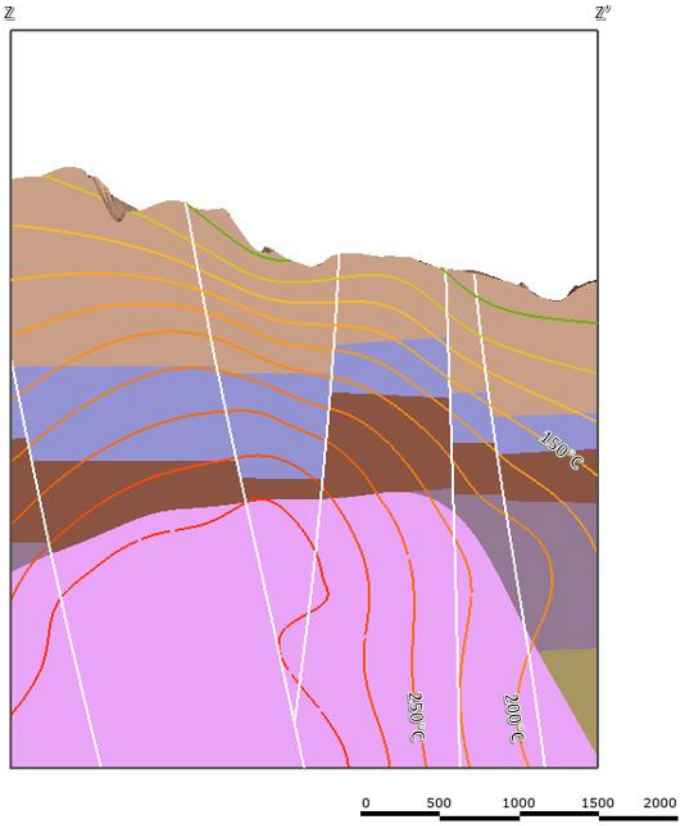

Figure 5.12: Southward view of the Tauhara field. Faults are marked in white. Isotherms occur in 25°C intervals. This shows relationship between the intrusive sequence and its relationship to surrounding units.

The highest temperatures at the field, other than in the intrusive sequence, are (1) in the Intercalated Dacite and Andesite Formation and Undifferentiated Silicic Formation (Fig. 5.10, 5.11, 5.13). This indicates these formations are the main stratigraphic conduits in the geothermal system. The model also shows that (2) the temperatures peak at the contact between the two formations. Both of these observations (1 & 2) are consistent throughout the field, even represented in fault blocks offset. These two units were erupted at about the same time. The older andesitic volcanic sequence contains lava, pyroclastic, and volcanic sediments and sediments, the younger silicic sequence contains mainly tuffs with minor lava, volcaniclastics, and lahar flows.

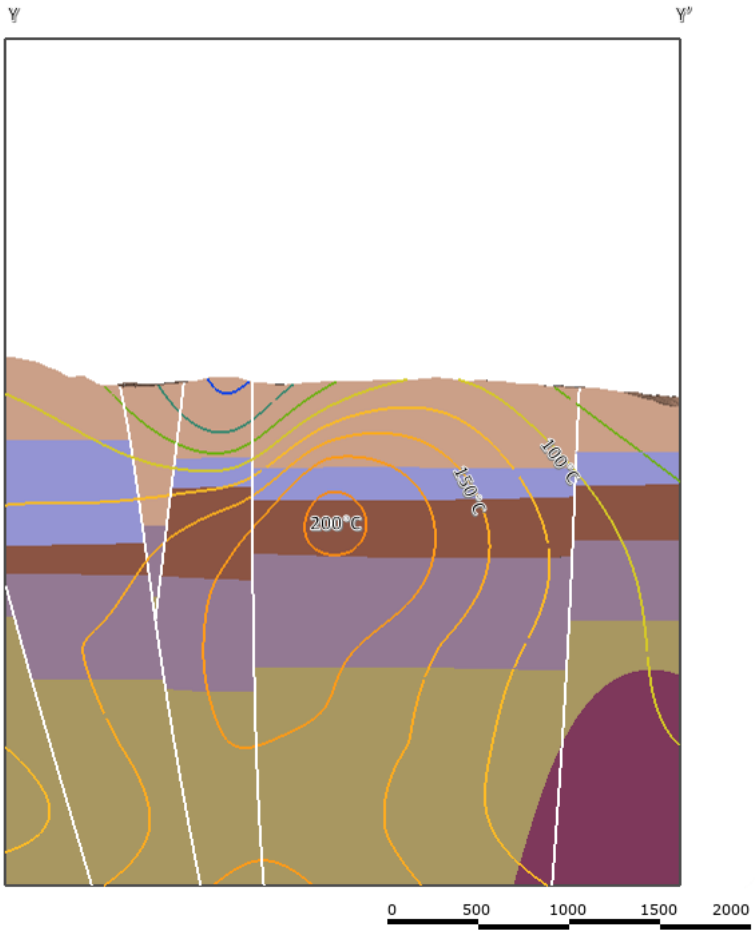

Figure 5.13: Southward view of the Muara Laboh field. Faults are marked in white; isotherms occur in 25°C intervals. This cross section is close to where the high temperature lobe pinches out

The feed zone models (Fig 5.14) indicate that there is a relationship between faulting and feed zones. It is difficult to distinguish whether these are related to the NW-SE older faults or the younger SW-NE Riedel shear in general, but the areas of" high" permeability occur along faults part of the cross-basin fault zone. Regardless, block model data indicates that there is average fault offset of 84m. These two factors indicate that there is a strong relationship between all faults and feed zone occurrence and the feed zones only occur within a relatively small buffer around these faults.

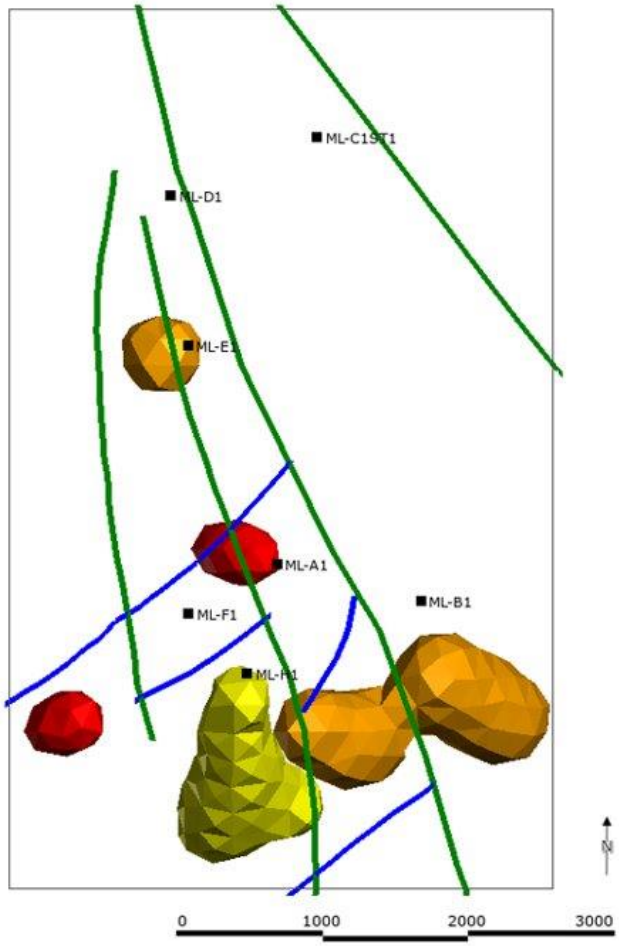

Figure 5.14: NS cross section of the Muara Laboh field. Faults are marked in white. Isotherms occur in 25°C intervals.

Part of the models and interpretations of the Muara Laboh study area are based on the 2016 Dyaksa temperature model. An updated model has since been developed by Stimac et al. (2019), however, due to parallel development of this model and those created for this thesis, several of these changes have not been implemented due to time restraints. The key difference is the use of resistivity surveys which identify one of the NW-SE faults as impermeable (see Fig. 5.14., the closest fault to east of well ML-D1). The impact of this is the partial restriction of high temperatures to the western side of the fault. This model also suggests a less prominent high temperature lobe that seen in Fig. 4.13 and 4.14. This changes the way that fluid flow travels through different lithologies and means that there is less distinction between each of the different units. The combined, block, and refined combined models used a temperature profile with a d lobe to the north. However, this change would have no effect to the average feed zone offset and would have little change on the depth of high temperature within the stratigraphy, this means that the models

created in this thesis still represent similar trends as would be the case had the updated temperature model been used and is therefore still representative of the fields geothermal properties.

5.3 Comparisons between Tauhara and Muara Laboh Geothermal Systems

Tauhara and Muara Laboh have similarities in faulting and volcanic influence. Both occur in oblique subduction zones that have resulted in areas of transtension and influenced by ring-faulting in caldera margins.

Tauhara geothermal field forms in the TVZ extensional system. Underlying this is likely to be a strike-slip faulting system within the basement rock, a function of the North Island Shear Zone which results in a transtensional fault system when the two fault trends are overlaid (Cole, 1990; Rowland et al., 2004). Areas where these features are superimposed are more susceptible to hydrothermal upwelling and the associated higher temperatures (McNamara et al., 2016; Rosenberg, 2017). These features can also make areas in the field more prone to meteoric water infiltration, resulting in colder temperatures. Tauhara field falls within the Whakamaru, Taupo and Waiora Calderas.

Muara Laboh Geothermal field forms in a transtensional pull-apart basin (Muraoka et al., 2010). A product of the Suliti and Siulak Fault segments of the GSF. The field is marginal to the Patah Sembilan Caldera. The extensional environment has resulting in the infiltration of dikes which are the source of the hydrothermal fluids (Stimac et al., 2019). The Patah Sembilan Caldera is beyond the study area constraints, which makes it difficult to interpret the magnitude of the associated normal faulting and its influence. However, it is hypothesized that the caldera contributes to the upwelling of hydrothermal fluids from the southwest.

The main difference between the two sites is the relationship between geology and permeability. Above the basement rock (Askari et al., 2009), hydrothermal fluids circulate through the Tahorakuri and Waiora Formations of Tauhara, which are high permeably and capped by the fine low permeability units (Huka Falls and younger) (Chi & Browne, 1991; Rosenberg et al., 2009a; Rosenberg, et al., 2009b Wilson & Browne, 2000). At Muara Laboh there is less reliance on geology but more on fracturing due to faulting. Two geological units are identified as the stratigraphic conduits: the andesitic volcanic sequence and the silicic volcanic sequence. But the average fault offset is 84 ± 69 m which indicates that fracturing only occurs in at a limited distance from faults. By contrast, the fault offset at Tauhara is 230 ± 120 m.

5.4 Limitations

There are potential limitations in this project. General constraints include the availability data, data accuracy, and time constraints, but each step of model building and model assessment introduces new features that effect the accuracy of the project. These limitations are mitigated, where possible, using literature and an understanding of geological principles but there are still opportunities for improvement.

There are two main errors in modelling geology, both in stratigraphy and structure. In terms of stratigraphy: the maximum well depth at both Tauhara and Muara Laboh does not contact the basement rock, meaning that that these contacts in both are inferred. This restricts the ability to assess the nature of fluid flow through these units, but is mitigated by using descriptions of the unit properties found at local sites (both of low permeability) and an understanding of the impact of the faulting relationships (both occur in extensional environments i.e. leading to fracturing).

At each site there are different reasons for limitations in temperature modelling. At Tauhara temperature modelling at depth is based on a few deep wells, clustered to the northwest and southwest, with little information available from the shallow wells between. This means that much of the temperatures modeled at the center of the reservoir are interpreted, but this is justified because little variability is recorded in the geology. The interpretations made about the areas of permeability in the field suggest that there will be major features which influence fluid flow between these two zones. At Muara Laboh there are two features that have introduced limitations of accuracy of the temperature model. The first is that some well logs measure temperature but not geology. The means that a unit at a set depth in the geological model has been interpreted from cross-sections, as opposed to recorded in well logs, and may be assigned a temperature that is not truly representative of that unit, meaning that temperatures (and respective fluid flow) is falsely attributed to a specific unit. This is most prevalent at the north of the site. This is difficult to mitigate but has been addressed by examining the trends of temperatures within lithologies elsewhere in the model to assess whether the temperature model shows similar trends. The second feature that has influenced confidence in the temperature model is the introduction of the Dyaksa et al. (2018) model. This suggests that the temperature is more closely aligned with the faulting, which is supported by the fault-feed zone offset relationship found in this thesis. This would cause the orientation of high temperature isotherms to trend SE-NW as opposed to S-N as shown in the temperature models of this project. Given the point in the project that this was realized, it was too late to make any adaptations. It is not thought however that such changes will make a substantive difference to the models.

In this project feed zone modelling had a high inherent uncertainty as the sites did not use the same feed zone measurement techniques, as well as the way the feed zone data was recorded. Firstly, the feed zones modelled in this project do not consider whether the feed zones are classified as injection or production. This is because the main aim is to identify trends in permeability, as opposed to optimizing hydrothermal productivity. Another feature that has affected both sites, particularly for comparison, is that the categories high, medium and low are artificial: neither site uses numerical values to assign these classifications.

There are two main issues unique to Tauhara, the first is the way that feed zone classification are measured. Classifications at Tauhara are assigned on observations made during drilling, well-by-well, meaning that a high measurement at one well may equate to a medium measurement at another. The second point of inconsistency in feed zone measurement is because there is often more than one feed zone encountered in a well. This is an issue because the fluid flow associated with each feed zone may cause interference when measuring the fluid flow other feed zones. This means that higher resolution analysis such as investigating the relationship between permeability and units within a specific well interval (e.g. Well WK208 from –125m to –200m between) is difficult to achieve with accuracy. This type of inaccuracy does not have a great impact on this project, given the scale, but should still be considered when examining the results. At Muara Laboh feed zones are not measured, rather, interpreted from borehole image fracture logs. This difference between feed zone measurement techniques is another aspect that makes fluid flow comparisons difficult between the two sites, although it is acceptable when examining the site by itself. There are, however, far fewer feed zone measurements (41 in total).

There are several limitations that occur within the combined models, both in terms of the accuracy of the input data, as well as the limitations of what they can represent. The combined models are a function of their input models, and they represent aspects of the modelled geology, feed zone, and temperature. This means that limitations to any of these models will compound within the combined model. There is no effective way to mitigate this other than to address the root issues of the input model. Another restriction is the simplification of the features being tested. For instance, at both Tauhara and Muara Laboh, there are no differences between the faults; in the model all faults are assumed to induce permeability, however, there are likely to be few faults which have any effect on this constraint. Another example is that there may be subtleties within the geology that change the nature of fluid flow that are not identified within the constraint model. Whether these be pockets of resistivity or specific impermeable layers within the geology, these are not specified in the model and each of the units are treated as though they are homogenous.

5.5 Future Recommendations

Should similar tests be carried out in the future there are several aspects that would improve the efficiency of the workflow, and there are also aspects that could be added to provide a more comprehensive assessment.

In terms of workflow optimization, this could be improved by the introduction of block model assessment prior to temperature modelling, and the removal of manual fault offset measurement techniques. This would result in a more time-efficient modelling process, removing the need for refining of the models, as they would already use the block model-calculated measurements. This was only a factor in this thesis as the block model tool was applied after having already made the combined models.

At Tauhara and Muara Laboh, there is an opportunity to incorporate more data. At Tauhara, at least one well drilled at the centre of the field would provide a much higher confidence in the interpretations on fluid flow. Additionally, this thesis uses only a few wells from the greater Wairakei-Tauhara field well dataset. Using all wells would generate a larger model which would provide greater opportunities to assess the parameters tested in this thesis. At Muara Laboh, the updated Stimac et al. (2019) model should be introduced and tested using the same processes as in this thesis.

There is also an opportunity to investigate specific faults as in this thesis all faults have been considered to have the same permeabilities or capacity for influencing fluid flow. The results of the modelling indicate that this may not be the case, that some faults do not have as greater control as others. A more selective combined model that uses only the faults which are identified as permeable would create a more representative assessment of the volume of the reservoir volumetric analysis.

Alteration is known to influence permeability. Creating an alteration model as another input alongside the geology, feed zone and temperature input would allow for a more comprehensive understanding of the fluid flow controls on the geothermal system.

5.6 Industry Application

This method used in the thesis establish an effective workflow for understanding the properties of a geothermal reservoir and how these properties influence hydrothermal fluid flow. This is important when considering geothermal resource analysis, where understanding potential areas of high permeability, the

volume of these areas, and whether these are zones of inflow or outflow of the reservoir (i.e. injection vs production) is so important.

6 Conclusions

This thesis examines two active geothermal systems: Tauhara (North Island New Zealand) and Muara Laboh (Sumatra, Indonesia). These fields were investigated to understand the properties of their geothermal reservoirs and what geological constraints there are that affect flow of hydrothermal fluids. The constraints identified at either site were compared against one another to identify points of similarity and difference. Academic studies and geothermal energy industry well exploration drilling provided data to build three-dimensional models to represent geology, feed zones and temperature using the Leapfrog Geothermal software. These models were tested using features within the same software: combined and block modelling. The results show that:

1. At Tauhara, permeability is associated with the Taupo Volcanic Zone (TVZ) and inferred strike slip faults related to the North Island Shear Belt (NISB), the Taupo and Whakamaru caldera sequence collapse structures and several of the geological units. Hydrothermal upwelling is sourced from magmas not observed in the well logs. These are found in intrusive bodies in the lower Waiora 1 or Tahorakuri but most likely to occur within the basement Torlesse, particularly at the southeast of the study area where there are recorded TVZ, NISB and caldera margins present. Infiltration of meteoric water of the Waikato River (inferred) percolate downward at the northeast of the study area where there are interactions between the TVZ and NISB faults. Fluid flow within the reservoir occurs mostly in the Tahorakuri Formation and Waiora Formation (mostly the Waiora 1 unit) and is capped by the Huka Falls Formation. The average offset distance of feed zones from faults (230±120m) indicates that geology is a larger control within the reservoir that faulting, however, temperature orientation from hottest in the southeast to the coldest in northwest shares the same orientation of the NISB faults and so geology and NISB faults are interpreted as the main controls on permeability within the reservoir margins.

2. At Muara Laboh permeability is closely confined to fractures as a result of extensional faulting within the pull-apart basin. The source of hydrothermal fluids is associated with the intrusive sequences at the southwest of the site, which intrude via the oblique faulting of the pull-apart basin (and hypothesized Mt Patah Sembilan caldera collapse). The silicic sequence and andesitic

sequence act as the main conduit for hydrothermal fluid, however, here is little difference in porosity between the different geological units and this is likely due upwelling fluids becoming trapped by the overlying clay cap. The average offset distance of feed zones from faults (84±70m) shows that feed zones occur close to faults indicating that fluid flow within the reservoir is controlled structurally controlled.

3. Despite having differences in the controls of fluid flow within the reservoirs, both sites are situated in oblique strike-slip environments which are attributed to the formation geothermal activity within the sites.

References

Ármannsson, H. (2013). Application of geochemical methods in geothermal exploration.

Ashwell, P., Kennedy, B., Gravley, D., von Aulock, F., Cole, J. (2013). Insights into caldera and regional structures and magma body distribution from lava domes at Rotorua Caldera, New Zealand. Journal of Volcanology and Geothermal Research 258, 187-202.

Askari, M., Azwar, L., Clark, J., & Wong, C. Injection Management in Kawerau Geothermal Field, New Zealand.

Balat, M., Balat, H., & Faiz, U. J. E. S., Part B. (2009). Utilization of geothermal energy for sustainable global development. 4(3), 295-309.

Baroek, M., Stimac, J., Sihotang, A. M., Putra, A. P., & Martikno, R. (2018). Formation and fracture characterization of the Muara Laboh geothermal system, Sumatera, Indonesia. In Proceedings Geothermal Resource Council (pp. 42).

Bibby, H. M., Risk, G. F., Caldwell, T. G., & Heise, W. (2009). Investigations of deep resistivity structures at the Wairakei geothermal field. Geothermics, 38(1), 98-107.

Bignall, G., Milicich, S. D., Ramirez, L. E., Rosenberg, M. D., Kilgour, G. N., & Rae, A. J. (2010, April). Geology of the wairakei-Tauhara geothermal system, New Zealand. In Proceedings Worlds Geothermal Congress (pp. 25-30).

Bixley, P. F., Clotworthy, A. W., & Mannington, W. I. (2009). Evolution of the Wairakei Geothermal Reservoir during 50 years of production. Geothermics, 38(1), 145-154.

Boden, D. R. (2016). Geologic fundamentals of geothermal energy: CRC Press.

Browne, P. (1978). Hydrothermal alteration in active geothermal fields. Annual Review of Earth and Planetary Sciences, 6(1), 229-248.

Browne, P. (1984). Lectures on geothermal geology and petrology: UNU Geothermal Training Programme, National Energy Authority Reykjavik.

Burton, P. W., & Hall, T. R. (2014). Segmentation of the Sumatran fault. Geophysical Research Letters, 41(12), 4149-4158.

Cant, J., Siratovich, P., Cole, J., Villeneuve, M., & Kennedy, B. J. G. E. (2018). Matrix permeability of reservoir rocks, Ngatamariki geothermal field, Taupo Volcanic Zone, New Zealand. Geothermal Energy 6(1), 2.

Cattell, H. (2015). Volcanic evolution of the Huka Group at Wairakei-Tauhara Geothermal Field, Taupo Volcanic Zone, New Zealand. Unpublished PhD thesis, University of Canterbury, Christchurch, New Zealand.

Cattell, H., Cole, J., Oze, C.. (2016). Volcanic and sedimentary facies of the Huka Group arc-basin sequence, Wairakei–Tauhara Geothermal Field, New Zealand. New Zealand Journal of Geology and Geophysics 59(2), 236-256.

Chambefort, I., Buscarlet, E., Wallis, I. C., Sewell, S., & Wilmarth, M. J. G. (2016). Ngatamariki geothermal field, New Zealand: Geology, geophysics, chemistry and conceptual model. 59, 266-280.

Chi, M., & Browne, P. (1991). Alteration mineralogy of sediments on the Huka Falls Formation of the Te Area, Wairakei. Paper presented at the Proc 13th New Zealand Geothermal Workshop.

Cole, J. W., & Spinks, K. D. (2009). Caldera volcanism and rift structure in the Taupo Volcanic Zone, New Zealand. Geological Society, London, Special Publications, 327(1), 9-29.

Cole, J., Milner, D., & Spinks, K. (2005). Calderas and caldera structures: a review. Earth Science Reviews 69(1-2), 1-26.

Cole, J.. (1978). Andesites of the Tongariro Volcanic Centre, North Island, New Zealand Journal of Volcanology and Geothermal Research 3(1-2), 121-153.

Cole, J... (1990). Structural control and origin of volcanism in the Taupo volcanic zone, New Zealand. Bulletin of Volcanology 52(6), 445-459.

Davidson, J. R. J. (2014). The Effect of Fractures on Fluid Flow in Geothermal Systems, Taupo Volcanic Zone, New Zealand. Unpublished doctoral dissertation). University of Canterbury, New Zealand.

Dyaksa, D. A., Ramadhan, I., & Ganefianto, N. (2016). Magnetotelluric Reliability for Exploration Drilling Stage: Study Cases in Muara Laboh and Rantau Dedap Geothermal Project, Sumatera, Indonesia. Paper presented at the 41st Workshop on Geothermal Reservoir Engineering Proceedings

Garg, S. K. (1984). Formation compaction associated with thermal cooling in geothermal reservoirs. Advances in Water Resources, 7(4), (pp. 188-191). doi:10.1016/0309-1708(84)90017-4

Hochstein, M. P., & Moore, J. N. (2008). Indonesia: Geothermal prospects and developments. Geothermics, 37(3), 217-219. doi:10.1016/j.geothermics.2008.04.002.

Hurwitz, S., Christiansen, L. B., & Hsieh, P. A. (2007). Hydrothermal fluid flow and deformation in large calderas: Inferences from numerical simulations. Journal of Geophysical Research - Solid Earth, 112(B2), B02206. doi:10.1029/2006JB004689.

Lagat, J. (2006). Hyrothermal alteration Mineralogy. Retrieved from https://orkustofnun.is/gogn/flytja/JHS-Skjol/Kenya%202006/0203JohnLagat.pdf

Lagat, J. K. E. (2007). Hydrothermal alteration mineralogy in geothermal fields with case examples from Olkaria domes geothermal field, Kenya. 001045504.

Mayer, K., Scheu, B., Montanaro, C., Yilmaz, T. I., Isaia, R., Aßbichler, D., & Dingwell, D. B. (2016). Hydrothermal alteration of surficial rocks at Solfatara (Campi Flegrei): Petrophysical properties and implications for phreatic eruption processes. Journal of Volcanology and Geothermal Research, 320, 128-143.

McNamara, D. D., Bannister, S., Villamor, P., Sepúlveda, F., Milicich, S. D., Alcaraz, S., & Massiot, C. (2016). Exploring structure and stress from depth to surface in the Wairakei Geothermal Field, New Zealand. In Proc. 41st Stanford Workshop on Geothermal Reservoir Engineering, SGP-TR-209.

Milicich, S. D., Bardsley, C., Bignall, G., & Wilson, C. J. N. (2014). 3-D interpretative modelling applied to the geology of the Kawerau geothermal system, Taupo Volcanic Zone, New Zealand. Geothermics, 51, 344-350.

Milicich, S. D., Pearson-Grant, S. C., Alcaraz, S., White, P. A., Tschritter, C. J. N.. (2018). 3D Geological modelling of the Taupo Volcanic Zone as a foundation for a geothermal reservoir model. New Zealand Journal of Geology and Geophysics 61(1), 79-95.

Muraoka, H., Takahashi, M., Sundhoro, H., Dwipa, S., Soeda, Y., Momita, M., & Shimada, K. (2010, April). Geothermal systems constrained by the Sumatran fault and its pull-apart basins in Sumatra, western Indonesia. In Proceedings World Geothermal Congress (pp. 1-9).

Mussofan, W., Baroek, M. C., Stimac, J., Sidik, R. P., Ramadhan, I., & Santana, S. (2018). Geothermal Resource Exploration along Great Sumatera Fault Segments in Muara Laboh: Perspectives from

Geology and Structural Play. Paper presented at the Proceedings, 43rd Workshop on Geothermal Reservoir Engineering, Stanford University. SGP-TR-213.

O'Brien, J. M. (2010). Hydrogeochemical Characteristics of the Ngatamariki Geothermal Field and a Comparison with the Orakei Korako Thermal Area, Taupo Volcanic Zone, New Zealand. Unpublished MSc thesis, University of Canterbury, Christchurch, New Zealand.

Oliver, N. H., & Bons, P. D. (2001). Mechanisms of fluid flow and fluid–rock interaction in fossil metamorphic hydrothermal systems inferred from vein–wallrock patterns, geometry and microstructure. Geofluids, 1(2), 137-162.

Oze, C., Cattell, H., & Grove, M.. (2017). 40Ar/39Ar dating and thermal modeling of adularia to constrain the timing of hydrothermal activity in magmatic settings. 45(1), 43-46.

Pambudi, N. A. (2018). Geothermal power generation in Indonesia, a country within the ring of fire: Current status, future development and policy. Renewable and Sustainable Energy Reviews, 81, 2893-2901.

Ratouis, T. M., & Zarrouk, S. J. (2016). Factors controlling large-scale hydrodynamic convection in the Taupo Volcanic Zone (TVZ), New Zealand. Geothermics, 59, 236-251.

Rosenberg, M. (2017). Volcanic and tectonic perspectives on the age and evolution of the Wairakei-Tauhara geothermal system. Unpubished PhD thesis, Victoria University of Wellington, New Zealand.

Rosenberg, M. D., Bignall, G., & Rae, A. J. (2009a). The geological framework of the Wairakei–Tauhara geothermal system, New Zealand. Geothermics, 38(1), 72-84.

Rosenberg, M., Ramirez, L., Kilgour, G., Milicich, S., & Manville, V. (2009b). Tauhara subsidence investigation project: geological summary of Tauhara Wells THM12-18 and THM21–22 and Wairakei Wells WKM14–15. GNS Science Consultancy Report 2009, 309.

Rowland, J. V., & Sibson, R. H. (2004). Structural controls on hydrothermal flow in a segmented rift system, Taupo Volcanic Zone, New Zealand. Geofluids, 4(4), 259-283.

Seebeck, H., Nicol, A., Villamor, P., Ristau, J., & Pettinga, J. (2014). Structure and kinematics of the Taupo Rift, New Zealand. Tectonics, 33(6), 1178-1199.

Sepúlveda, F., Rosenberg, M. D., Rowland, J. V., & Simmons, S. F. (2012). Kriging predictions of drill-hole stratigraphy and temperature data from the Wairakei geothermal field, New Zealand: Implications for conceptual modeling. Geothermics, 42, 13-31.

Situmorang, J., Martikno, R., Putra, A. P., & Ganefianto, N. (2016). A Reservoir Simulation of the Muara Laboh Field, Indonesia. Paper presented at the 41st Workshop on Geothermal Reservoir Engineering.

Spinks, K. D., Acocella, V., Cole, J. W., & Bassett, K. N. (2005). Structural control of volcanism and caldera development in the transtensional Taupo Volcanic Zone, New Zealand. Journal of Volcanology and Geothermal Research, 144(1-4), 7-22.

Stelling, P., Shevenell, L., Hinz, N., Coolbaugh, M., Melosh, G., & Cumming, W. (2016). Geothermal systems in volcanic arcs: Volcanic characteristics and surface manifestations as indicators of geothermal potential and favorability worldwide. Journal of Volcanology and Geothermal Research, 324, 57-72.

Stimac, J., Ganefianto, N., Baroek, M., Sihotang, M., Ramadhan, I., Mussofan, W., ... & Martikno, R. (2019). An overview of the Muara Laboh geothermal system, Sumatra. Geothermics, 82, 150-167.

Struthers, J. D. (2017). Geological modelling workflows to contribute to a better evaluation of slope stability, at Pinnacle Ridge (Ngā Tohu), Mt Ruapehu, New Zealand. Unpublished Professional Master of Engineering Geology Thesis. University of Canterbury, Christchurch, New Zealand.

Truesdell, A. H., Lippmann, M. J., Quijano, J. L., & D'Amore, F. (1995). Chemical and physical indicators of reservoir processes in exploited high-temperature, liquid-dominated geothermal fields. In Proceedings of the World Geothermal Congress (Vol. 3, pp. 1933-1938)

White, B. R., & Chambefort, I. (2016). Geothermal development history of the Taupo Volcanic Zone. Geothermics, 59, 148-167. doi:10.1016/j.geothermics.2015.10.001

Wilson, C. J. N., & Rowland, J. V. (2016). The volcanic, magmatic and tectonic setting of the Taupo Volcanic Zone, New Zealand, reviewed from a geothermal perspective. Geothermics, 59, 168-187. doi:10.1016/j.geothermics.2015.06.013

Wisnandary, C. M., Alamsyah, O., & Energy, S. (2012). Zero Generation of Muara Laboh Numerical Model: Role of Heat Loss and Shallow Wells Data on Preliminary Natural State Modeling. GRC Transactions, 36, 825-830.

Wood, C. P. (1994). The Waiora Formation geothermal aquifer, Taupo Volcanic Zone, New Zealand. In Proceedings of the 16th New Zealand Geothermal Workshop (pp. 121-126). University of Auckland Geothermal Institute

Wood, C., & Browne, P. (2000). Wairakei Geothermal Power Project 40th anniversary: geology and hydrothermal alteration. Paper presented at the Proceedings 22nd New Zealand Geothermal Workshop. (pp. 285-290).

Wu, J. E., McClay, K., Whitehouse, P., & Dooley, T. (2009). 4D analogue modelling of transtensional pull-apart basins. Marine and Petroleum Geology, 26(8), 1608-1623. doi:10.1016/j.marpetgeo.2008.06.007

Wyering, L. D. (2015). The influence of hydrothermal alteration and lithology on rock properties from different geothermal fields with relation to drilling. Unpublished PhD thesis, University of Canterbury, Christchurch, New Zealand

Appendices

Appendix A: Tauhara and Muara Laboh Wells

Tauhara				
Well ID	Northing	Easting	Elevation	Max Depth
WK208	5717829	1866365	440.06	863.72
WK226	5718137	1868322	409.25	1082
TH02	5716767	1870060	407	1207
TH03	5713856	1871947	464	1092
TH04	5715576	1870102	417.1	1040
TH06	5716485	1870257	413.859	1003.73
TH08	5716312	1868991	402.088	575
TH07	5716183	1869144	402	277.47
TH11	5714440	1872884	472.11	1994.64
TH09	5712593	1872012	509.83	2416.67
TH13	5715318	1871825	469.05	1869
TH14	5715128	1871891	484.74	938.0692
THM12	5715667	1871472	432.27	376.6
THM13	5716168	1870025	414.61	414
THM14	5713638	1871019	449.22	389
THM15	5711950	1870749	455.02	152.68
THM16	5712664	1870285	446.27	800.45
WK401	5716909	1867148	443.6859	1512.7
THM17	5714980	1869833	413.78	294
TH15	5716039	1868692	389.81	735
THM18	5715059	1869549	404.06	717.4
TH16	5715713	1869579	403.37	345
THM19	5713978	1871829	465.286	380
WK402	5715759	1867158	426.3454	1194
WK404	5716751	1867463	430.48	2916.85

WK407	5716747	1867505	430.3381	2928.669
WK403	5716180	1866928	436.0039	1200
TH19	5716102	1868750	389.84	2393.595
TH20	5715509	1871417	437.46	1201.136
WK408	5716727	1867069	442.8	3011.7
WK409	5716709	1867059	442.88	2629.088
WK409A	5716709	1867059	442.88	2798.926
WK410	5716690	1867048	442.84	2252.904
THM12	5715674	1871317	432.53	377.2
THM13	5716167	1870027	414.788	416.2
THM14	5713687	1870969	449	388.6
THM17	5714979	1869833	413.455	289.8
THM18	5715059	1869549	405	716.8
THM19	5713978	1871829	374.2	374.2
TH18	5716786	1874338	445	878

Muara Laboh				
Well ID	Northing	Easting	Elevation	Max Depth
ML-A1	737224	9819913	1432.45	1550
ML-A2	737231	9819913	1431.26	2254
ML-A3	737239	9819916	1423.25	2000
ML-A4	737224	9819913	1423.25	1600
ML-B1	738203	9819666	1399.4	2280
ML-C1oh	737497	9822827	1118.4	966
ML-C1ST1	737497	9822827	1118.4	2510
ML-C1ST2	737497	9822827	1118.4	2510
ML-H1	737020	9819167	1571.7	2000
ML-H2	737027	9819166	1571.7	2564.8
ML-H2RD	737027	9819166	1571.7	2691

ML-H3	737043	9819164	1559.7	2800
ML-H4	737052	9819164	1559.7	3100
ML-D1	736502	9822428	1135.8	2500
ML-D1ST2	736854	9823401	1100	977
ML-D2	736502	9822428	1145	1510
ML-E1	736619	9821404	1222.4	2100
ML-E2	736627	9821400	1222.4	1900
ML-E2ST	736627	9821400	1222.4	1400
ML-F1	736624	9819579	1459	3100
ML-F1ST	736624	9819579	1459	2500
ML-F2	736624	9819579	1459	2520

Appendix B: Combined Model Numeric Outputs

Tauhara - Original Combined Model	Potential	Actual	Summary
Lithology	Volume (m^3)	Volume (m^3)	Volume (m^3)
Karapiti 2a Rhyolite	54,350,000	-	-
Spa Andesite	35,839,000	-	-
Middle Huka Falls Formation	37.612	-	-
Lower Huka Falls Formation	55,880,000	-	-
Waiora Formation (Wa5)	701,540,000	5,335,100	701,540,000
Waiora Formation (Wa3-4)	2,781,100,000	30,230,000	2,781,100,000
Waiora Formation (Wa1)	25,120,000,000	109,320,000	25,120,000,000
Tahorakuri Formation	33,979,000,000	37,399,000	33,979,000,000
Whakamaru Group (Wairakei Ignimbrite)	138,940,000	-	-

Muara Laboh - Original Combined Model	Potential	Actual	Summary
Lithology	Volume (m^3)	Volume (m^3)	Volume (m^3)
PS Andesite Fm	275,230,000	5,289,600	275,230,000
Undif Silicic Fm	1,545,100,000	42,564,000	1,545,100,000
Intercalated Dacite & Andesite Fm.	2,165,900,000	5,634,900	2,165,900,000
Painan Fm.	1,931,800,000	7,982,600	1,931,800,000
Pb - Bukit Barisan Fm	1,195,800,000	-	-
Intrusion Sequence	3,376,200,000	40,677,000	3,376,200,000

Appendix C: Refined Combined Model Numeric Outputs

Tauhara – Refined Combined Model	Potential	Actual	Summary
Lithology	Volume (m^3)	Volume (m^3)	Volume (m^3)
Karapiti 2a Rhyolite	51,005,000	-	-
Spa Andesite	27,301,000	-	-
Middle Huka Falls Formation	37.612	-	-
Lower Huka Falls Formation	41,564,000	-	-
Waiora Formation (Wa5)	548,910,000	2,084,400	548,910,000
Waiora Formation (Wa3-4)	2,129,200,000	21,421,000	2,129,200,000
Waiora Formation (Wa1)	19,493,000,000	64,273,000	19,493,000,000
Tahorakuri Formation	26,655,000,000	31,846,000	26,655,000,000
Whakamaru Group (Wairakei Ignimbrite)	134,370,000	23,148	134,370,000

Muara Laboh – Refined Combined Model	Potential	Actual	Summary
Lithology	Volume (m^3)	Volume (m^3)	Volume (m^3)
PS Andesite Fm	126,330,000	1,560,700	126,330,000
Undif Silicic Fm	731,350,000	27,465,000	731,350,000
Intercalated Dacite & Andesite Fm.	1,061,700,000	5,504,000	1,061,700,000
Painan Fm.	1,022,000,000	3,900,200	1,022,000,000
Pb - Bukit Barisan Fm	533,290,000	-	-
Intrusion Sequence	1,611,300,000	27,129,000	1,611,300,000